From the Institute for Nutrition Medicine

of the University of Lübeck

Director: Prof. Dr. med. Christian Sina

The role of IL-6 in vaccine-induced IgG Fc glycosylation

Dissertation

for Fulfillment of

Requirements

for the Doctoral Degree

of the University of Lübeck

from the Department of Natural Sciences

Submitted by

Yannic Christoph Bartsch

from Neustadt am Rübenberge

Lübeck 2019

UNIVERSITÄT ZU LÜBECK

First referee: Prof. Dr. Marc Ehlers

Second referee: Prof. Dr. Rudolf Manz

Date of oral examination: 07.05.2019

Approved for printing: Lübeck, 17.10.2019

Table of content

Abstract

Vaccinations against pathogens are an effective and preventive treatment, the success of which is often correlated with the induced IgG antibody titers. The effector function of IgG antibodies (abs) dependents on the IgG subclass and the respective IgG Fc N-glycosylation pattern at asparagine 297 in the Fc part. Non-fucosylated (afucosylated) IgG abs show an increased pathogenic potential due to increased affinity to activating Fcγ receptors. Furthermore, agalactosylated and asialylated IgG abs are associated with pro-inflammatory and pathogenic effector functions in autoimmune diseases, and an increased potential of these IgG glycan patterns is nowadays discussed in the defense against pathogens. Accordingly, the type of naturally or vaccine-induced IgG Fc glycosylation pattern might be considered more in the future.

One aim of this thesis is to improve and apply the IgG Fc glycosylation analysis of murine and human IgG antibodies. In particular, the effect of different adjuvants on the IgG Fc glycosylation pattern after immunization and the corresponding mechanism should be investigated. Therefore, mice were immunized with different adjuvant, and the resulting antigen-specific IgG subclass distribution analyzed by ELISA, while IgG Fc glycosylation patterns were analyzed via HPLC or LC-MS based methods. Additionally, T and B cell responses were investigated via flow cytometry.

The analysis revealed that the specific IgG Fc glycosylation varies upon different adjuvant treatments in mice. The level of IgG Fc sialylation correlated with α-2,6 sialyltransferase (St6gal1) expression levels in adjuvant-induced splenic plasma cells. This research thereby demonstrated for the first time that the cytokine interleukin (IL)-6 is indispensable for the induction of pro-inflammatory IgG glycosylation patterns (low galactosylation and low sialylation). Interestingly, IL-6 was crucial for the induction of Th17 T helper cells as well as T follicular helper cells in the germinal center. Likewise, it was shown that IL-17A as well as the germinal center reaction were important for the induction of pathogenic plasma cells, which expressed low levels of St6gal1 and subsequently produced low-sialylated IgG abs.

The results indicate the importance of IL-6 to the immunization-induced IgG glycosylation pattern. In the future, novel vaccines and adjuvants may be selected due to the capability of inducing IL-6 and low-sialylated IgG abs via the described mechanisms. Furthermore, these mechanisms may play a role in other contexts, for example, anti-tumor vaccination or inflammatory autoimmunity diseases. Parts of the results presented in this thesis were already published in the peer-reviewed journals *The Journal of Allergy and Clinical Immunology* and *Frontiers in Immunology* (Epp et al., 2018; Bartsch et al., 2018; Twisselmann et al., 2019).

Zusammenfassung

Impfungen gegen Pathogene sind eine effektive präventive Maßnahme. Der Erfolg einer Impfung wird in der Regel mit dem induzierten IgG Antikörpertiter korreliert. Jedoch ist die Effektorfunktion von IgG Antikörpern von deren Subklasse und N-Glykosylierungsmuster an Asparagin 297 im Fc Teil abhängig. IgG Antikörpern mit „nicht-fucosyliertem“ Fc Glycan wird ein höheres pathogenes Potential durch eine erhöhte Affinität zu aktivierenden FcγRezeptoren zugeschrieben. „Nicht-galaktosylierte“ und „nicht-sialinisierte“ IgG Antikörper werden mit pro-inflammatorischen und pathogenen Effektorfunktionen bei Autoimmunerkrankungen assoziiert und inzwischen auch im Kontext der Bekämpfung von Infektionen diskutiert. Entsprechend könnte in Zukunft die natürliche oder Impf-induzierte Art der IgG (Subklassen) Fc Glykosylierung im Kampf gegen Pathogene stärker in den Fokus rücken.

Ein Ziel dieser Arbeit war es, die IgG Fc Glykoanalyse von humanen und murinen Antikörpern weiter zu entwickeln und anzuwenden. Insbesondere sollte dann nach Immunisierung mit verschiedenen Adjuvantien, deren Einfluss auf die IgG Fc Glykosylierung und der entsprechende Mechanismus untersucht werden. Dazu wurde nach Immunisierung von Mäusen die Antigen-spezifische Serum IgG Subklassen-Verteilung mittels ELISA und deren Fc Glykosylierung mittels HPLC und LC-MS Methode untersucht. Die resultierenden T und B Zellantworten wurden mittels Durchflusszytometrie analysiert.

Die Analysen ergaben, dass das spezifische IgG Subklassen Fc-Glykosylierung abhängig vom jeweiligen Adjuvans ist, und dass die IgG Fc Sialinisierung mit der Expression der α-2,6-Sialyltransferase (St6gal1) in den Impf-induzierten Plasmazellen korreliert. Des Weiteren konnte hier erstmalig gezeigt werden, dass das Zytokin Interleukin (IL)-6 für eine pro-inflammatorische IgG Fc Glykosylierung („nicht galaktosyliert“ und „nicht-sialinisiert“) obligatorisch ist. IL-6 war dabei entscheidend für die Induktion von Th17 und follikulären T Helferzellen im Keimzentrum, welche die B Zellantwort steuern. Entsprechend konnte nachgewiesen werden, dass sowohl IL-17 als auch die Keimzentrumsreaktion für die Entstehung von „pathogenen“ Plasmazellen mit niedriger St6gal1 Expression und nicht- sialinisierten IgG Antikörpern entscheidend sind.

Die Ergebnisse weisen darauf hin, dass IL-6 einen entscheidenden Einfluss auf das induzierte IgG Fc Glykosylierung nach Immunisierung hat. In Zukunft könnten neue Impfstoffe und Adjuvantien speziell für die Anregung von IL-6 und einer entsprechend der beschriebenen Mechanismen niedrig sialinisierten IgG Antwort ausgewählt werden. Die beschriebenen Mechanismen zur Entstehung von verschieden glykosylierten IgG Antikörpern könnten auch auf weitere Bereiche wie Tumorvakzinierung oder der Entstehung von Autoimmunerkrankungen eine wesentliche Rolle spielen. Teile der Ergebnisse dieser Arbeit wurden bereits in den „peer review“ Fachzeitschriften „The Journal of Allergy and Clinical Immunology“ und „Frontiers in Immunology“ veröffentlicht (Epp et al., 2018; Bartsch et al., 2018; Twisselmann et al., 2019).

1 Introduction

1.1 Vaccination

One of the most common causes of morbidity and mortality worldwide are the consequences and complications of infectious diseases. Pathogens such as bacteria, viruses, fungi and intra- and extracellular parasites can cause acute or chronic infection. In some cases, the immune system is not able to clear an infection, which can cause cancer, organ failure and death. Although modern treatments such as antibiotics and vaccination have dramatically reduced the burden of infectious diseases, pathogens that cannot be treated by modern medicine nevertheless remain (Khabbaz et al., 2014).

Even in ancient times, it was recognized that people who experienced and survived distinct infections were protected from reinfection. Variolation describes a process wherein small amounts of smallpox particles from infected patients were administered to people, and the survivors of this treatment were protected from reinfection (Murphy et al., 2012). Edward Jenner (*1749 †1823) first demonstrated that a similar protection to smallpox can be achieved by infecting individuals with the cowpox virus, which led to milder disease symptoms compared to the often-fatal infection of the smallpox virus (Riedel, 2005). Jenner coined the term vaccination, which is derived from the Latin word for cow, *vacca* (Riedel, 2005).

Since then, vaccinations have been developed for several diseases and pathogens, and after a mass vaccination campaign, smallpox was declared by the WHO to be eradicated in 1980 (World Health Assembly, 1980). In other severe diseases such as poliomyelitis or measles, a clear reduction in incidence has been seen after the release of an efficient vaccination (Ada, 2005). Until the present, treatments for some acute infections have been limited, and vaccination is the only effective agent to prevent fatal infections (e.g., tick-borne encephalitis; Lindquist & Vapalahti, 2008). Vaccination refers to the inoculation of an attenuated or heat-killed strain or a harmless antigen (e.g., a surface molecule toxoid) to induce a protective immune response (Pschyrembel et al. (eds.), 2007).

The term vaccination is often used not only for immunizations against pathogens; for example, advances have been made in developing vaccinations against tumor antigens (Chiang et al., 2011). In the context of allergies, antigen-specific immune therapy (AIT) protocols include adjuvanted or non-adjuvanted immunizations with the allergen (Larché et al., 2006). In such inoculations, the immune system is skewed to non-pathogenic responses (Larché et al., 2006; Epp et al., 2018). Comparable approaches are currently being

investigated to induce non-pathogenic or even tolerogenic responses to auto-antigens in the context of autoimmunity (Anderson & Jabri, 2013; Oefner et al., 2012; Bartsch et al., 2018). Hereafter, the term vaccination is used to refer to the induction of an immune response to an antigen in the context of different adjuvants.

1.1.1 Vaccine principles

The aim of a vaccination is to trigger an immune response without inducing actual disease or harm to the vaccinated person. After vaccination, the subject is equipped with immunological tools (e.g., neutralizing or opsonizing antibodies, memory cells) that facilitate a proper immune response upon infection with the corresponding pathogen. Even if the circumstances do not allow a person to be vaccinated, herd immunity describes the protection of transmission to non-vaccinated persons due to high vaccination rates among the normal population (Rashid et al., 2012). Mechanisms that lead to this protective immunity are described below (see 1.2).

The WHO currently lists 26 different pathogens to which vaccinations are available (Tab. 1.1; Ada, 2005). Due to the diversity of pathogens, different types of vaccines have been developed. Moreover, certain types of vaccine principles may be contraindicated in some circumstances (e.g., due to allergy or immune suppression) (McNeil & DeStefano, 2018; Bonilla, 2018).

Tab. 1.1 Overview of pathogens or diseases to which vaccination is currently available. Vaccines may be available from different vendors and may differ in formulation (e.g., strain, antigen-content, stabilizers or preservatives, adjuvant). Vaccine may only be effective for certain sub-strains of the pathogens indicated. Vaccines for the listed pathogens may not be licensed for use in humans in all countries. (Source: http://www.who.int/immunization, retrieved:09/2018).

Pathogen/disease name	type of pathogen	Vaccine principles	adjuvant
Cholera	bacteria	killed/inactivated	-
Dengue	virus	live attenuated	-
Diphtheria	bacteria	inactivated toxin	aluminum salts
Hepatitis A	virus	live attenuated	-
		inactivated	aluminum salts
Hepatitis B	virus	purified antigen	aluminum salts
Hepatitis E	virus	purified antigen	aluminum salts
***Haemophilus influenzae* type b**	bacteria	polysaccharide conjugated to carrier protein	none or aluminum salts
Human papillomavirus	virus	purified antigen	aluminum salts

Influenza	virus	live attenuated	-
		inactivated	-
		inactivated	MF59
Japanese encephalitis	virus	live attenuated	-
		inactivated	aluminum salts
Malaria	parasite	recombinant protein fused to Hepatitis B antigen	QS-21+MPLA
Measles	virus	live attenuated	-
Meningococcal meningitis	bacteria	polysaccharide conjugated to carrier protein	none or aluminum salts
		purified polysaccharides	-
Mumps	virus	live attenuated	-
Pertussis	bacteria	killed/inactivated	aluminum salts
		purified antigen	various
Pneumococcal disease	bacteria	polysaccharide conjugated to carrier protein	aluminum salts
		purified polysaccharides	-
Poliomyelitis	virus	live attenuated	-
Rabies	virus	inactivated	
Rotavirus	virus	live attenuated	-
Rubella	virus	live attenuated	-
Tetanus	bacteria	inactivated toxin	aluminum or calcium salts
Tick-borne encephalitis	virus	inactivated	aluminum salts
Tuberculosis	bacteria	live attenuated	-
Typhoid	bacteria	polysaccharide conjugated to carrier protein	aluminum salts
		purified polysaccharides	-
		live attenuated	-
Varicella	virus	live attenuated	-
Yellow fiber	virus	live attenuated	-

1.1.1.1 Attenuation and inactivation

As mentioned above, Jenner inoculated cowpox virus to protect from smallpox infections. The immune response that developed was sufficient to establish immunity to both the cowpox and smallpox viruses (Riedel, 2005). While several further examples exist of naturally occurring strains that can be used for vaccination, for most diseases, no reasonable counterpart exists or has yet been discovered (Ada, 2005). Currently, most viable vaccines are developed artificially by attenuating the pathogenic strain. Attenuation can be achieved by exposing the pathogen to “sub-optimal” conditions, and mutants that adapt to the altered conditions are more likely to survive and be selected for the next round. Due to short generation time and high mutation rates, this often works well for viral diseases (Ada, 2005).

After several rounds, the resulting strain may be non-pathogenic and transmittable between hosts while remaining immunogenic when a person is vaccinated (Murphy et al., 2012; Ada, 2005). Another way to decrease pathogenicity is to inactivate or kill whole pathogens or toxins, for example, by heat, chemically or by only using immunogenic fragments (Salk et al., 1954a; Ada, 2005).

Poliomyelitis, a disease caused by strains of the polio virus, is an example of a disease prevented by inactivated and attenuated vaccines (Kew et al., 2005). The first polio vaccine was developed and licensed in the 1950s, with formalin inactivated variants of three polio virus strains used to inoculate people (Salk et al., 1954a; Salk et al., 1954b). A few years later in the early 1960s, the first viable attenuated polio vaccine was released, generated by adapting isolated human viruses to monkey cells (Sabin & Boulger, 1973). Due to successful vaccination regimens, polio viruses have been nearly eradicated (Kew et al., 2005).

However, viable vaccines may lead to pronounced infections and may transmit the disease to others. For the viable polio virus vaccine, the attenuating mutations can reverse, resulting in a pathogenic vaccine-derived virus that can be transmitted and cause outbreaks of poliomyelitis (Kew et al., 2005). In addition, the immune system of immunocompromised people may not develop pronounced immunity to the disease from the vaccine, and in severe cases, these patients fail to defend against the attenuated strain which contraindicates a vaccination with viable strains (Eibl & Wolf, 2015).

1.1.1.2 Adjuvant based vaccination

Attenuated or inactivated vaccines have an endogenous ability to trigger an adequate immune response. However, these vaccines do not cover all diseases and often lead to safety and efficacy concerns (Coffman et al., 2010; Di Pasquale et al., 2015). It has been recognized that protective immune responses do not require whole pathogens; rather, smaller subunits, toxins or even single (surface-) protein or polysaccharide antigens may be sufficient (Ada, 2005). These antigens often lack immunogenicity, in response to which additional immune-activating substances (adjuvants) must be administered (Coffman et al., 2010).

In the 1930s, Jules Freund described the strong adjuvant effects of mineral oil supplemented with (heat-killed) tuberculosis mycobacteria (Complete Freund’s Adjuvant, CFA) (Freund et al., 1937). The exact mode of action of CFA is still not understood, though it is theorized that aside from inducing general tissue damage (“danger signal”), it might activate certain receptors (e.g., the Mincle receptor) (Ishikawa et al., 2009). Due to its toxicity and severe side effects, however, CFA was not licensed for use in humans (Petrovsky & Aguilar, 2004). New mineral oil preparations have since been licensed in some countries for anti-tumor vaccinations where more side effects are tolerated (Chiang et al., 2011).

Aluminum salts (Alum) were described as a potent adjuvant as early as the 1920s (Glenny et al., 1926; Marrack et al., 2009); however, their adjuvant effects are also not completely understood (Marrack et al., 2009). However, they have long been the only licensed adjuvant for human vaccination (Di Pasquale et al., 2015) and are used in numerous vaccines against viral and bacterial pathogens (Petrovsky & Aguilar, 2004; Tab. 1.1). The requirements for protective immunity are determined by the pathogen, so the choice of adjuvant should aim for one that induces immune responses comparable to naturally induced responses (Coffman et al., 2010).

Today, adjuvants are developed that target distinct pattern recognition receptors (PRR) or cytokine receptors on immune cells (Coffman et al., 2010; Petrovsky & Aguilar, 2004). Adjuvants can be chosen by the type of PRR or cytokine profile that is activated by the targeted pathogen. For example, Monophosphoryl Lipid A (MPLA) is licensed for human vaccine use, as it is a less-toxic derivate of lipopolysaccharide (LPS) from gram negative bacteria that targets Toll-like Receptor (TLR) 4 (Mata-Haro et al., 2007).

1.1.1.3 Future vaccine strategies

Successful vaccination has dramatically reduced the burden of infectious diseases (Hinman, 1999); however, new advances continue to be necessary to cover the full range of pathogens (Ada, 2005). Research for new attenuated or adjuvanted vaccines is continuous, and completely new vaccination approaches are also under development and may be licensed in the future.

Promising results have been obtained from DNA vaccines, wherein DNA plasmids coding for the antigen of interest are administered directly into the muscle. From here, the DNA is taken up and expressed by muscle and antigen-presenting cells. Aside from conventional adjuvant, the plasmid itself can further contain sequences for the expression of cytokines or CpG motifs to enhance immunogenicity (Saade & Petrovsky, 2012).

Another approach is cloning endogenous protein antigens into existing vaccine viruses. The cloned antigen is then expressed together with normal viral antigens and targeted by the immune system. In this way, multiple antigens with different epitopes or even from different pathogens can be combined (Boursnell et al., 1996).

1.2 Vaccination-induced immune responses

The immune system is traditionally divided into the innate and the adaptive immune systems. The innate immune system recognizes pathogen-associated molecular patterns (PAMP) or danger-associated molecular patterns (DAMP) via PRR (Matzinger, 2002; Kawai & Akira, 2010). After vaccination or infection, innate immune cells are immediately activated, and

neutrophils and macrophages phagocyte intruders and release effector molecules like cytokines and chemokines. Antigen-presenting cells (APC) such as dendritic cells process and present pathogen antigens in the context of major histocompatibility complex (MHC) II on their surface to CD4+ T cells. Additionally, infected cells present foreign antigen peptides in the context of MHC I molecules to CD8+ (cytotoxic) T cells, which in turn can lead to lysis of the infected cell (Murphy et al., 2012).

In contrast to PRR that recognize conserved pathogenic structures, adaptive antigen receptors of T and B cells are much more diverse. During the development of these cells, somatic recombination fuses a random V, (D) and J element in the variable region of the DNA sequence of their corresponding receptor chains (Matthews et al., 2014), which generates clones with individual receptor specificities (Schatz & Ji, 2011). Moreover, after the infection (or vaccination) is resolved, activated T and B cells may develop into long-lived memory cells that can respond rapidly after reinfection (Ahmed & Gray, 1996). This secondary adaptive immune response is much faster and more specific to the pathogen and, hence, more effective.

In 1890, Behring and Kitasato described how immunity to Tetanus and Diphtheria can be transferred onto unvaccinated animals by serum (Behring & Kitasato, 1890), with the resultant antiserum then used to treat diphtheria – an infection that often led to death – in children (Llewelyn et al., 1992). The protective moiety was later identified as antibodies neutralizing the toxin (Browning, 1955), and even currently, such purified antibodies can be used as post-exposure prophylaxis as an alternative to active vaccination (Llewelyn et al., 1992; Rothstein et al., 1982). Although cellular immunity – for example, the cytolytic activity of CD8+ cytotoxic T cells (CTL) – can contribute to protective immunity (Schmitz et al., 1999), specific antibody titers often correlate with immune protection. Accordingly, antibody titers are used to assess the level of protection after vaccination (Plotkin, 2010). In the following, the means by which B cells are activated and differentiated to antibody secreting plasma cells are described.

1.2.1 T cell dependent B cell immune responses

Upon infection or vaccination, APCs present foreign antigen peptides loaded on MHC II molecules on their surface. After the CD4+ T cell receptor (TCR) recognizes the MHC II:antigen complex (Signal 1) and additional activating signals occur (e.g., CD28 stimulation by CD80/86; Signal 2), naïve CD4+ T helper cells that are passing by are activated. Specific soluble mediators, such as the cytokines that are released from activated APCs, skew the T cell differentiation to a certain T cell subtype (Signal 3) (Murphy et al., 2012). In contrast to T cells, B cells can be directly activated upon antigen binding to the B cell receptor (BCR) (Malkiel et al., 2018). Both activated T and B cells upregulate chemokine receptors and

migrate into lymphoid organs (Malkiel et al., 2018), and at the T:B cell border in secondary lymphoid organs, T cell activation is augmented by recognition of MHC II:antigen complex and additional co-stimulatory molecules on B cells. Sustained B cell activation is subsequently mediated by binding of CD40 to CD40L on T cells. (Malkiel et al., 2018), and B cells can further differentiate into antibody producing (short-lived) extrafollicular plasma cells or germinal center (GC) B cells (Malkiel et al., 2018). Most of the early antibodies are non-class-switched, low-affinity antibodies mediating a first line of defense (Eisen, 2014; Miyauchi et al., 2016). However, extrafollicular plasma cells may also undergo class-switch to other immunoglobulin heavy chains. For this process, activation-induced cytidine deaminase (AID) induces specific DNA breaks in the heavy chain region (Muramatsu et al., 2000), so the old heavy chain locus is excised, and DNA repair fuses the sequence of the new isotype to the variable region. Class-switch recombination is tightly regulated by cytokines (Matthews et al., 2014). High affinity, class-switched antibodies, however, are the product of GC derived plasma cells (Victora & Nussenzweig, 2012), making the GC particularly important for the generation of vaccine-induced, high affinity protective antibodies (Bentebibel et al., 2013; Pallikkuth et al., 2012).

1.2.1.1 Germinal Center

Germinal centers are follicular structures in secondary lymphoid organs (Fig. 1.1). Stimulation of B cells at the T:B cell border favors upregulation of the transcription factor Bcl-6 and differentiation into GC B cells (Cattoretti et al., 1995; Malkiel et al., 2018). Likewise, antigenic stimulation of the TCR and respective co-stimulation can lead to upregulation of Bcl-6 in CD4+ T cells and migration into the GC (Nurieva et al., 2009). Germinal center B cells proliferate in the dark zone and migrate to the GC light zone. Here, follicular dendritic cells (FDC) present intact antigen in the form of immune complexes (IC) on their surface. Follicular dendritic cells are derived from stromal cells and build a structural backbone (Allen & Cyster, 2008). The GC B cells compete with their BCR for antigen binding. B cells with high affine BCRs can displace the antibodies in the IC and take up the antigen, which is than presented as peptides in the context of MHC II on the B cell's surface. Cognate follicular T helper cells (T_{FH}) recognize the peptide antigen and provide respective T cell help (e.g., CD40L, IL-4 or IL-21 secretion) (Crotty, 2011). Germinal center B cells that do not receive a BCR signal or sufficient T cell help are negatively selected and become apoptotic (Victora & Nussenzweig, 2012). After positive selection, GC B cells return to the dark zone to proliferate further. In addition, in the dark zone, GC B cells can undergo class-switching and incorporate hypermutations into the BCR antigen binding site (Victora & Nussenzweig, 2012), processes which are also influenced by T cells. For example, T_{FH}-derived IL-4 has been described as an important factor in inducing IgG1 class-switch in GC B cells, and IL-4-deficient mice had reduced IgG1 serum antibodies (Reinhardt et al., 2009; Crotty, 2011).

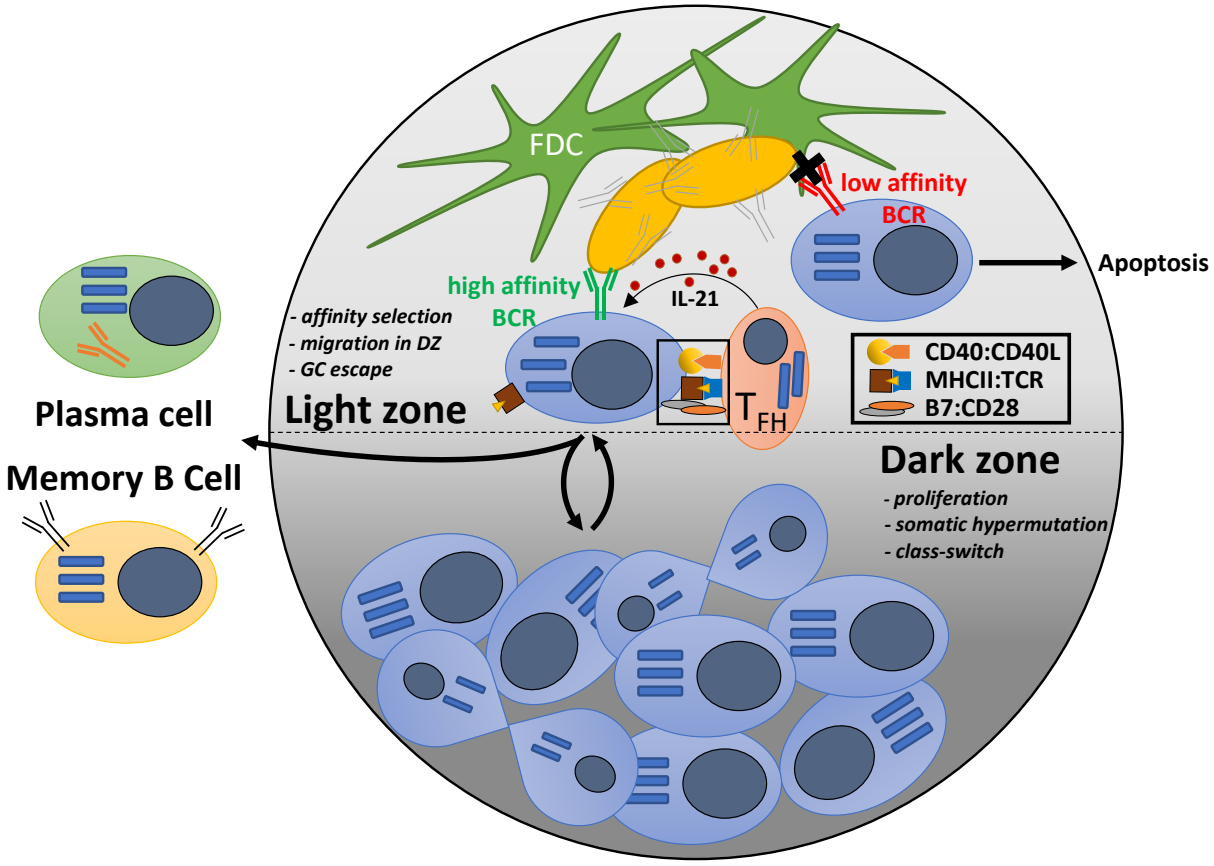

Fig. 1.1 ***Schematic overview of the germinal center.*** *The germinal center (GC) is histologically structured into the dark (lower part) and light (upper part) zone. Germinal center B cells (blue cells) proliferate in the dark zone and somatic hypermutation and class-switch of the B cell receptor (BCR) occur. In the light zone, follicular dendritic cells (FDC) provide the structure for antigen immune complexes. Low affinity GC B cells receive no BCR stimulation or T cell help and undergo apoptosis. Germinal center B cells with higher affinities receive BCR stimulation and T_{FH} cell help (e.g., CD40 stimulation, IL-21). These positive selected GC B cells can return to the dark zone or exit the GC and terminally differentiate into Memory B cells or plasma cells.*

Deamination mediated by AID of DNA bases in the DNA sequence of the antigen binding site results in nucleotide substitution (Muramatsu et al., 2000; Di Noia & Neuberger, 2007). The induced point mutation can be translated into amino acid changes in the antigen-recognizing region of the BCR and may influence affinity and specificity. B cells then migrate once more into the light zone where they are selected for affinity (Victora & Nussenzweig, 2012). Furthermore, auto-reactive B cell clones, which might develop upon hypermutations, can then be eliminated (Malkiel et al., 2018).

High affine clones, however, receive sufficient survival signals and return to the dark zone to further proliferate and improve receptor affinity. However, some positive selected light-zone B cells escape the GC and further differentiate into plasma and memory cells, though which signals make the decision for the fate of the B cells is not yet known. The observation

that plasma cells bare higher affinity receptors than memory cells led to the conclusion that memory cells may develop early in the GC reaction while plasma cells arise later (Weisel et al., 2016; Kräutler et al., 2017). This was confirmed by another study that found the highest level of memory B cell generation early after the onset of GC (Shinnakasu et al., 2016). However, early GC-derived plasma cells have also been observed (Zhang et al., 2018). After exiting the GC, plasma cells begin to produce massive amounts of specific antibodies, and some may become long lasting antibody producers and occupy special niches (e.g., in the bone marrow) (Manz et al., 1997; Kometani & Kurosaki, 2015). Memory B cells stay in circulation or become resident in tissue, and after reencountering the antigen, they quickly differentiate into plasma cells or new GC B cells (Weisel & Shlomchik, 2017). Both high-affinity long-lived plasma cells and memory B cells provide protection against reinfection and are crucial for effective and sustained vaccination (Victora & Nussenzweig, 2012), which underlines the importance of the GC reaction for vaccination.

Antigen-specific GC B cells can still be observed after resolving infections, ensuring the development of protective adaptive immunity. Dysregulated, sustained GC reactions, however, have been associated with the development of auto-reactive antibodies and the respective auto-immune diseases (Vaeth et al., 2014; Sage & Sharpe, 2015). Therefore, under physiological conditions, the termination of GC reactions is facilitated by Foxp3 expressing regulatory follicular T cells (T_{FR}), which in turn express as T_{FH} cells, Bcl-6 and CXCR5 (Wollenberg et al., 2011; Chung et al., 2011). However, some data has indicated that Foxp3-expressing T_{FR} cells do not arise from the naïve T cell pool but from thymus derived (natural) regulatory Foxp3+ T cells (nTregs) (Chung et al., 2011; Ritvo et al., 2018).

The mechanism by which T_{FR} cells downregulate GC responses is uncertain (Sage & Sharpe, 2015). Anti-inflammatory cytokines expression (e.g., IL-10 and TGFβ), as well as direct cell interaction with T_{FH} or GC B cells and cytolysis, has been discussed (Sage & Sharpe, 2015). Nevertheless, the importance of the inhibitory receptor CTLA4 (cytotoxic T-lymphocyte-associated Protein 4) for T_{FR} function is evident (Sage et al., 2014; Wing et al., 2014). CTLA4 is expressed on regulatory T helper cells (Tregs) as well as on T_{FR} cells and can bind to co-stimulatory molecules (e.g., B7) on B cells or other APCs with high affinity, thereby competing the binding of stimulatory receptors like CD28, which leads to attenuated co-stimulation of the T_{FH} cell (Sage & Sharpe, 2015).

1.2.2 T cell independent B cell immune responses

Non-protein antigens cannot be presented on MHC II molecules, which makes CD4+ T cell activation impossible; however, B cells may be activated and facilitate proper antibody responses. B1 cells are a distinct B cell subset that has been described as responding to T cell independent antigens (Martin et al., 2001) and has a low-affinity polyreactive BCR

repertoire that recognizes conserved pathogenic structures (Malkiel et al., 2018). Another important B cell subset can be found in the marginal zone (MZ) of the spleen. These cells respond quickly to blood-borne antigens via TLR and can differentiate into plasma cells (Martin et al., 2001). T cell independent (TI) activation is facilitated via massive crosslinking of BCR by the antigen (e.g., repetitive antigen motifs; TI-type II) or via engagement of additional PRR (e.g., TLR; TI-type I) (Mond et al., 1995). For example, the polyvalent-pneumococcal vaccine consists of up 23 non-protein pneumococcal polysaccharide antigens (Caya et al., 2015), which have an endogenous adjuvant effect by activating PRRs such as TLR 2 (Sen et al., 2005). Antigen-specific B cells are activated after antigen binding and may differentiate into plasma cells. After activation, signals from APCs can also induce class-switching to IgG, IgA or IgE (Litinskiy et al., 2002). Likewise, T cell independent anti-pneumococcal vaccination leads to sustained formation of anti-pneumococcal antibodies. However, titers, and therefore protection, decrease over time (Mufson et al., 1991; Jackson et al., 1999), and re-vaccination does not lead to enhanced formation of new antibodies compared to the primary immunization (Mufson et al., 1991; Jackson et al., 1999). Likewise, affinity maturation is low because B cells require T cell help and GC formation for extensive BCR affinity maturation (Victora & Nussenzweig, 2012).

1.3 IgG-mediated effector functions

Plasma cells secrete massive amounts of their antigen receptor (i.e., BCR) as antibodies. These antibodies are particularly important to the defense against pathogens. IgG antibodies are the dominant isotype in serum and pathogen-specific IgG titers are markers of a current or past infection or vaccination and often correlate with the level of respective protection (Plotkin, 2010). Four different IgG subclasses have been described in humans (IgG1-4) and mice (IgG1, IgG2a/c, IgG2b and IgG3) (Vidarsson et al., 2014; Shade & Anthony, 2013), each differing in its ability to bind to Fcγ receptors (FcγR)or activate complement (Bruhns & Jönsson, 2015; Lilienthal et al., 2018). IgG antibodies are composed of two identical heavy and light chains that form a Y-shaped molecule (Arnold et al., 2007)(Fig. 1.2). The heavy chain consists of three constant immunoglobulin and an N-terminal variable domain (CH 1-3 and VH, respectively), while the light chain is comprised of one constant and one variable domain (CL and VL; respectively). Light and heavy chains are connected N-terminal at the first constant immunoglobulin domain via disulfide bonds and form the Fab portion of the IgG antibody (Vidarsson et al., 2014). The variable domains of the heavy and light chains form the antigen-binding site. Two heavy chains are connected via disulfide bonds in the flexible hinge region, and the “lower” parts of the heavy chains are intertwined and form the Fc part. Antigen-binding is mediated by the Fab part, which may inhibit viral entry or neutralize pathogenic toxins. Fc mediated effector functions, however, are often indispensable for a protective immune response (see below).

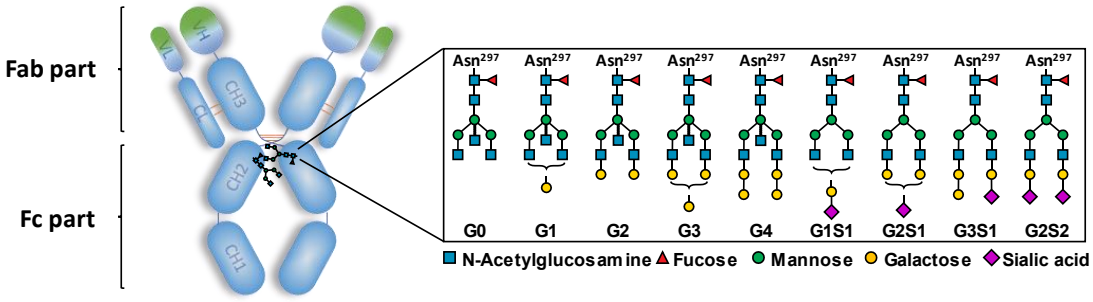

Fig. 1.2 ***Schematic IgG molecule and main Fc glycan structures.*** *IgG consists of two identical heavy and light chains, which are connected by disulfide bonds (orange lines). Each heavy chain has three constant immunoglobulin domains (CH1-3) and one variable domain (VH). The light chain has one constant (CL) and one variable domain (VL). The variable parts are insinuated in green. Antigen-binding is mediated by the Fab part and effector functions by the Fc part. Each IgG heavy chain bares one conserved N-glycosylation site at Asn297 in the CH2 domain. The attached N-glycan is a biantennary complex-type glycan. The main observed structures and the corresponding abbreviations are sketched.*

1.3.1 IgG Fc glycosylation

Antibodies have long been recognized to be post-translationally glycosylated. IgM, IgD, IgE and IgA antibodies carry several glycosylation sites (Arnold et al., 2007). IgG, however, bares just one N-conserved glycosylation site at asparagine 297 in the sequence of the constant heavy chain (Howell et al., 1967; Edelman et al., 1969). The IgG glycan has been identified as a complex-type biantennary N-glycan (Fig. 1.2); that is, a chain of two N-acetylglucosamines (“chitobiose core”) is connected to the protein backbone. Three branched mannoses are connected to chitobiose and build the foundation for the two antennae (Parekh et al., 1985). The glycan core structure is completed by the addition of N-acetylglucosamine (GlcNAc) to the terminal mannoses. The antennae can be further elongated by galactose and, subsequently, by sialic acid (Moremen et al., 2012). Fucosylation can occur at the protein-bound GlcNAc, and the addition of GlcNAc at the branched mannose leads to bisection. These modifications can be found in all combinations, making the structure of the IgG N-glycan highly diverse (Arnold et al., 2007). IgG glycosylation is initiated by the protein N-glycosylation enzyme machinery in the endoplasmic reticulum (ER), where it acts as quality control. Un- or misfolded proteins that were not correctly glycosylated are retained in the ER. Glycosylation is completed by the respective enzymes during the protein transport chain in the Golgi apparatus (Moremen et al., 2012).

The significance of the IgG Fc glycan is emphasized by the observation that (artificially) aglycosylated IgG hardly binds to FcγR or fixes complement (Tao & Morrison, 1989). Similar observations regarding receptor binding have been made for aglycosylated IgE (Shade et al., 2015). Furthermore, IgG glycosylation patterns have been associated with inflammatory diseases. An increase in the non-galactosylated (agalactosylated; G0) IgG

pattern is observed in patients with rheumatoid arthritis (RA), systemic lupus erythematosus (SLE), multiple sclerosis (MS) or inflammatory bowel diseases (IBD) (Parekh et al., 1985; Vučković et al., 2015; Wuhrer et al., 2015; Trbojević Akmačić et al., 2015). The observation that agalactosylated IgG has an increased pathogenic potential suggests a role in the pathophysiology in these diseases (Ito et al., 2014). Moreover, when IgG antibodies from RA patients were analyzed in an antigen-specific manner, this observation was even more pronounced and might be even used as a prognostic marker (Scherer et al., 2009; Rombouts et al., 2015). Intriguingly, pregnancy or therapy induced remission in RA patients correlated with decreased proportions of G0 glycans and higher proportions of galactosylated and sialylated glycans, which have less inflammatory or even anti-inflammatory effector functions (Croce et al., 2007; van de Geijn et al., 2009; Karsten et al., 2012; Oefner et al., 2012; Collin & Ehlers, 2013; Hess et al., 2013; Ito et al., 2014; Bartsch et al., 2018; Epp et al., 2018; Anthony et al., 2011).

1.3.2 The role of Fc glycosylation on IgG effector functions

IgG can respond specifically to an antigen challenge via the antigen-binding domain in the Fab part. While antigen-masking alone might be sufficient for toxin neutralization or inhibiting viral entry (Plotkin, 2010), in most cases, additional effector functions for a sufficient defense against a pathogen might be required. The constant Fc part plays an important role in mediating effects and activating innate and adaptive immune cells and factors. Although vaccine titers often correlate with successful vaccination, vaccine failures independent of the titer have been observed (Taranger et al., 2000; Coudeville et al., 2010). For example, anti-influenza IgG levels have been highly correlated with the level of protection; however, nevertheless, in 50% of the cases, intermediate anti-influenza IgG titers do not protect efficiently (Coudeville et al., 2010). IgG subclass analysis in connection with IgG subclass Fc glycosylation analysis may help determine the protectivity of an antibody response upon vaccination (Alter et al., 2018). In the following, IgG Fc mediated effector functions and the influence of Fc glycosylation are introduced.

1.3.2.1 Fcγ receptor binding

Specific FcγR on innate and adaptive effector cells can bind to the Fc part of IgG. In mice and humans, four and six different classical FcγR have been described, respectively. The receptors differ in their affinities to the individual IgG subclasses as well as in their expression on the different effector cells (Bruhns & Jönsson, 2015). For example, an IgG1 dominated immune response is more likely to activate human macrophages that express FcγRI instead of basophils which lack the receptor (Bruhns & Jönsson, 2015). Although under physiological conditions FcγR may be occupied by IgG, activation requires receptor multimerization, for example, after binding to an immune complex (Bruhns & Jönsson,

2015; Dekkers et al., 2018). Intracellular signaling of most activating FcγRs is mediated via the "common gamma chain." The human FcγRIIIB mediates signaling via a glycophosphatidylinositol (GPI) anchor, while human FcγRIIA and human FcγRIIC have a signaling moiety in their intracytoplasmic tail (Bruhns & Jönsson, 2015). Signaling via these tails or via the common gamma chain occurs upon receptor crosslinking, which is initiated by phosphorylation of tyrosine residues in the intra-cellular immunoreceptor tyrosine-based activation motif (ITAM) by SRC family kinases. This recruits spleen tyrosine kinase (SYK) family kinases, which mediate the signaling further downstream (Nimmerjahn & Ravetch, 2008). FcγRIIB is, in humans and mice, the only inhibitory classical Fcγ receptor. At an intracellular level, the ITAM is replaced by an ITIM (cellular immunoreceptor tyrosine-based inhibitory motif), which, after co-ligation with other ITAM-bearing Fc receptors and subsequent phosphorylation, recruits SHIP phosphatases. These SHIP phosphates can then dephosphorylate the ITAM of activating Fc receptors and thereby modulate the cellular activation threshold (Bruhns & Jönsson, 2015; Nimmerjahn & Ravetch, 2008).

Intriguingly, pooled intravenous IgG from healthy donors can have an immunosuppressive effect when administered in relatively high doses (1–2g/kg) (Schwab & Nimmerjahn, 2013). The protective effect of sialylated IgG abs has been shown to depend on the upregulation of the inhibitory FcγRIIB after the binding of sialylated IgG Fc to the lectin receptor SIGN-R1 (Kaneko et al., 2006; Anthony et al., 2011). From this, it was suggested that upregulated FcγRIIB increases the cellular activation threshold (Anthony et al., 2012). Additional receptors interacting with galactosylated (e.g., Dectin-1) or sialylated (e.g., CD23, Dendritic cell immunoreceptor; DCIR) IgG Fc have been identified (Karsten et al., 2012; Pincetic et al., 2014; Massoud et al., 2014; Wang et al., 2015). All these C-type lectin receptors are associated with an anti-inflammatory function.

Furthermore, sialylated antigen-specific IgG has been shown in mouse models to induce tolerance and attenuate rheumatic diseases (Oefner et al., 2012; Pagan et al., 2018; Bartsch et al., 2018). Consequently, agalactosylated IgG was concluded to has a pro-inflammatory effect, while galactosylated or sialylated IgG Fc is less inflammatory or immunosuppressive, respectively (Collin & Ehlers, 2013).

The effects of activation are highly dependent on the respective cell type, as FcγR can induce the release of cytokines and chemokines (e.g., granulocytes), phagocytosis and antigen-presentation (e.g., macrophages and DCs) or antibody-dependent cytotoxicity (ADCC) (e.g., Natural killer cells and macrophages) (Nimmerjahn & Ravetch, 2008; Bruhns & Jönsson, 2015; Li et al., 2017). How and which cells are activated depends on the IgG subclass and the receptor expression pattern on the cells. Moreover, the IgG Fc glycan itself was also shown to be involved in modulating the affinities to FcγR (Li et al., 2017; Dekkers et al., 2018). Remarkably, sialylation of IgG1 Fc glycan was associated with reduced FcγRIIIA

binding and decreased ADCC (Scallon et al., 2007). Similarly, de-fucosylation of monoclonal IgG1 increased FcγRIIIA affinity and led to an increased ADCC (Shields et al., 2002; Li et al., 2017). Likewise, increased non-fucosylated antigen-specific IgG has been linked to overcoming persistent infections of lymphocytic choriomeningitis virus in mice (Wieland et al., 2018) or enhanced antibody-dependent cell-mediated virus-inhibition (ADCVI) in HIV elite controllers (Ackerman et al., 2013). Interestingly, the elite controllers also showed reduced levels of galactosylated and sialylated IgG Fc, which is linked to an enhanced FcγR stimulation and pro-inflammatory responses and increased vaccine-induced protection (Ito et al., 2014; Scallon et al., 2007; Vaccari et al., 2016).

1.3.2.2 Complement activation

The complement system is a cascade of self-activating proteases that can result in the membrane attack complex (MAC) and subsequent lysis of the pathogen or infected cell, and during activation, several immuno-stimulatory mediators (anaphylatoxins) are released (Ricklin et al., 2010). The complement system has been recognized as an important defense mechanism against infectious diseases. IgG antibodies play a critical role in the activation of the classical complement pathway. Upon antigen-binding, the complement factor C1q can bind to IgG Fc and initiate the complement cascade (Ricklin et al., 2010). Fc glycans with terminal galactose seem to favor C1q binding while sialylation abrogates C1q binding and the subsequent complement-dependent cytotoxicity (Quast et al., 2015; Lilienthal et al., 2018). Furthermore, agalactosylated IgG antibodies may recognized by the Mannose binding protein (MBP), which triggers activation of the lectin-complement pathway (Malhotra et al., 1995).

1.3.3 Regulation of IgG glycosylation

IgG Fc glycosylation appreciably influences IgG effector functions, with levels of fucosylation, galactosylation and sialylation having been found to influence IgG effector functions. Specific enzymes hierarchically modify the glycan during the vesicular transport from the ER to the Golgi and the plasma membrane (Moremen et al., 2012), and glycosylation is dependent on the availability of enzymes, substrates and acceptor molecules. For example, the α-2,6-sialyltransferase (St6gal1) requires a galactosylated glycan for the addition of cytidine monophosphate (CMP) activated sialic acid. Consistently, St6gal1 expression levels in plasma cells correlates with IgG Fc sialylation (Oefner et al., 2012; Hess et al., 2013; Pfeifle et al., 2017; Bartsch et al., 2018), and furthermore, plasma cells that were conditionally knocked-out for St6gal1 failed to produce sialylated IgG antibodies (Ohmi et al., 2016). Likewise, genome-wide association studies in humans found strong associations between galactosylation and sialylation with the glycosyltransferase β-1,4-galactosyltransferase 1 (B4galt1) and St6gal1, respectively (Lauc et al., 2013; Wahl et al.,

2018). Additionally, correlations of IgG glycosylation with other factors such age or ethnicity have been found (Pucić et al., 2011; Mahan et al., 2016).

An active (and aberrant) regulation of IgG glycosylation has been suggested for the alteration observed in inflammatory auto-immune diseases. Here, IgG glycosylation is more pro-inflammatory (low levels of galactose and sialic acid) during disease flare and becomes less inflammatory upon treatment (e.g., with anti-TNFα abs) or pregnancy associated remission (Collins et al., 2013; van de Geijn et al., 2009). Similarly, pro-inflammatory IgG glycosylation patterns have been correlated with chronic and active infections in Hepatitis B (Ho et al., 2015a). In line, specific IgG from patients with active tuberculosis infections were more pro-inflammatory than patients with latent (asymptomatic; no inflammation) infection (Lu et al., 2016). Furthermore, vaccination can induce characteristic Fc glycosylation patterns (Selman et al., 2012a; Mahan et al., 2016; Kao et al., 2017), and vaccination-induced IgG Fc glycosylation patterns have been linked to a more pro-inflammatory phenotype (e.g., reduced sialylation), which is also advantageous for defense against the infection (Vaccari et al., 2016).

Although the first studies to investigate the influence of different adjuvant on the IgG glycosylation pattern have been conducted, only limited data about the mechanisms by which differently glycosylated IgG antibodies develop is available. These initial studies have shown that T cell dependent vaccination leads to decreased St6gal1 expression and lower sialylation of antigen-specific IgG Fc compared to T cell independent vaccinations (Hess et al., 2013). The downregulation of St6gal1 has been associated with the induction of pathogenic Th17 cells in the context of auto-immunity (Pfeifle et al., 2017). However, there is a considerable lack of knowledge concerning the mechanisms that contribute to IgG glycosylation regulation.

1.4 Aim of the thesis

Vaccination against pathogens is an effective preventive treatment, and the burden of infectious diseases has dramatically decreased since introduction of the first vaccines more than 200 years ago. However, even currently, effective vaccination is not available to prevent numerous infectious diseases, and the efficiency of some vaccines, even when IgG antibodies are induced, has been questioned. New vaccines and vaccination strategies are constantly under development, however, induced IgG titers alone might not be sufficient to predict the level of protection. The induction and quality of memory T and B cells and the induced IgG subclass distribution and their Fc glycan patterns are critical determining factors of pathogenic immune effector mechanisms and may explain sufficient or insufficient immunity upon vaccination.

T cell dependency and the co-stimulus (adjuvant) seems to be important in inducing distinct antigen-specific IgG Fc glycosylation patterns. The choice of the right co-stimulus (adjuvant) may help to induce protective IgG glycosylation patterns and overcome present obstacles in the development of new vaccines. However, the means by which IgG glycosylation is regulated are poorly understood, but sound knowledge on the mechanisms that regulate IgG glycosylation could help in the targeted development of novel vaccines.

The first aim of the thesis is to establish a high-throughput HPLC-based approach for the analysis of human and mouse IgG Fc glycans. This approach should then be used to analyze the IgG Fc glycosylation of different cohorts, for example, a cohort of individuals with a deficiency in their *CTLA4* allele and respective controls.

Secondly, IgG Fc glycosylation in mice should be investigated upon vaccination with the model antigen Ovalbumin and different adjuvants. Aside from antigen-specific IgG Fc glycosylation, plasma cell differentiation and St6gal1 expression should be analyzed by flow cytometry.

The third aim of this thesis is to explore how IgG glycosylation is regulated upon immunization with a T cell dependent antigen and different adjuvants. In adjuvanted vaccination mouse models, the immune mechanisms of cytokines like IL-6 and IL-17 on T and B cell responses should be analyzed further.

The results of these studies may increase the understanding of how pathogenic IgG glycosylation patterns are induced, which can then be used to develop new vaccination strategies and improve the induced immunity. Furthermore, these findings may help to achieve a more basic understanding of how IgG glycosylation is regulated.

2 Material and Methods

2.1 Materials

2.1.1 Human samples

Fourteen heterozygous *CTLA4* mutation carriers from five unrelated families were identified by Sanger (Schubert et al., 2014; Schwab et al., 2018). Serum samples and clinical information from all *CTLA4* mutation carriers were collected after obtaining informed written consent under local ethics board–approved protocols 239/99_BG, 27 251/13_KW, and 282/11_SE version 140023 (Ethics Committee of the Albert-Ludwigs-University of Freiburg, Germany).

Thirty control serum samples from human participants aged 8–20 years were collected after obtaining informed written consent under local ethics board-approved protocol 12-006 (Ethics Committee of the Medical Faculty of the University of Lübeck, Germany).

An additional eighty control serum samples from human participants aged 25–59 years from a community-based cohort were provided by the PopGen biobank. The samples were collected following informed written consent under local ethics board-approved protocol A 156/03 (Ethics Committee of the Medical Faculty of the University of Kiel, Germany).

2.1.2 Mice

C57BL/6 wildtype (WT) mice were purchased from Janvier Laboratories or Charles River Laboratories and bred in the internal facility. IL-17RA-deficient (Il-17Ra KO), IL-17A-deficient (IL-17A KO), IL-6-deficient (Il-6 KO), soluble sp130 transgenic (sgp130Fc tg), IL-6R$^{fl/fl}$ x CD4-Cre (Cd4-Cre) and IL-6R$^{fl/fl}$ x CD11c-Cre (Cd11c-Cre), IL-22-deficient (Il-22 KO), IL-23p19 -deficient (Il23 KO) and NFATc1$^{fl/fl}$ x Foxp3-IRES-Cre (Nfat) mice were developed as described and maintained in accordance with institutional guidelines (Ye et al., 2001; Nakae et al., 2002; Kopf et al., 1994; Rabe et al., 2008; Heink et al., 2017; Zheng et al., 2007; Ghilardi et al., 2004; Vaeth et al., 2012). If possible, only 8–12-week-old male mice were analyzed in the experiments. If mixed genders were used, genders were distributed equally between the investigated groups. However, no differences between male and female mice were observed. All experiments were conducted in accordance with the regulatory guidelines and ethical standards of the University of Lübeck and with the approval of the Federal Ministry of Energy, Agriculture, the Environment and Rural Areas Schleswig-

Holstein (License numbers: 39_45-4-17; 39_42-3-17; 39_48-6-18; 39_125-10-16; 19_53-4-17) or the respective authorities of collaboration partners.

2.1.3 Consumables

3-way stop cock	Braun (Melsungen, Germany)
8-well tube strips	Kisker Biotech (Steinfurt, Germany)
96-well PP plate (conical, 450µl/well)	Thermo Fisher (Waltham, MA, USA)
Costar Assay plates (high binding), 96 well	Corning (Kennebunk, ME, USA)
FACS tube 5 ml	Sarstedt (Sarstedt, Germany)
Falcon 70µm cell strainer	Corning (Kennebunk, ME, USA)
Falcon tubes (15, 50 ml)	Greiner Bio-one (Kremsmünster, Austria)
HPLC vial ND11	Carl Roth (Karlsruhe, Germany)
Maxi Column	G Biosciences (St, Louis, MO USA)
Micro inserts HPLC vials	Carl Roth (Karlsruhe, Germany)
Multiscreen filter plate (0.45µm, low binding)	Merck (Darmstadt, Germany)
Needle 26G 0.45x13mm	Braun (Melsungen, Germany)
Needle 26G 0.45x25mm	Braun (Melsungen, Germany)
Pipett tips with and without Filter (10 µl, 100 µl, 200 µl, 1000 µl)	Sarstedt (Sarstedt, Germany)
Pipette tips (10, 200, 1000 µl)	Sarstedt (Nümbrecht, Germany)
Reaction tubes (1.5, 2.0 ml)	Sarstedt (Nümbrecht, Germany)
Serological pipettes (5, 10, 25, 50 ml)	Sarstedt (Nümbrecht, Germany)
Serological pipette (1 ml. 5 ml. 10 ml. 25 ml)	Sarstedt (Nümbrecht, Germany)
Single-use syringes, 1 ml	Braun (Melsungen, Germany)

Single-use syringes, 3 ml	Braun (Melsungen, Germany)
Tissue culture 6-well suspension plate	Sarstedt (Nümbrecht, Germany)
Vial lid ND11 PTFE Septum	Carl Roth (Karlsruhe, Germany)
XBridge BEH Glycan 1.7µm HPLC-column	Waters Corporation (Milford, MA, USA)

2.1.4 Chemicals

Acetic acid	Carl Roth (Karlsruhe, Germany)
Acetonitrile Rotisolv HPLC Gradient	Carl Roth (Karlsruhe, Germany)
AlexaFluor 488 Abs labeling kit	Thermo Fisher (Waltham, MA, USA)
Allhydrogel (Alum)	Invivogen (Toulouse, France)
Aminobenzamide (2-AB) p.a.	Sigma-Aldrich (St, Louis, MO, USA)
Ammonia (25%)	Carl Roth (Karlsruhe, Germany)
Ammonium chloride (NH_4Cl)	Merck (Darmstadt, Germany)
BD Opteia (TMB substrate)	BD Bioscience (San Diego , CA, USA)
Blotto Immunoanalytical Grade (Non-Fat Dry Milk)	Rockland (Limerick, PA, USA)
Brefeldin-A (1000x)	Biolegend (San Diego, CA, USA)
BSA	GE Healthcare (Little Chalfont, UK)
Carbonate/Bicarbonate-Puffer	Sigma-Aldrich (St, Louis, MO, USA)
Carbonate-bicarbonate	Sigma-Aldrich (St, Louis, MO, USA)
Cellulose	Merck (Darmstadt, Germany)
CNBr-activated Sepharose 4B	GE Healthcare (Little Chalfont, UK)
DL-Dithiothreitol solution 1 M in H2O	Sigma-Aldrich (St, Louis, MO, USA)
DMSO (dried)	Merck (Darmstadt, Germany)
Dulbecco´s Phosphate buffered saline	Thermo Fisher (Waltham, MA, USA)

EDTA	Sigma-Aldrich (St, Louis, MO, USA)
Endoglycosidase S (EndoS)	Provided by Mattias Collin (University of Lund)
Ethanol	Carl Roth (Karlsruhe, Germany)
Fetal bovine serum	Thermo Fisher (Waltham, MA, USA)
Formic acid p.a.	Fluka (St, Louis, MO, USA)
Gelatin	Sigma-Aldrich (St, Louis, MO, USA)
Glycerol	Sigma-Aldrich (St, Louis, MO, USA)
Glycine	Merck (Darmstadt, Germany)
Fixable viability dye (eFluor780)	Thermo Fisher (Waltham, MA, USA)
Ovalbumin AF647 conjugated	Thermo Fisher (Waltham, MA, USA)
Streptavidin BV605 conjugated	Biolegend (San Diego, CA, USA)
Streptavidin BV421 conjugated	Biolegend (San Diego, CA, USA)
Legendplex mouse Th17 kit	Biolegend (San Diego, CA, USA)
Legendplex mouse IL-23p19 beads	Biolegend (San Diego, CA, USA)
Legendplex mouse IL-12p40 beads	Biolegend (San Diego, CA, USA)
Legendplex mouse Cytokine panel 2 standard	Biolegend (San Diego, CA, USA)
Legendplex mouse Cytokine panel 2 detection antibodies	Biolegend (San Diego, CA, USA)
Graphite (Carbograph)	Grace (Columbia, MD, USA)
HCl	Merck (Darmstadt, Germany)
HEPES (N-(2-Hydroxyethyl) piperazin-N'-(2-ethansulfonacid))	Thermo Fisher (Waltham, MA, USA)
Incomplete Freund‘s Adjuvant	Sigma-Aldrich (St, Louis, MO, USA)
Intratect® (IVIG)	Biotest AG (Langen, Germany)
Ionomycin	Biolegend (San Diego, CA, USA)

Ketamin 10 mg/ml	WDT (Garbsen, Germany)
Methanol	AppliChem (Darmstadt, Germany)
Monensin (1000x)	Biolegend (San Diego, CA, USA)
Monophosphoryl Lipid A (MPLA)	Invivogen (Toulouse, France)
Mycobacterium tuberculosis H37 Ra (killed)	BD Bioscience (San Diego , CA, USA)
Sodium chloride (NaCl)	Merck (Darmstadt, Germany)
Ovalbumin Grade VI	Sigma-Aldrich (St, Louis, MO, USA)
Penicillin Streptomycin	Thermo Fisher (Waltham, MA, USA)
PMA	Invivogen (Toulouse, France)
Protein G resin	GeneScript (Piscataway, NJ, USA)
Rompun 2% (Xylazine)	Bayer (Lerverkusen, Germany)
RPMI1640 (L-Glutamine)	Thermo Fisher (Waltham, MA, USA)
Saponin	Sigma-Aldrich (St, Louis, MO, USA)
Sodium bicarbonate (NaHCO3)	Merck (Darmstadt, Germany)
Sodium cyanoborohydride	Merck (Darmstadt, Germany)
Sodium hydrogen phosphate	Sigma-Aldrich (St, Louis, MO, USA
Sodium hydroxide (NaOH)	Merck (Darmstadt, Germany)
Sodium azide	AppliChem (Darmstadt, Germany)
Sulfuric acid	Sigma-Aldrich (St, Louis, MO, USA)
Trifluoracetic acid	Merck (Darmstadt, Germany)
Tris-HCl	Sigma-Aldrich (St, Louis, MO, USA)
Trizma base (Tris)	Sigma-Aldrich (St, Louis, MO, USA)
Tween 20	Sigma-Aldrich (St, Louis, MO, USA)
β-Mercaptoethanol	Sigma-Aldrich (St, Louis, MO, USA)
Cytofix/Cytoperm	BD Bioscience (San Diego, CA, USA)

True Nuclear transcription factor buffer	Biolegend (San Diego, CA, USA)
FoxP3 / Transcription Factor Staining Buffer Set	Thermo Fisher (Waltham, MA, USA)

2.1.5 Antibodies

Epitope	clone	Species/ isotype	conjugate	Vendor
anti-mouse-FAS	Jo2	hamster IgG2	BV510	BD Bioscience (San Diego, CA, USA)
anti-mouse-Foxp3	MF-23	rat IgG2b	AF647	
anti-mouse-IgG1	polyclonal	goat IgG	HRP	Bethyl Labs, (Montgomery, TX, USA)
anti-mouse-IgG2b	polyclonal	goat IgG	HRP	
anti-mouse-IgG2c	polyclonal	goat IgG	HRP	
anti-mouse-IgG3	polyclonal	goat IgG	HRP	
anti-mouse-IgG Fc	polyclonal	goat IgG	HRP	
anti-mouse-IgM	polyclonal	goat IgG	HRP	
anti-mouse-IgG Fc	polyclonal	goat $F(ab)_2$	PE	
anti-mouse/human-B220	RA3-6B2	rat IgG2a	BV786	Biolegend (San Diego, CA, USA)
anti-mouse-CD138	281-2	rat IgG2a	BV711	
anti-mouse/human-GL7	GL7	rat-IgM	PerCP-Cy5.5	
anti-mouse-IgG1	RMG1-1	rat IgG	BV421	
anti-mouse-CD4	RM4-5	rat IgG2a	BV711	
anti-mouse-CD8a	53-6.7	rat IgG2a	AF700	
anti-mouse/human-ICOS	C398.4A	hamster IgG	Pe-Cy7	
anti-mouse-CXCR5	L138D7	rat IgG2b	Biotin	
anti-mouse-CD3	17A2	rat IgG2b	AF488	
anti-mouse-IFNγ	XMG1.2	rat IgG1	AF647	
anti-mouse-IL-6R	MR16-1	rat IgG1	non	Chugai Pharmaceutical (Tokyo, Japan)

anti-human-St6gal1	polyclonal	goat	non	R&D Systems (Minneapolis, MN, USA)
anti-mouse-IgM	eB121-15F9	rat IgG2a	Pe-Cy7	Thermo Fisher (Waltham, MA, USA)
anti-mouse/rat-IL-17A	eBio17B7	rat IgG2a	PE	

2.1.6 Buffers

100 mM Ammoniumformat (Eluent A)	3.77 ml/L formic acid adjusted to pH 4.5 with Ammonia (25%)
1x PBST	1x PBS 0.5 ml/L Tween 20
Blocking buffer (Ova coupling)	0.1 M Tris-HCl adjusted to pH 8 with HCl
ELISA Puffer	30 g BSA 1g gelatin 7.9 ml 0.38 M EDTA ad 1L with 1x PBS
Erylysis buffer	150 mM NH4Cl 100 µM EDTA 1 mM NaHCO3 adjusted to pH 7.2
FACS buffer	0.5% BSA 0.05% sodium azide in 1x PBS
Perm/Wash buffer	0.05x PBS 0.05% saponin 0.01% NaN3

T Cell Medium	1% Penicillin Streptomycin 10% Fetal bovine serum 1mM HEPES 50µM β-Mercaptoethanol in RPMI1640 Medium (L-Glutamine)
Wash buffer I (Ova coupling)	0.1 M Acetic acid 0.5 M NaCl adjusted to pH 4 with NaOH
Wash buffer II (Ova coupling)	0.1 M Tris-Hcl 0.5 M NaCl adjusted to pH 8 with HCl

2.1.7 Instruments

Attune Flow Cytometer	Thermo Fisher (Waltham, MA, USA)
Autoclave VX-75	Systec (Linden, Deuschland)
Barnstead GenePure Pro (Ultrapure water)	Thermo Fisher (Waltham, MA, USA)
Centrifuge 5424R	Eppendorf (Hamburg, Germany)
Centrifuge Megafuge 8	Thermo Fisher (Waltham, MA, USA)
Chromeleon Software V6.9	Thermo Fisher (Waltham, MA, USA)
Concentrator plus (speed-vac)	Eppendorf (Hamburg, Germany)
Electronic balance	Kern & Sohn (Balingen-Frommern, Germany)
ELISA-ReaderMultiskan EX	Thermo Fisher (Waltham, MA, USA)
Prism v. 6.04	GraphPad Software (San Diego, CA, USA)
HPLC Ultimate 3000 system	Thermo Fisher (Waltham, MA, USA)
Incubator AutoFlow NU-5510	NuAir (Plymouth, MN, USA)
MACSQuant Analyzer flow cytometer	Miltenyi Biotec (Bergisch Gladbach , Germany)

Megastar 3.0 Centrifuge	VWR (Radnor, PA, USA)
Microcentrifuge Heraeus Pico 17	Thermo Fisher (Waltham, MA, USA)
Confocal Laser Scanning Biological Microscope FV1000	Olympus (Hamburg, Germany)
NanoDrop-2000C	peqlab Biotechnologie GmbH (Erlangen, Germany)
pH Meter FiveEasy F20	Mettler-Toledo (Columbus, OH, USA)
Pipetboy Accu 2	Integra Bioscience (Zizers, Schweiz)
Pipette (eight- or twelve multi-channel)	VWR (Radnor, PA, USA)
Pipette (single-channel)	Eppendorf (Hamburg, Germany)
Pipette Multi-channel Eppendorf Xplorer® plus	Eppendorf (Hamburg, Germany)
Thermomixer C	Eppendorf (Hamburg, Germany)
Thermomixer Compact	Eppendorf (Hamburg, Germany)
Tube Rotator „end-over-end“ shaker	VWR (Radnor, PA, USA)
Vacuum pump MZ2C	Vacuubrand (Wertheim, Germany)
Vortex-Genie 2	Scientific Industries (Bohemia, NY, USA)

2.2 Methods

2.2.1 Antibody purification

2.2.1.1 Total IgG purification with Protein G and IgG glycan release

Purification of total IgG was accomplished via affinity chromatography with agarose coupled Protein G, which is a S*treptococcal* protein that binds to the CH_2 domain of the Fc part of IgG (Kato et al., 1995). The used Protein G is a recombinant variant that lacks the albumin-binding site.

One hundred µl of Protein G resin slurry was packed into wells of a 96-well filter plate (Merck, Darmstadt, Germany), and storage solution was removed by applying negative

pressure on a vacuum manifold. The Protein G was reconstituted by washing it three times with 200 µl PBS. Fifty µl of serum samples were diluted with 150 µl of PBS prior to loading and were subsequently incubated on the resin for 2 hours at room temperature (RT) with agitation by a plate shaker (300 rpm). Afterwards, the supernatant was removed and Protein G washed at least five times with 200 µl of PBS. IgG was than eluted two times with 200 µl of 0.1 M formic acid (pH 2.7). The pH value of the elution was adjusted to neutral (pH ~7) with 20 µl of 1 M ammonium-bicarbonate (pH 9), and the IgG purification was then confirmed by ELISA (Fig. A.1).

The Fc glycan of the purified IgG was then released by EndoS, an endoglycosidase derived from *Streptococcus pyogenes* that is described to cleave N-glycans specifically at the IgG Fc (Collin & Olsén, 2001). Ten µl of a 1 mg/ml EndoS solution in PBS was added to each well, and the plate was incubated for at least 4 hours at 37°C. Samples were stored at –20°C until further use.

2.2.1.2 Preparation of Ova-Sepharose

The coupling principle is based on the immobilization of primary amines to activated agarose beads by the cyanogen bromide method. The coupling was conducted as described in the manufacturer's manual (GE Healthcare).

In brief, lyophilized agarose beads were resuspended in 1 mM HCl (10 ml per 1 g beads) and transferred to a Maxi Column. The beads were washed with 1 mM HCl and Ovalbumin (Ova) was weighed out and dissolved in coupling buffer to 10 mg/ml. The Ovalbumin solution was then added to the washed beads (1 ml Ova solution to 1 ml beads) and the Maxi Column closed at both ends, at which point the bead-Ova mixture was incubated at 4°C end-over-end overnight. The beads were washed with coupling solution after incubation to rinse residual Ova, after which any uncoupled binding sites on the beads were blocked with blocking buffer for 2 hours at RT. The beads were then washed, alternating three times between wash buffer 1 and wash buffer 2. Ova-coupled Sepharose was stored in 20% ethanol in PBS at 4°C until use.

2.2.1.3 Ova-specific antibody purification and IgG Fc glycan release

One hundred µl of Ova-beads were packed into wells of a 96-well filter plate (Merck, Darmstadt, Germany), and storage solution was removed by applying negative pressure on a vacuum manifold. The Ova-beads were reconstituted by washing three times with 200 µl of PBS, and 100 µl of serum samples were diluted with 100 µl of PBS prior loading and subsequent incubation for 4 hours at RT with agitation on a plate shaker (300 rpm). Afterwards, supernatant (containing serum components including non-Ova-specific IgG) was removed and Ova-beads washed at least five times with 200 µl of PBS. IgG Fc glycans were then released by EndoS. Therefore, 200 µl of a 0.2 x PBS containing 10µg EndoS was

added to each well and incubated for 4 hours at 37°C. Afterwards, the released glycans were collected in a 96 well plate and stored at –20°C for further analysis. IgG was eluted five times with 200 µl of 0.1 M formic acid (pH 2.7), and the beads were washed with three times with 200µl of PBS and stored in 20% ethanol in PBS at 4°C. Purification of Ova-specific IgG was then confirmed by ELISA (Fig. A.2).

2.2.2 IgG Fc glycan analysis by HPLC

2.2.2.1 Graphite purification

After the EndoS glycan release, the glycan samples were desalted and subsequently enriched by graphitized carbon (graphite) purification. The released glycans and proteins were retained by the graphite while other compounds (e.g., salts) were washed away. Acidification was required to neutralize the charged residue and facilitate the binding of sialylated glycans. Elution conditions were adjusted for the preferential elution of glycans (Packer et al., 1998).

Ten µl filter pipette tips were filled with graphite above the filter, and filled tips were inserted into a 96 well centrifuge adapter. All spinning steps were conducted at 500 x g for 30 seconds. After the initial spinning, the graphite tips were washed 5 times with 50 µl of 80% ACN + 0.1% TFA each. Afterwards, the graphite was reconstituted 5 times with 50 µl of 0.1% TFA. The pH of the samples was adjusted to pH 3–4, with 10% TFA solution directly before the sample was added to the graphite. pH for each sample was confirmed with pH indicator paper. Lager sample volumes were added in several 50 µl aliquots. Next, the graphite was washed 5 times with 50 µl of 0.1% TFA, and glycans were subsequently eluted by 3 times 30 µl of 25% ACN + 0.1% TFA. The elution was collected in a 96 well plate and immediately vacuum dried in a vacuum centrifuge. Dried glycans were then stored at –20°C until further use.

2.2.2.2 2-AB labeling

For the detection, graphite purified glycans were labeled with the fluorophore 2-aminobenzamide (2-AB), which was covalently linked to the reducing end of the released glycan via reductive amination, as described previously (Bigge et al., 1995). Sodium cyanoborohydride ($NaBH_3CN$) was used as reducing agent, and 2-AB was solved to 50 mg/ml in a 7:3 (v:v) mixture of DMSO and glacial acetic acid. This solution was then used to solve $NaBH_3CN$ to 60 mg/ml, after which 10 µl of this solution was used per sample. Labeling was done for 2 hours at 65°C with agitation on a plate shaker (300 rpm).

Excessive labeling solution was removed with cellulose chromatography. Therefore, cellulose was filled in 10 µl pipette filter tips, which were inserted into a 96 well centrifuge adapter. All spinning steps were conducted at 500 x g for 30 seconds. Cellulose tips were

washed 8 times with 50 µl of H2O and then reconstituted 5 times with 50 µl of 80% ACN. Labeled samples were mixed with 50 µl of 80% ACN prior to loading on the cellulose. The loaded cellulose was then washed 5 times with 50 µl of 80% ACN to remove excessive labeling solution. Labeled glycans were eluted 3 times with 30 µl of H_2O, after which the elutions were collected in a 96 well plate and subsequently vacuum dried in a vacuum centrifuge. Dried glycans were stored at –20°C until further use.

2.2.2.3 HPLC analysis

The N-glycan distribution of the released and labeled IgG Fc glycans was analyzed via high performance liquid chromatography (HPLC). The labeled glycans were separated via hydrophobicity on a column (hydrophilic interaction liquid chromatography; HILIC), and their fluorescent intensity was measured by a fluorescence detector (FLD). The more hydrophobic groups the glycan has, the longer the retention.

Dried, labeled glycans were reconstituted in an appropriate volume of 80% ACN (at least 10 µl), and at least 5 µl of the sample was transferred into a HPLC vial with a micro-insert and the vial closed with pierceable septum cap.

HILIC-HPLC was performed on a modular Ultimate 3000 instrument equipped with a BEH glycan column. One hundred mM ammonium formate (pH 4.5) was used as eluent A and ACN as eluent B. The column compartment was heated to 60°C, and the autosampler from which the samples were drawn automatically was set to 6°C. Two point five µl of sample were used for analysis, and 80% of the ACN was used as carrier solution. Glycan separation was performed by a linear gradient of 78.0% eluent B to 55.9% eluent B at a flow rate of 0.5 ml/min over the course of 22 minutes. Fluorescence was detected at the FLD at 420 nm (emission) after excitation at 330 nm wavelength. Afterwards, the gradient was set to 100% eluent A within 2 min, and the column was washed with 100% eluent A at a flow of 0.25 ml/min for 5 min. The gradient was then increased together with the flow rate to 78% eluent B and 0.5 ml/min, respectively, within 5 minutes. The column was allowed to reconstitute before next sample could be loaded for 6 minutes. Hence, the total analysis time was 40 minutes per sample.

Respective chromatograms were analyzed with Chromeleon 6 software. Peaks for G0, G0GNAc, G1, G1GNAc, G2, G2GNAc, G1S1, G2S1 and G2S2 were assigned by retention time. The area of each peak was integrated by the software and the relative fraction of each peak calculated by dividing the area of the peak by the sum area of all nine assigned peaks. The following traits were calculated by the sum of the relative fractions: agalactosylated/G0 (G0+G0GNAc), sialylated (G1S1+G2S1+G2S2) or bisection (G0GNAc+G1GNAc+ G2GNAc). Bisection was only observed in the analysis of human IgG.

2.2.3 IgG Fc glycan analysis by LC-MS

The Fc glycan analysis by Liquid Chromatography-Mass Spectrometry (LC-MS) is based on the analysis of respective glycopeptides after tryptic digestion of purified IgG. Glycopeptides for human IgG1, IgG2/3 and IgG4 could be discriminated. For C57BL/6 murine IgG, glycopeptides for IgG1, IgG2(b and c) and IgG3 could be discriminated. The analysis was performed by the PhD student in our laboratory, Alexander Wagt, at the Center for Proteomics and Metabolomics (Prof. Manfred Wuhrer), Leiden University Medical Center, Leiden, the Netherlands (Selman et al., 2012b; Haan et al., 2017) .

For the analysis, relative fractions of glycopeptides containing agalactosylated glycans (G0), sialylated glycans (sialylation), bisected glycans (bisection) or fucosylated glycans (fucosylation) were summed for the individual subclasses. Afucosylated glycans were under the detection limit for all mouse and human IgG4 analysis. Not all subclasses were observed for all samples, and in general, IgG1 gave the best signal for both human and mouse samples.

2.2.4 Mouse handling

2.2.4.1 Immunizations

If not otherwise indicated, mice were immunized by intraperitoneal (i.p.) injections of 200 µl of the prepared Ova-Adjuvant mixtures. Before the mixture with the adjuvant, Ova was dissolved to 1 mg/ml in PBS.

2.2.4.1.1 Ova-eCFA

Enriched Complete Freund's Adjuvant (eCFA) was prepared by adding 100 mg heat killed mycobacteria tuberculosis (Mtb.) to 20 ml incomplete Freund's adjuvant (IFA). Ova-eCFA emulsions were prepared by syringe mixing on the day of injection, and two syringes were filled with equal volumes of either Ova-solution or eCFA. The two syringes were connected via a 3-way-stopcock. Air-bubbles were removed beforehand as good as possible. Watery Ova-solution was then pushed into the eCFA oil phase. Emulsification was performed by repeatedly pushing the mixture from one syringe into the other (> 50 times). The emulsification was completed when a drop of the emulsion did not dissolve in water (water drop method; (Dvorak & Dvorak, 1974)). Two hundred µl of the emulsion corresponded to 100 µg Ova and 500 µg mycobacteria.

2.2.4.1.2 Ova-Alum

Alum was added dropwise into an equal total volume Ova-solution while vortexing. Afterwards, the mixture was incubated for 2 hours of end-over-end shaking at 4°C to allow the Ova to be absorbed into the Alum. Two hundred µl of the mixture correspond to 100 µg Ova and ~1 mg aluminum.

2.2.4.1.3 Ova-LPS

Three hundred µg/ml LPS from an *Escherichia coli* stock-solution was prepared by dissolving LPS in PBS, and equal volumes of LPS stock and Ova-solution were mixed. Two hundred µl of the mixture correspond to 100 µg Ova and 30 µg LPS.

2.2.4.1.4 Ova-MPLA

MPLA was dissolved in DMSO for a stock of 1mg/ml, and for injection, the MPLA stock was diluted 1:10 in PBS, and this solution equally mixed (v:v) with Ova-solution. Two hundred µl of the mixture correspond to 100 µg Ova and 10 µg MPLA.

2.2.4.2 Serum collection

On the indicated day, mice were anesthetized with a solution of Ketamine/Xylazine i.p. (80mg/kg Ketamin and 10mg/kg Xylazin), and the final blood collection was conducted via heart puncture. A 23G needle was pushed through the sternum, and the correct position was indicated by aspirated blood flows (Hoff, 2000), with as much blood as possible being collected. The mice were sacrificed by cerebral dislocation immediately after blood collection. Blood was drawn into serum gel tubes and allowed to coagulate for at least 20 minutes. Tubes were spun at 4,000 g for 5 minutes and the serum was pipetted into a tube. Until further use, the serum was stored at –20°C.

2.2.5 Ova-specific ELISA

For Ova-specific ELISA, 50 µl/well of 10 µg/ml Ova was coated on a high binding ELISA plate, which was then either incubated for 2 hours at RT or overnight at 4°C. After incubation, each well was washed 4 times with 100 µl of PBST, and unspecific binding sites were blocked for 1 hour with 100 µl of ELISA buffer. Samples were diluted in ELISA buffer, and 50 µl per well was incubated for 1 hour at RT. After washing with PBST, 50 µl of the respective HRP-labeled secondary antibody against the various mouse Ig isotypes or IgG subclasses was added to each well in a 1:5,000 dilution and incubated for another hour at RT. After washing with PBST, 50 µl of freshly prepared TMB substrate was added to each well. The reaction was stopped with 0.5 M sulfuric acid after the appropriate interval. Absorption at 450nm wavelength was then measured on an ELISA plate reader.

2.2.6 Cytokine multiplex assay

IL-6, IL-10, IL-12p40, IL-17A, IL-17F, IL-21, IL-22, IL-23p19, IFNγ and TNFα were measured via Legendplex^{TM} cytokine assay, which has the ability to measure all cytokines simultaneously. Anti-cytokine-antibodies are immobilized on specific beads, and for each cytokine, the beads differ in size or fluorescent intensity, or both, in the APC channel. After binding to the beads, the cytokines are detected by a secondary antibody that is coupled to

PE. Hence, cytokine concentration correlates with fluorescent intensity in the PE channel and is calculated by a standard curve.

The cytokines analyzed here where measured with the pre-defined mouse Th17 panel, to which IL-12p40 and IL-23p19 were added. First, a bead master mix was pipetted. Per sample, 0.61 µl of each cytokine bead and 1.9 µl 1x assay buffer were required. The Th17 kit standard and the Cytokine panel 2 standard that contains IL-12p40 and IL-23p19 were reconstituted with 125 µl of assay buffer to generate a 2-fold stock. The two standard stocks were mixed 1:1 directly before use, after which the standard solution that was generated was diluted 1:4, 1:16, 1:64. 1:256, 1:1024 and 1:4096 in a serial dilution with the assay buffer. The assay was performed in a 96 well plate. Before use, the detection antibodies of the Th17 kit and the Cytokine panel 2 kit were mixed 1:1.

For the cytokine standard probe, 8 µl of the provided Matrix B were added together with 8 µl of the respective standard, 8 µl of beads master mix and 8 µl of detection antibody mixture. For the serum samples, 12 µl of assay buffer was added in each well together with 4 µl of sample, 8 µl of beads master mix and 8 µl of detection antibody mixture. The plate was then covered and incubated overnight in the dark. The next day, 8 µl of streptavidin-PE was added to each well and the samples incubated for 30 minutes on a plate shaker with agitation (300 rpm). Afterwards, the plate was centrifuged at 1,000g for 5 minutes and the supernatant discarded. The beads were then resuspended in 200 µl of 1 x wash buffer and centrifuged again at 1,000g for 5 minutes. The supernatant was removed and the beads resuspended in 150 µl of wash buffer. A MACSQuant Analyzer flow cytometer equipped with a plate reader was used to analyze 70 µl of the beads.

The standard curve and concentration of the serum sample were analyzed with Legenplex Software version 8.

2.2.7 Flow cytometry

Single cell suspensions of freshly collected organs were prepared by carefully meshing the organ through a 70 µm cell strainer into a 50 ml tube. The strainer was washed with 15 ml PBS and the cells subsequently centrifuged at 340 g for 6 minutes at 4°C. The supernatant was discarded and the cell pellet dissolved with 5 ml of Erylysis buffer and the samples incubated for 5 minutes at RT. The erylylsis buffer was than diluted with 20 ml PBS and the cells spun down at 340 g for 6 minutes at 4°C. The supernatant was discarded and the cell pellet dissolved in 1 ml FACS buffer. The cell concentration was estimated by flow cytometry using a 1:20 (10 µl + 190 µl PBS) dilution of this suspension.

2.2.7.1 Anti-St6gal1 antibody labeling

Anti-St6gal1 polyclonal IgG was coupled with an Alexa Fluor 488 Abs labeling kit according to manufacturer's protocol. In brief, 100 µg of the lyophilized anti-St6gal1 IgG was reconstituted with 100 µl 0.1 M ammonium bicarbonate. This solution was then transferred to a vial containing the activated Alexa Fluor 488 (AF488) dye. The vial was closed and inverted until the dye was completely dissolved, and the reaction was allowed to occur for 1 hour at RT in the dark. To quench the remaining active groups from the dye, 50 µl of 1 M Tris (pH 8) was added, and the solution was allowed to incubate in the dark at RT for another 20 minutes. Afterwards, 350 µl of FACS buffer was added, and hence, the final concentration of the AF488 labeled anti-St6gal1 antibody was 0.2 mg/ml. Until further use, the labeled antibody was stored at 4°C in the dark. The specificity and binding pattern was confirmed by ELISA and confocal microscopy (Fig. A.3).

2.2.7.2 B cell staining

B cells were stained for markers of plasma cells (CD138) and GC B cells (B220+, GL7+, FAS+). Cells were further characterized by staining for IgG, IgG1 and IgM as well as for St6gal1and the ability to bind to Ova.

The volume corresponding to 5 x 10^6 splenocytes of the prepared cell suspension was transferred into a 96 well plate. The cells spun down (340g for 6 min at 4°C) and the supernatant discarded by inverting the plate on a tissue. For the staining of extracellular markers, the cell pellet was resuspended with 100 µl of a master mix containing the following antibodies and reagents in FACS buffer using a multichannel pipet:

Tab. 2.1 Antibodies and reagents used for extracellular staining of B cells

Marker	Dye	Dilution
Fixable-viability dye	eFluor 780	1:1000
B220	BV786	1:200
CD138	BV711	1:200
GL7	PerCP-Cy5.5	1:200
FAS	BV510	1:200
IgG	Pe	1:200
IgG1	BV421	1:200
IgM	Pe-Cy7	1:500
Ova	AF647	1:500

Cells were stained for 20 minutes on ice in the dark. 200 µl of FACS buffer was added afterwards and the cells spun down, as above. The supernatant was discarded, and the cell pellet resuspended in 200 µl of a Cytofix/Cytoperm fixation buffer. The plate was incubated for at least 30 minutes at RT in the dark. Afterwards, 150 µl of PermWash buffer was added and the cells spun down. The supernatant was discarded and the cell pellet was resuspended

with 100 µl of a master mix containing the following antibodies/reagents for intracellular staining in PermWash buffer:

Tab. 2.2 Antibodies and reagents used for intracellular staining of the B cells

Marker	Dye	Dilution
IgG	Pe	1:200
IgG1	BV421	1:200
IgM	Pe-Cy7	1:500
Ova	AF647	1:500
St6gal1	AF488	1:50

Cells were stained for 30 minutes on ice in the dark, after which 200 µl PermWash buffer was added and the cells spun down, as above. The cells were washed two additional times with 200 µl PermWash buffer before they were resuspended in 200 µl FACS buffer, at which point the samples were measured with an Attune flow cytometer.

2.2.7.3 Foxp3- T follicular helper and Foxp3+ T follicular regulatory cell staining

The volume corresponding to 2.5 x 10^6 splenocytes of the prepared cell suspension was transferred into a 96 well plate. The cells were spun down (340 g for 6 min at 4°C) and the supernatant discarded. For the extracellular T cell marker staining, the cell pellet was resuspended with 100 µl of a master mix containing the following antibodies and reagents in FACS buffer using a multichannel pipet:

Tab. 2.3 Antibodies and reagents used for extracellular staining of the Foxp3 T cell panel

Marker	Dye	Dilution
Fixable-viability dye	eFluor 780	1:1000
B220	BV786	1:200
CD4	BV711	1:200
CD8	AF700	1:200
ICOS	Pe-Cy7	1:100
CXCR5	Biotin	1:100

The cells were stained for 45 minutes on ice in the dark, after which 200 µl FACS buffer was added and the cells spun down, as above. The supernatant was discarded, and the cell pellet was resuspended in 100 µl of the FACS buffer containing Strepavidin-BV605 (dilution 1:100). The cells were incubated for 20 minutes, and 200 µl of FACS buffer was afterwards added. After spinning, the supernatant was discarded and the cells fixed with 200 µl of TrueNuclear™ fixation solution, which was freshly prepared by diluting the fixation stock 1:4 with the respective diluent. The cells were incubated for 1 hour at RT in the dark before being spun down and washed three times with 200 µl of 1 x eBioscience™ Foxp3 Perm buffer. The cells were then stained with 100 µl of Foxp3 Perm buffer containing antibodies for FoxP3-AF647 (1:200) and Rorγt-BV421 (1:100). The staining was incubated for 45

minutes at RT in the dark, after which 200 µl of the Foxp3 perm buffer was added and the cells spun down. The supernatant was discarded and the cells washed two additional times with 200 µl of the Foxp3 perm buffer before the cells were resuspended in 200 µl of FACS buffer and subsequently measured at the Attune flow cytometer.

2.2.7.4 T cell cytokine staining

The production of cytokines by T cells was analyzed upon *in vitro* stimulation with ionomycin and Phorbol-12-myristat-13-acetat (PMA). Cytokine secretion was inhibited with the protein transport inhibitors Brefeldin A and Monensin.

10×10^6 splenocytes were seeded in 3 ml T cell medium supplemented with 500 ng/ml PMA, 1 µg/ml Ionomycin, 5 µg/ml Brefeldin A and 2 µM Monensin in a 6-well suspension culture plate. The cells were incubated for 5 hours at 37°C and 5% CO_2, after which they were collected in a 15 ml tube and spun down (340 g, 6 minutes at 4°C). The supernatant was then discarded and the resuspended pellets transferred into a 96 well plate. After another centrifugation step, the supernatant was again discarded and the cells resuspended in 100 µl of a master mix containing the following antibodies and reagents in FACS buffer using a multichannel pipet:

Tab. 2.4 Antibodies and reagents used for extracellular staining of the Cytokine T cell panel

Marker	Dye	Dilution
Fixable-viability dye	eFluor 780	1:1000
B220	BV786	1:200
CD3	AF488	1:200
CD4	BV711	1:200
CD8	AF700	1:200
ICOS	Pe-Cy7	1:100
CXCR5	Biotin	1:100

The cells were stained for 45 minutes on ice in the dark, after which 200 µl of FACS buffer was added and the cells spun down as above. The supernatant was then discarded and the cell pellet resuspended in 100 µl of FACS buffer containing Strepavidin-BV421 (dilution 1:100). The cells were incubated for 20 minutes and 200 µl of FACS buffer subsequently added. After spinning, the supernatant was discarded and the cells fixed with 200 µl of Cytofix/Cytoperm for 30 minutes at RT. Hereafter, 150 µl PermWash buffer was added and the cells spun down. The supernatant was discarded and the cell pellet was resuspended with 100 µl of a master mix containing the following antibodies and reagents for intracellular staining in PermWash buffer:

Tab. 2.5 Antibodies and reagents used for intracellular staining of the Cytokine T cell panel

Marker	Dye	Dilution
CD3	AF488	1:200
CD4	BV711	1:200
IL-17A	Pe	1:200
IFNγ	AF647	1:200

The cells were stained for 30 minutes on ice in the dark, after which 200 µl of PermWash buffer was added and the cells spun down as above. The cells were then washed two additional times with 200 µl of PermWash buffer before they were resuspended in 200 µl of FACS buffer. The samples were then measured with an Attune flow cytometer.

2.2.8 Statistical analysis

Statistical analysis was performed using GraphPad Prism version 6.0. Normal distribution was assumed, and differences between two normally distributed groups were analyzed by two-tailed t-tests. Comparison of more than two groups was performed by One-way Analysis of Variance (ANOVA). $P < 0.05$ was considered as an indicator of significant difference (*$P < 0.05$, **$P < 0.01$, ***$P < 0.001$ and **** $P<0.0001$). Unless otherwise stated, murine data were taken from one representative out of at least two individual experiments or combined from multiple experiments. The bar graphs are presented as the mean and error bars indicate the standard error of the mean (+ SEM). For St6gal1 expression levels, the median fluorescent intensities of the respective population in the St6gal1 channel was calculated for the individual samples by FlowJo. The mean (+ SEM) of the individual MFIs per group is shown in the figures.

3 Results

3.1 Analysis of the IgG Fc glycan

The effector function of IgG antibodies depends on their subclass and Fc glycosylation pattern. Inflammatory disease conditions in patients with autoimmune diseases are associated with agalactosylated IgG antibody enrichment, whereas galactosylated and terminal sialylated IgG antibodies are associated with less inflammatory conditions and can even have anti-inflammatory functions (Collin & Ehlers, 2013; Kaneko et al., 2006; Anthony et al., 2011; Pagan et al., 2018; Bartsch et al., 2018). Likewise, a more protective effector function has been suggested of vaccine-induced agalactosylated and asialylated IgG (Ackerman et al., 2013; Alter et al., 2018).

Several methods to analyze IgG glycosylation have been developed depending on specific requirements and conditions (e.g., equipment, sample size) (Huffman et al., 2014). In our laboratory, a HPLC-based method was established to analyze human or murine IgG Fc glycans (Fig. 3.1). This method was further improved here, and a workflow developed to process and analyze 96 samples simultaneously. The IgG Fc N-glycans were enzymatically released from purified IgG antibodies by EndoS – an endoglycosidase that is specific to IgG Fc parts but not for Fab glycosylation or other immunoglobulin isotypes (Collin & Olsén, 2001; Vanderschaeghe et al., 2018).

During the HPLC analysis, glycans were separated in an analytical column due to their hydrophobicity. The more hydrophobic groups the glycan have, the better the interaction with the column and the longer the retention time. As a rule of thumb, the more sugars are attached (the larger the glycan is), the later it is detected at the fluorescent detector (Fig. 3.1).

The IgG Fc glycan is a biantennary complex type N-glycan that is attached to asparagine (N) 297 of both heavy chains of the IgG protein. It consists of a core structure consisting of 4 GlcNAcs and three mannoses (G0) that can be further prolonged by adding galactose (G1, G2) and sialic acid (G1S1, G2S1, G2S2) to the antenna (Fig. 1.2). The first GlcNAc can be modified by adding fucose, and the branching mannose can carry a “bisecting” GlcNAc (bisection). Interestingly, bisection was observed in humans but scarcely at all in mice (Fig. 3.1). Aside from the lack of bisecting glycans in the mouse IgG chromatogram, mouse and human chromatograms differed considerably in the retention times for sialylated glycan species. In mice, N-acetylneuraminic acid (Neu5Ac) is enzymatically converted into N-glycolylneuraminic acid (Neu5Gc). Humans acquired a loss of function mutation in the gene of the responsible enzyme, that is, CMP-N-acetylneuraminic acid hydroxylase (Brinkman-

Van der Linden et al., 2000). Hence, in humans, sialylation occurs only with Neu5Ac, whereas in mice only Neu5Gc is detectable. Due to an additional hydroxyl group (-OH) in Neu5Gc compared to Neu5Ac, the respective murine glycans are retained longer during HPLC.

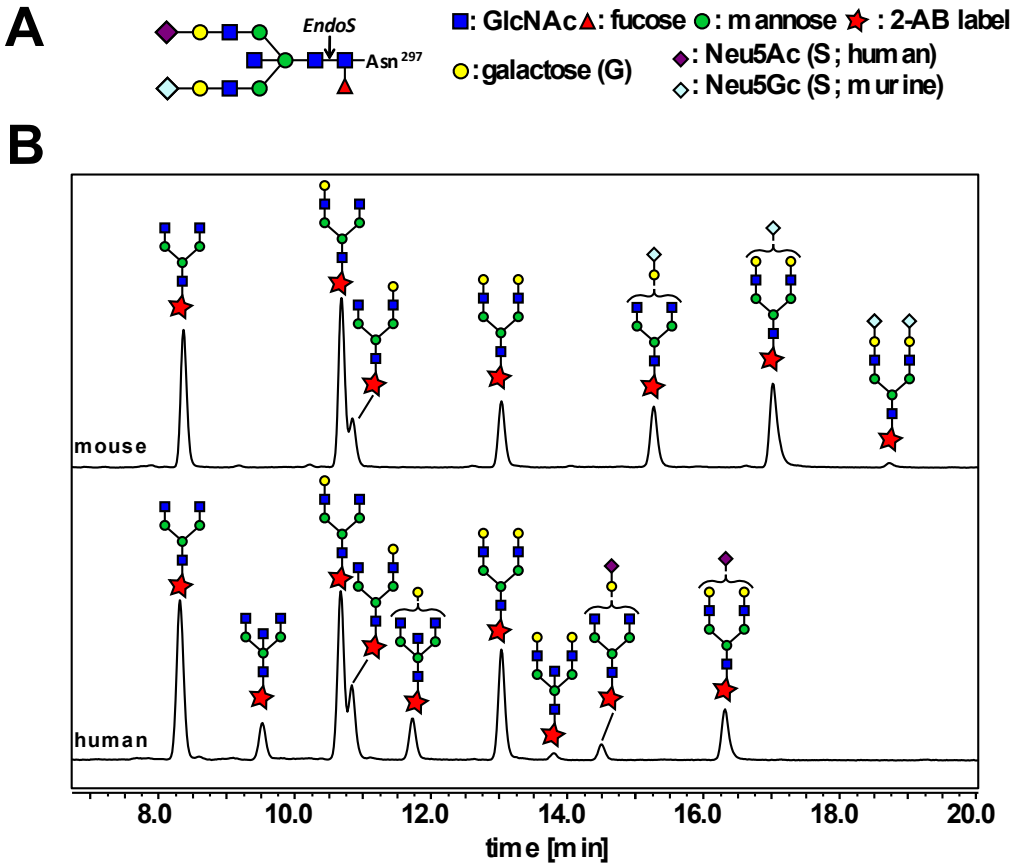

Fig. 3.1 ***Representative HILIC-HPLC IgG glycan analysis after EndoS release and subsequent 2-AB labeling from mouse or human serum IgG****. (A) The IgG Fc glycan is a complex type biantennary glycan. The core structure consists of four N-Acetylglucosamines and three mannoses. The arms can be furthered modified with galactose and sialic acid. Fucosylation can be found on the first GlcNAc and a bisecting GlcNAc on the branching mannose. The EndoS hydrolysis site between the first and second GlcNAc is indicated by the arrow. (B) Serum IgG of either mouse (C57BL/6; upper chromatogram) or human (lower chromatogram) was purified by Protein G and the EndoS released IgG Fc glycan labeled with 2-AB. Glycan composition was then measured by HILIC-HPLC. G0, G1 and G2 was measured for both species. Bisection was only observed in humans. Sialylation with N-Glycolylneuraminic acid (Neu5Gc) or with N-Acetylneuraminic acid (Neu5Ac) was observed in mice and humans, respectively. For humans, IgG bi-sialylation was only observed in traces.*

For example, the IgG Fc glycosylation patterns of pre-term infants of different gestational ages were analyzed. Pre-term infants with extremely low gestational ages (born after < 28 weeks of gestation) had decreased proportions of galactosylated, sialylated and bisecting N-Acetylglucosamine-containing IgG Fc glycans compared to preterm infants born after ≥ 28 weeks of gestation and term infants. Interestingly, early pre-term infants have higher susceptibility to the development of chronic inflammatory bronchopulmonary dysplasia

(BPD). Increased non-galactosylated IgG Fc was associated with the development of BPD (Fig. A. 4).

These experiments were published in Twisselmann N*, Bartsch YC*, Pagel J, Wieg C, Hartz A, Ehlers M and Härtel C. IgG Fc glycosylation patterns of preterm infants differ with gestational age. *Frontiers in Immunology*, 2019 (*these authors contributed equally).

3.1.1 Altered IgG Fc glycosylation pattern in CTLA4-deficient individuals

The above described establishment of a high throughput analysis allowed the measurement of large quantities of samples as shown here in the analysis of 14 human CTLA4 (cytotoxic T-lymphocyte-associated Protein 4) mutation carriers, which were prone, for example, to developing inflammatory autoimmune diseases compared to a total of 110 healthy human control samples.

CTLA4 is a receptor that is expressed on different T cell subsets and is described as an inhibitory receptor. This receptor is particularly important for the function of regulatory Foxp3+ T helper cells (Tregs), for example, in suppressing B cell responses (Wing et al., 2008; Sage et al., 2014). Hence, the question of whether CTLA4 deficiency affects IgG Fc glycosylation in humans should be investigated here.

Tab. 3.1:The IgG Fc glycosylation of 14 individuals from five different families with different types of CTLA4 mutation was investigated. The mutations are shown at the cDNA (c.X) and protein (p.X) level. The number indicates the position and the change is given in a single letter code for nucleotides or amino acids, respectively (= premature stop codon). IBD = inflammatory bowel disease. The samples were analyzed in cooperation with Bodo Grimbacher (University of Freiburg, Freiburg, Germany) (Schubert et al., 2014; Schwab et al., 2018).*

Family	mutation	identifier	age	gender	primary diagnosis
A	c.105C > A; p.C35*	A.II.10	50	m	unaffected
		A.II.3	58	f	unaffected
		A.III.1	27	f	neurological symptoms due to non-caseating brain granulomas
		A.III.5	22	f	unaffected
		A.III.6	19	f	unaffected
B	c.110+1G > T intron 1 splice donor site	B.II.1	56	f	unaffected
		B.II.3	50	m	Hodgkin lymphoma
		B.II.4	43	f	IBD
		B.III.3	17	f	unaffected
C	c.208C > T p.R70W	C.II.4	12	f	unaffected
G	c.347T > C p.I116T	GG.I.1	46	m	unaffected
		GG.II.2	17	m	unaffected
		GG.II.3	13	f	unaffected
H	c.407C > T p.P136L	H.I.2	52	f	IBD

The CTLA4 deficiency is hereditary, and individuals from five different families with different types of mutation were investigated (Tab. 3.1). Although these patients still had an intact variant of their *CTLA4* gene, reduced CTLA4 protein expression levels were observed (Schwab et al., 2018). The symptoms were diverse and range from hypogammaglobulinemia to inflammatory syndromes like inflammatory bowel disease (IBD) to higher prevalence for certain cancers (e.g., Hodgkin lymphoma). However, the onset of disease or whether a mutation carrier was affected at all varied considerably between individuals and was not linked to a certain type of mutation (Schubert et al., 2014; Schwab et al., 2018). At the time of serum sampling, patients were not under immunosuppressive therapy or receiving therapeutic antibodies that could interfere directly with the measurement. As healthy controls, serum samples of 30 children with unrelated non-inflammatory diseases (age range: 8-20y, median age:13.5y, male:female ratio: 1:1) were kindly provided by Christoph Härtel (Clinic for Pediatrics, UKSH Lübeck, Lübeck, Germany). In addition, serum samples from 80 healthy adults (age range: 25–59y, median age: 39.5y, male : female ratio: 1:1) from the Popgen cohort (Wolfgang Lieb, UKSH Kiel, Kiel, Germany) were used.

3.1.1.1 HILIC-HPLC analysis of total IgG Fc glycans

The IgG Fc glycan from purified serum IgG of CTLA4 mutants or healthy controls was released by EndoS and, after subsequent 2-AB labeling, analyzed by HILIC-HPLC. The analysis revealed significant differences between the two groups (Fig. 3.2). CTLA4 mutants had a higher degree of agalactosylated (G0) and bisected (bisection) IgG Fc glycans and a lower degree of sialylated IgG Fc glycans compared to the controls. Higher proportions of G0 as well as lower sialylation are linked to more pro-inflammatory IgG glycosylation. The data indicate that the deficiency in CTLA4 may lead to more pronounced inflammation that is reflected in the IgG glycosylation pattern.

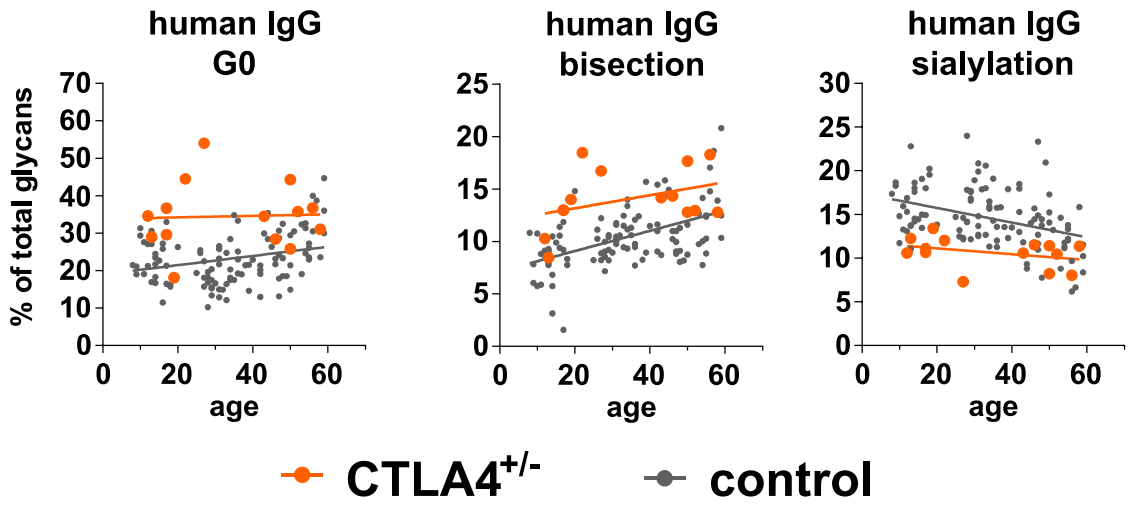

Fig. 3.2 ***IgG Fc glycosylation is altered in patients with heterozygous deficiency in the* CTLA4 *allele****. Serum IgG of 14 CTLA4 mutation carriers and 110 matched controls was purified with Protein G, and the EndoS released IgG Fc glycan was labeled with 2-AB and subsequently analyzed via HILIC-HPLC. Depicted are the percentages of G0, bisected and sialylated IgG against the age of the individual subjects. The lines show a linear regression analysis. Statistical significance between the groups was observed for all glycan traits by a moderated t-test correcting for gender and age ($p < 0.05$; calculation was performed in cooperation with Hauke Busch, University of Lübeck, Lübeck, Germany).*

3.1.1.2 LC-MS analysis of IgG subclass Fc glycans

To verify the results obtained by HILIC-HPLC, the IgG Fc subclass glycosylation of the same serum samples of the CTLA4 deficient families and the controls were analyzed via an independent liquid-chromatography-coupled mass spectrometry (LC-MS) system (Fig. 3.3). Similar to the HPLC method, IgG was purified from serum by protein G. In contrast to the EndoS glycan release, IgG was proteolytically cleaved into smaller peptides by Trypsin. The generated peptides were than subject to the LC-MS analysis (Tab. 3.2). During the LC part, glycopeptides were separated from non-glycosylated peptides by C18 column. The eluted glycopeptides were then analyzed for their mass to charge (m/z) value by the coupled MS. The glycopeptides for different IgG subclasses possess different amino acid sequences, which allows the discrimination of the signals for the different subclasses; however, the sequences of the IgG2 and IgG3 glycopeptides are identical, meaning that both glycopeptides have the same mass and could not be distinguished from each other (Wuhrer et al., 2007).

Tab. 3.2 Human IgG subclass glycopeptides detected by LC-MS, noting whether the different subclass glycopeptide for the depicted glycan structure was detected (yes) or not detected (n.d.). G0 = agalactosylated, G1 = mono-galactosylated, G2 = bi-galactosylated, S1 = mono-sialylated, S2 = bi-sialylated, F = fucosylated, B = bisected. The expected glycan structures are depicted: blue square = N-Acetylglucosamine, green circle = Mannose, yellow circle = Galactose, purple diamond = Neuraminic acid (sialic acid), red triangle = Fucose.

Glycan	Group	Structure	IgG1	IgG2/3	IgG4
G0	G0	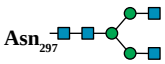	YES	YES	n.d.
G0F		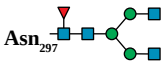	YES	YES	YES
G0B		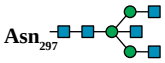	YES	n.d.	n.d.
G0BF		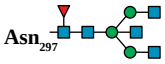	YES	YES	YES
G1	G1	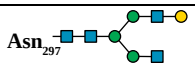	YES	YES	n.d.
G1F		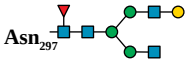	YES	YES	YES
G1B		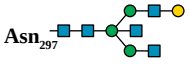	YES	n.d.	n.d.
G1FB		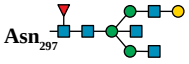	YES	YES	YES
G2	G2	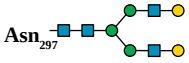	YES	YES	n.d.
G2F		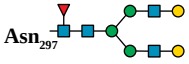	YES	YES	YES
G2BF		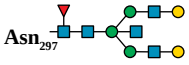	YES	YES	YES
G1FS1	G1S1	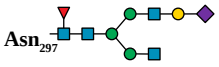	YES	YES	YES
G1BFS1		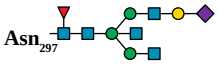	YES	YES	YES
G2S1	G2S1	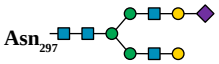	YES	YES	n.d.
G2FS1		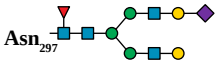	YES	YES	YES
G2BFS1		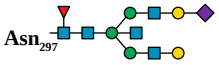	YES	n.d.	n.d.
G2FS2	G2S2	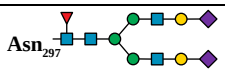	YES	YES	n.d.

The LC-MS analysis revealed significant differences in the IgG Fc glycosylation for G0, bisection and sialylation among all subclasses (Fig. 3.3). In addition, the degree of fucosylation on IgG1 and IgG2/3 appeared to be lower in the CTLA4 group. This modification, however, could not be analyzed by the HPLC analysis, because after EndoS release, the first GlcNAc to which fucose is linked remained on the protein backbone. IgG4 together with IgG3 usually occur much less frequently compared to IgG1 and IgG2 in normal human serum (Vidarsson et al., 2014). The low proportion of IgG4 glycopeptides could therefore only be analyzed for some samples. Furthermore, some spectra had to be excluded

from analysis due to signals that were too low, which proved an issue for non-fucosylated IgG4 glycopeptides as well. Therefore, only fucosylated IgG4 glycopeptides were analyzed.

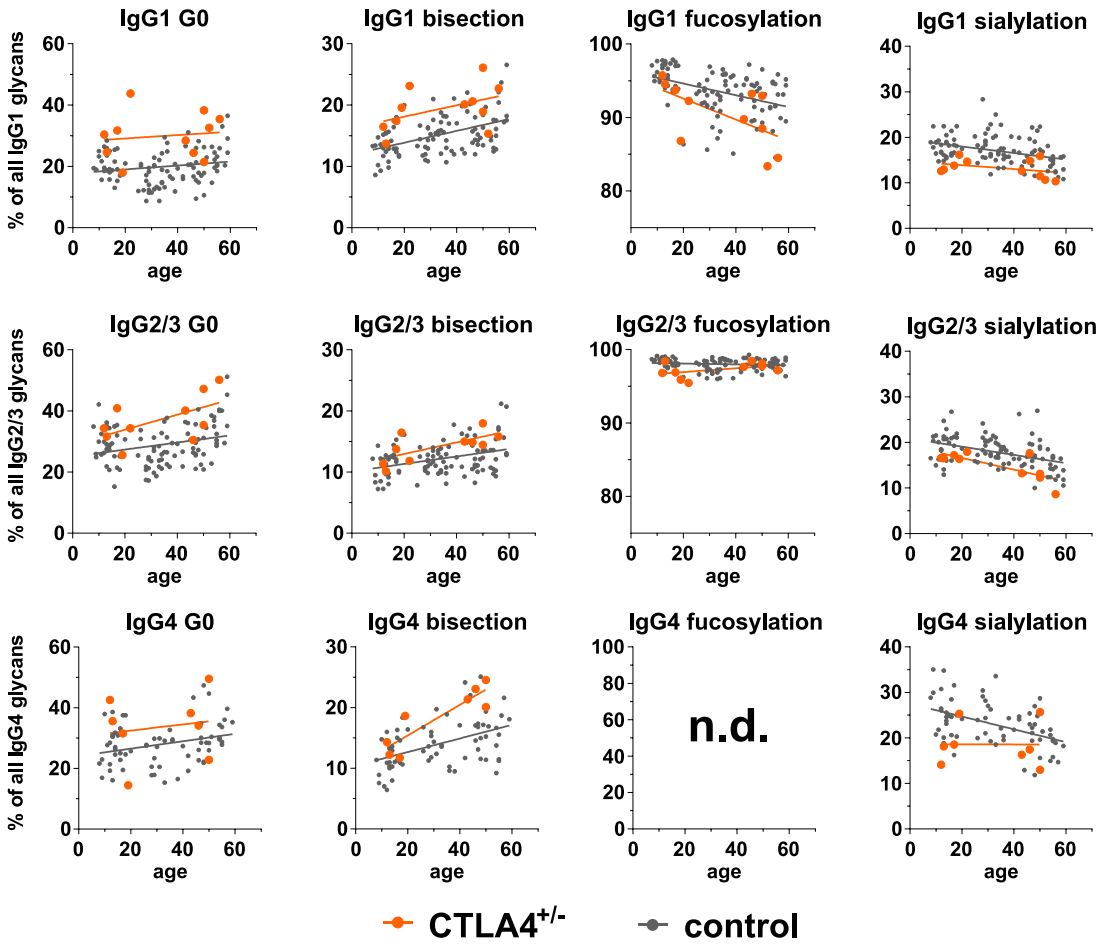

Fig. 3.3 ***Confirmation of the IgG Fc glycosylation profile observed with HILIC-HPLC by LC-MS****. IgG glycosylation of serum samples of CTLA4 mutation carriers and controls that were analyzed by HILIC-HPLC were re-analyzed by LC-MS. After protein G purification IgG samples were trypsinized and glycopeptides analyzed by LC-MS. Depicted are the percentages for G0, bisected, fucosylated and sialylated IgG1, IgG2/3 and IgG4, respectively. Fucosylation could technically not be determined for IgG4 (n.d. = not determined). Statistical significance between the groups was observed for all glycan traits and subclasses (except IgG4 fucosylation) by a moderated t-test correcting for gender and age (and the calculation was performed in corporation with Hauke Busch, University of Lübeck). The LC-MS analysis was done by the PhD student in our laboratory, Alexander Wagt, at the Center for Proteomics and Metabolomics (in collaboration with Manfred Wuhrer), Leiden University Medical Center, Leiden, the Netherlands.*

The IgG Fc glycosylation patterns of IgG1 and IgG2/3 were comparable, while IgG4 tended to be slightly more galactosylated and sialylated compared to IgG1 and IgG2/3. However, as mentioned, IgG4 is the least common subclass, and its contribution to the overall (bulk) glycosylation pattern is minimal. Consistently, the G0, bisection and sialylation values for IgG1 and IgG2/3 were comparable to the results obtained for bulk IgG by HPLC (Fig. 3.2 and Fig. 3.3).

Thus, the IgG (subclass) Fc glycosylation pattern of CTLA4 mutations carriers showed less galactosylation and sialylation compared to healthy controls, which might contribute to an enhanced risk of developing inflammatory autoimmune diseases. Furthermore, the results suggest that CTLA4 is directly or indirectly involved in the regulation of IgG Fc glycosylation.

3.1.2 Fc glycosylation of normal C57BL/6 mouse serum IgG

To further analyze the development of differently Fc glycosylated IgG antibodies, mouse IgG Fc glycosylation was analyzed. At first, serum was taken from naïve C57BL/6 WT mice and IgG-Fc glycosylation analyzed by HPLC and LC-MS.

The HPLC analysis was performed on EndoS-released IgG glycans without discrimination of IgG subclasses. By contrast, the LC-MS glycopeptide analysis allowed discrimination between the murine IgG subclasses. The sequences of the IgG2b and IgG2c glycopeptides differed only in isoleucine and leucine, respectively (Haan et al., 2017). Accordingly, the observed mass was equal between both glycopeptides and could not be discriminated here. In contrast to the human analysis, pronounced differences were observed in galactosylation and sialylation of the Fc part among the different murine IgG subclasses. IgG2b/c was heavily galactosylated and sialylated, whereas IgG1 was mostly agalactosylated. Naïve IgG3 glycosylation was between the levels of IgG1 and IgG2b/c (Fig. 3.4), as were the galactosylation and sialylation levels observed by HPLC analysis (Fig. 3.4). Afucosylated or bisected murine IgG glycans were not detected in all samples investigated in this thesis.

The frequencies of the IgG subclasses were calculated under the assumption that the signal intensity in the LC-MS analysis was proportional to the quantity of the corresponding subclass. Interestingly, ~60% of the serum IgG was IgG2b/c, followed by ~35% IgG1 and ~5% IgG3 (Fig. 3.4).

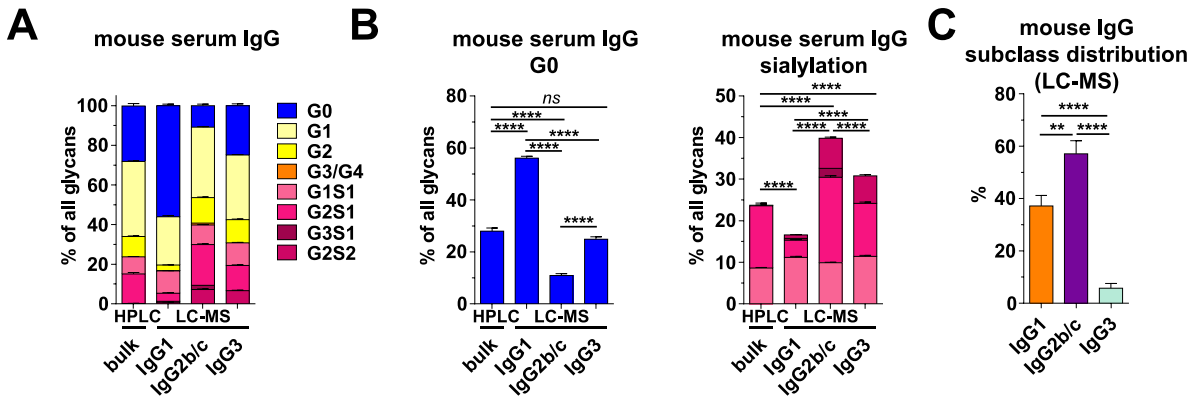

Fig. 3.4 ***IgG subclasses are differently glycosylated in naïve C57BL/6 WT mice****. IgG from serum of naïve C57BL/6 WT mice was purified by Protein G. The Fc glycosylation of EndoS-released glycans or trypsinized glycopeptides were analyzed by HILIC-HPLC or LC-MS, respectively. (A) Glycosylation profile of bulk IgG as determined by HPLC (n = 24) or of IgG1, IgG2b/c and IgG3 subclasses as determined by LC-MS (n = 20). Mouse IgG showed no bisection and non-fucosylated IgG Fc glycans. In contrast to the human analysis, traces of G3, G4 and G3S1 peaks were detected. (B) Percentages of G0 and sialylated glycans of bulk IgG (HPLC) and corresponding IgG subclass glycopeptides (LC-MS). (C) The subclass distribution of normal serum IgG was calculated by the dividing the intensities of the observed signals for IgG1, IgG2b/c and IgG3 in the LC-MS analysis by the sum of all these intensities. The LC-MS analysis was conducted by the PhD student in our laboratory, Alexander Wagt, at the Center for Proteomics and Metabolomics (in collaboration with Manfred Wuhrer), Leiden University Medical Center, Leiden, the Netherlands.*

3.1.3 Immunization with different adjuvants leads to distinct IgG glycosylation patterns

Previously, it had been suggested that the type of immune response might influence the induction of the IgG Fc glycosylation pattern (Selman et al., 2012a; Hess et al., 2013). Here, the serum IgG Fc glycosylation pattern was analyzed after vaccination with the model antigen Ova and different adjuvants. The advantages of the Ova-model are that it is a foreign protein that is not expressed by mice and that Ova-specific antibodies can be easily purified, which allows analysis of antibodies that developed entirely due to the vaccination stimulus. Complete Freund's adjuvant with enhanced content of mycobacteria (5 mg/ml; eCFA) and lipopolysaccharide (LPS) were already established for immunizations in the laboratory. Additionally, the adjuvants Monophosphoryl Lipid A (MPLA; an LPS derivate) and aluminum hydroxide (Alum) were tested, as these are currently licensed for vaccine preparations in humans (Tab. 1.1).

C57BL/6 wildtype (WT) mice were immunized intraperitoneally (i.p.) and serum samples taken 14 days later. The analysis of the Ova-specific IgG Fc N-glycan by HPLC revealed considerable differences between the different adjuvants (Fig. 3.5). Among these differences, the oil-in-water emulsion eCFA showed the lowest Fc galactosylation and sialylation levels, which were downregulated compared to naïve mice (Fig. 3.4). In addition, a downregulation for galactose and sialic acid was observed for the immunization with Ova-Alum compared to naïve untreated samples, although the downregulation was milder

compared to eCFA (Fig. 3.5). Immunizations with Ova-LPS and MPLA led to a more galactosylated and sialylated glycosylation profile comparable to that of naïve mice (Fig. 3.5). These analyses show that the bulk IgG glycosylation was highly dependent on the adjuvant. However, it remained unclear whether all IgG subclasses were affected in the same manner.

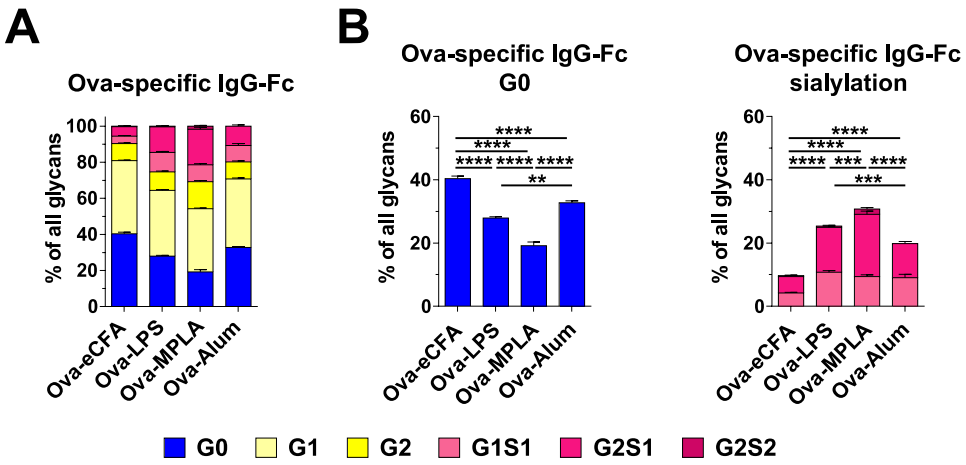

Fig. 3.5 ***Different adjuvants lead to distinct IgG glycosylation patterns.*** *C57BL/6 WT mice were immunized i.p. with 100 µg Ova and the respective adjuvant. Fourteen days after immunization, the mice were bled and the IgG Fc glycans of Ova-specific serum IgG antibodies analyzed by HILIC-HPLC. (A) Ova-specific IgG Fc glycosylation profiles. (B) Percentages of G0 and sialylated Ova-specific IgG Fc. Data presented in this figure were published in Epp, et.al., 2018. ($n_{Ova\text{-}eCFA}$ = 18, $n_{Ova\text{-}LPS}$ = 14, $n_{Ova\text{-}MPLA}$ = 5, $n_{Ova\text{-}Alum}$ = 5).*

LC-MS glycopeptide analysis of IgG from naïve mice had already indicated a certain bias towards higher galactosylation and sialylation of IgG2b/c compared to IgG1 (Fig. 3.4). Indeed, Ova-specific IgG2b/c showed a higher degree of galactosylation and sialylation compared to the IgG1 counterparts (Fig. 3.6). However, the reduction of Fc galactosylation and sialylation for Ova-eCFA compared to the other immunizations or untreated naïve controls was confirmed in both observed subclasses (IgG1 and IgG2b/c) (Fig. 3.6). Surprisingly, Ova-Alum showed Fc galactosylation and sialylation levels comparable MPLA for IgG1 (Fig. 3.6). Although IgG2b/c was under the detection limit for Ova-Alum immunizations here, comparing the pooled serum from Ova-MPLA or Ova-Alum immunized mice showed similar levels of IgG2b/c Fc sialylation (Epp et al., 2018). This result diverges from the results of the HPLC analysis, wherein Ova-Alum immunizations led to lower frequencies of galactosylated and sialylated glycans compared to Ova-MPLA immunization (Fig. 3.5).

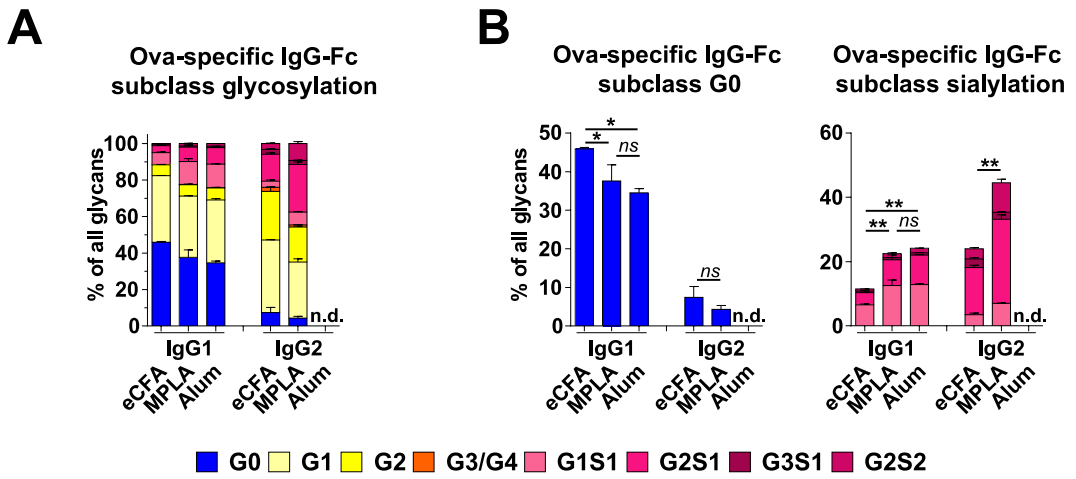

Fig. 3.6 ***Subclass-specific analysis of Ova-specific IgG upon immunization reveals no difference between MPLA and Alum adjuvant induced IgG1 Fc glycosylation pattern****. Serum samples analyzed in Fig. 3.5 were re-analyzed by LC-MS approach (A) Fc glycosylation profile of Ova-specific IgG1 and IgG2. (B) Percentages of G0 and sialylated Ova-specific IgG1 Fc and IgG2 Fc. (n.d. = not detectable). Ova-specific IgG3 was not detected. The LC-MS analysis was performed by the PhD student in our laboratory, Alexander Wagt, at the Center for Proteomics and Metabolomics (in collaboration with Manfred Wuhrer), Leiden University Medical Center, Leiden, the Netherlands.*

A possible explanation might be that Alum and MPLA/LPS induced different amounts of IgG1 and IgG2b/c, which then led to an apparent shift in the bulk IgG glycosylation measured by HPLC. In fact, the Ova-specific subclass ELISA demonstrated that Alum induced preferentially IgG1 antibodies, whereas for MPLA, more IgG2b and IgG2c antibodies were observed (Fig. 3.7).

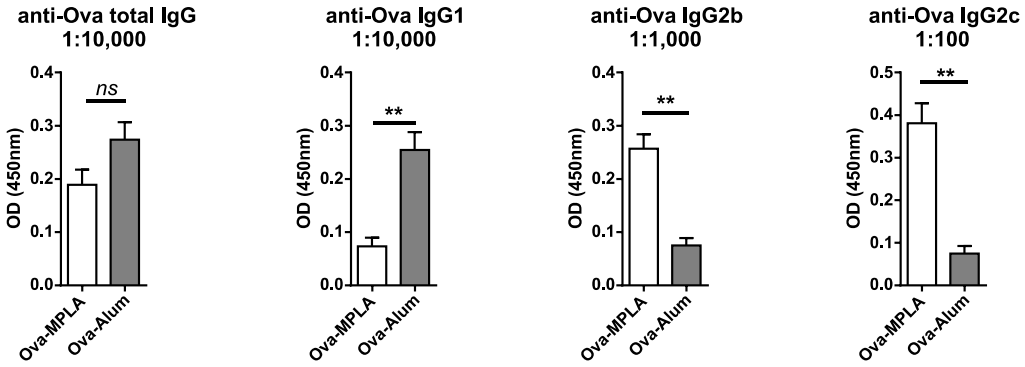

Fig. 3.7 ***Immunization with Ova-Alum or Ova-MPLA leads to different subclass distribution.*** *Mice were immunized with either Ova-Alum or Ova-MPLA and bled 14 days later. The relative amounts of Ova-specific total IgG or IgG1, IgG2b or IgG2c subclasses were then determined by Ova-specific ELISA. The serum was diluted as indicated in the graphs (n_{MPLA} = 5, n_{Alum} = 3).*

In summary, the results showed a clear influence of the adjuvants on the resulting IgG subclass glycosylation as well as the IgG subclass distribution. Ova-eCFA immunizations exclusively led to a more pro-inflammatory IgG glycosylation pattern. Although, the Fc glycosylation of IgG subclasses was affected by the adjuvant in the same manner, murine IgG subclasses were generally glycosylated in a considerably different manner, which led to

an apparent downregulation of IgG sialylation after Ova-Alum immunization in the HPLC analysis compared to Ova-MPLA immunization. However, the downregulation could be explained solely by a predominant induction of IgG1 antibodies. Consequently, murine IgG Fc glycosylation should be investigated in a subclass-specific manner, especially when differences in the subclass distribution are expected.

Part of these experiments were published in: Epp A*****, Hobusch J*, Bartsch YC*, Petry J*, . . . , Ehlers M. Sialylation of IgG antibodies inhibits IgG-mediated allergic reactions. *J Allergy Clinic Immunol 2018* (*these authors contributed equally).

3.1.4 Vaccination-induced antigen-specific IgG subclass level and IgG Fc subclass glycosylation pattern varies over time

The investigation above showed that the immune response to a foreign pathogen or protein is highly dependent on the co-stimulus. To investigate how dynamic the IgG subclass level and Fc glycosylation pattern react against Ova with different adjuvants and how antigen (Ova) re-exposure (boost) influences the IgG response, the antigen-specific IgG subclass level and Fc glycosylation pattern were analyzed on different days after immunization with Ova-eCFA or Ova-LPS. Ova-eCFA was chosen as an exemplar of a high inflammatory immunization and Ova-LPS as an exemplar of a much less inflammatory immunization. On day 28 after the initial immunization, a booster immunization with Ova (without adjuvant) was performed. Here, the IgG subclass levels were analyzed by ELISA (Fig. 3.8) and the IgG subclass Fc glycosylation was analyzed by LC-MS (Fig. 3.9).

The development of Ova-specific IgM, IgG and the different IgG subclasses were investigated by ELISA over time (Fig. 3.8). On day 7, both immunizations had similar amounts of specific IgM and IgG (all subclasses together) antibodies. However, Ova-LPS tended to have more IgG2b, IgG2c and IgG3 antibodies on day 7 compared to Ova-eCFA immunization. While up to day 14 only a minor increase in the Ova-specific IgG antibodies could be observed for Ova-LPS (mainly due to an increase in the IgG1 titer), antibody titers decreased from day 14 until day 28. For Ova-eCFA immunizations, the titers for all IgG subclasses increased tremendously until day 28. Antigen re-exposure after boost led to an increase in antigen-specific IgM and IgG titer for both adjuvants. It remained unclear whether the IgG titer increase for Ova-eCFA immunization was due to the boost, given that it was rising in a comparable manner before the boost. Although, the Ova-LPS group did not reach the IgG level seen in the Ova-eCFA group, the increase of the antigen-specific IgG titer after boost in the Ova-LPS group was remarkable. This may indicate induced memory upon primary immunization. Notably, in contrast to the Ova-eCFA group, Ova-LPS did not induce Ova-specific IgG3 antibodies after day 7.

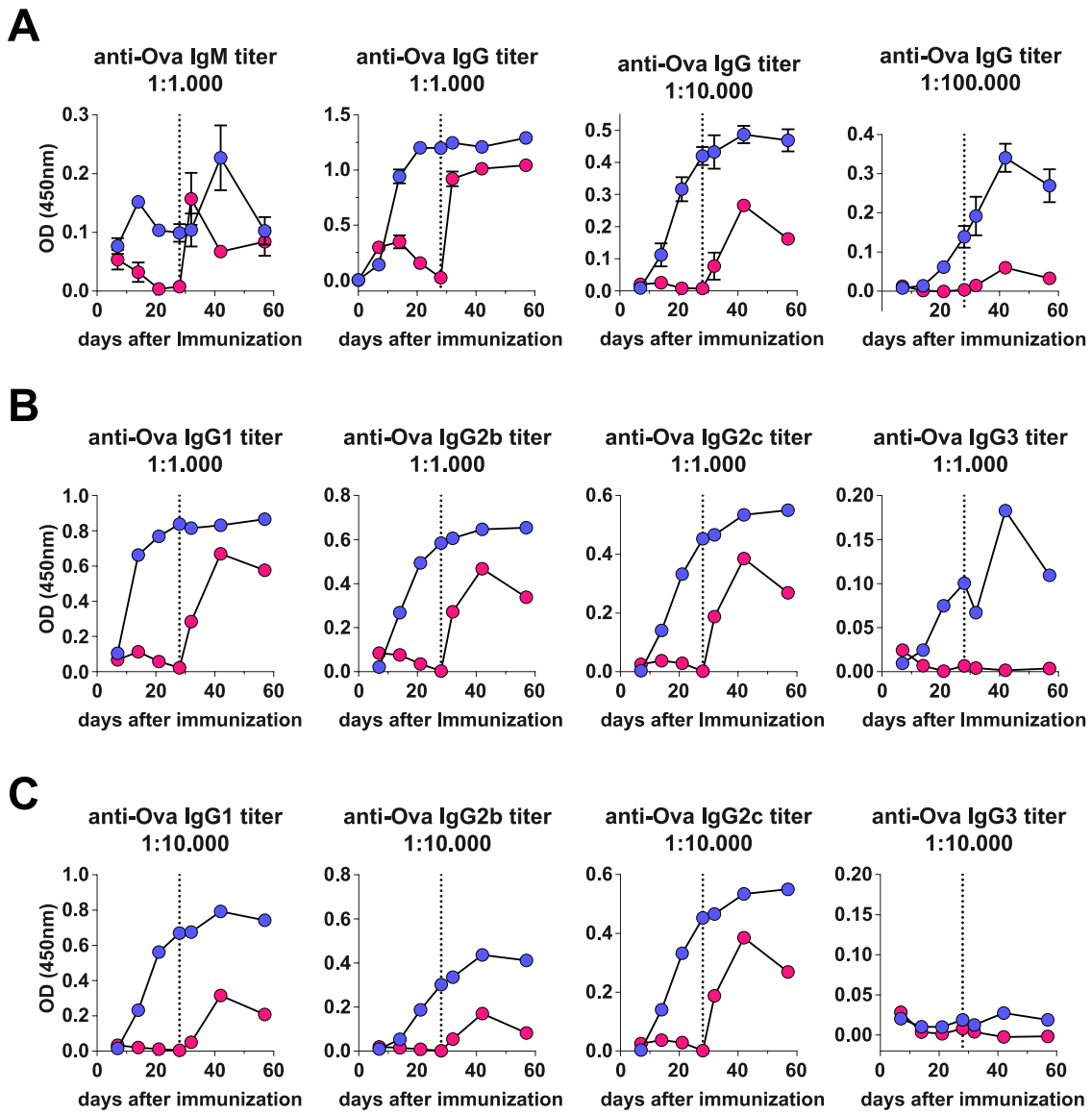

Fig. 3.8 ***Ova-specific IgG subclass distribution over the time.*** *Mice were immunized with either Ova-LPS (red) or Ova-eCFA (blue) and bled on days 7, 14 21 and 28 thereafter. A boost immunization with 100µg Ova was performed on day 28 (vertical dashed line), and the mice were subsequently bled on days 32, 42 and 57. (A) Ova-specific ELISA of different time points for anti-Ova IgM and anti-Ova total IgG in different dilutions (serum dilutions as indicated in the graph). (B, C) Ova-specific ELISA for IgG1, IgG2b, IgG2c and IgG3 with 1:1,000 (B) and 1:10,000 (C) serum dilution. n = 2–4 mice per group and time point.*

The Fc glycosylation of Ova-specific IgG1 and IgG2b/c antibodies upon Ova-eCFA immunization became more pro-inflammatory over time until day 28 and compared to Ova-LPS immunization. On day 7 after immunization, galactosylation and sialylation levels were considerably high and comparable to the Fc glycosylation pattern observed for Ova-LPS induced IgG subclass antibodies (Fig. 3.9). Interestingly, for IgG1, the galactosylation and sialylation levels appeared even higher than the mean levels before immunization (dashed horizontal line). While the glycosylation after Ova-LPS maintained relatively high levels of galactosylation (low levels of G0) and sialylation, both levels dropped substantially after Ova-eCFA immunization until day 28 (Fig. 3.9). After the boost

with pure Ova, however, increased galactosylation and sialylation was observed for both adjuvant groups on day 32 (Fig. 3.9). However, until day 42, both levels decreased again and tended to reach the glycosylation levels of prior to the boost on day 28.

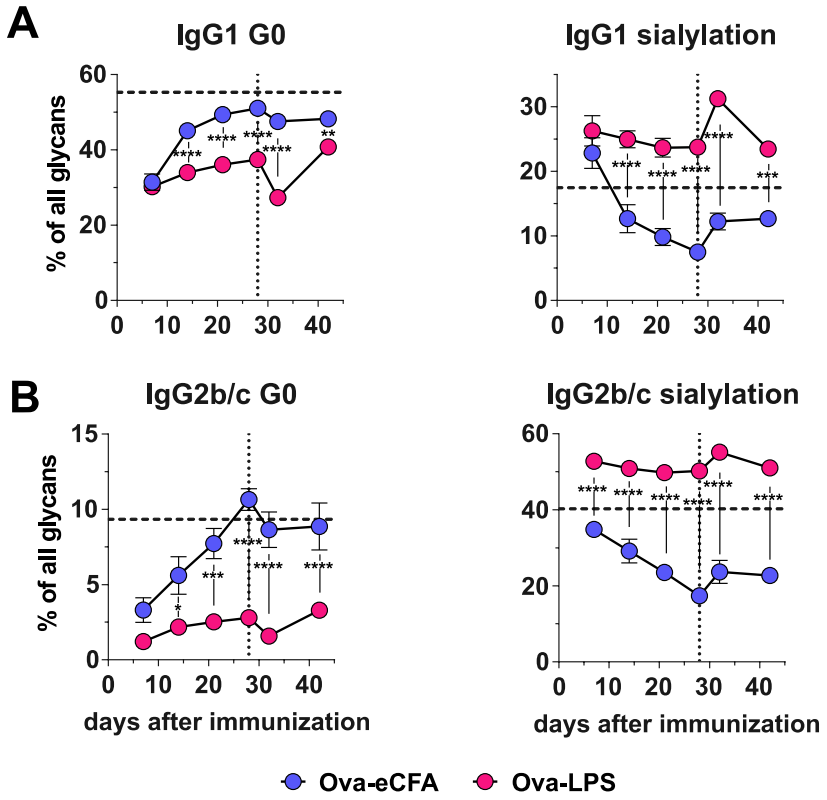

Fig. 3.9 ***Ova-specific IgG Fc subclass glycosylation varies over the duration of an immune reaction****. Mice were immunized with either Ova-LPS (red) or Ova-eCFA (blue) and bled on days 7, 14 21 and 28 thereafter. A boost immunization with 100µg Ova was performed on day 28 (vertical dashed line), and the mice were subsequently bled on days 32 and 42. Anti-Ova IgG Fc subclass glycopeptide analysis of the individual mice on the individual days was performed by LC-MS. (A) Average (± SEM) percentage of G0 and sialylated IgG1 (A) or IgG2b/c (B) on the indicated days. The horizontal line represents the average glycosylation of bulk IgG subclasses before immunization. n = 2–4 mice per group and time point. To test for statistical significance, the values for the different adjuvant were compared on the individual days, correcting for multiple testing (one-way-ANOVA). Significant differences between Ova-eCFA and Ova-LPS on the respective days are indicated by asterisks. The LC-MS analysis was performed by the PhD student in our laboratory, Alexander Wagt, at the Center for Proteomics and Metabolomics (in collaboration with Manfred Wuhrer), Leiden University Medical Center, Leiden, the Netherlands.*

Interestingly, upon primary (adjuvanted) and secondary (not adjuvanted) vaccination, an induction of highly sialylated antigen-specific IgG antibodies was observed on days 7 and 32 for both adjuvant groups, respectively. After day 7 and day 32 the IgG Fc sialylation dropped. These results may indicate that fast (early) and slow (late) immune mechanisms may induce different glycosylation patterns. Furthermore, the induction of new IgG antibodies upon boost may indicate the induction of a memory response.

3.1.5 Vaccination induced IgG sialylation correlates with St6gal1 protein expression level in plasma cells

The main source of IgG antibodies are B cells that were differentiated into plasma cells (Nutt et al., 2015). Murine plasma cells are characterized by high expression of surface CD138 (Sydecan-1) (Sanderson et al., 1989). Antigen (Ova)-specific IgG Abs were already observable on day 7 post-immunization with Ova-eCFA and Ova-LPS. To investigate the cellular plasma cell response and identify the optimal time points for more in-depth analysis of the B cell response, the mice were immunized with Ova-eCFA or Ova-LPS and the frequencies of PCs in the spleen investigated on different days (Fig. 3.10).

Under naïve conditions (d0), approximately 0.2% of the splenocytes were CD138+ plasma cells. The frequency of plasma cells rose upon immunization, with Ova-LPS immunization leading to a moderate increase in PC frequencies between days 4 and 8 post-immunization. By contrast, Ova-eCFA led to a strong induction of plasma cells, which peaked at day 8 and slowly declined afterwards. However, until day 21, increased plasma cell levels were still observable for Ova-eCFA immunization (Fig. 3.10).

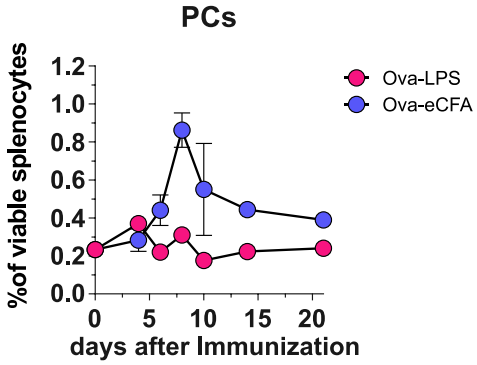

Fig. 3.10 ***Splenic plasma cells are induced after vaccination****. C57BL/6 WT mice were immunized with either Ova-LPS (red) or Ova-eCFA (blue), and their spleens were harvested on the indicated days. Mean (± SEM) frequencies of CD138+ cells of viable single lymphocytes are shown, respectively. Day 0 corresponds to the frequency of plasma cells from untreated naïve mice (n = 2–5 mice per group and day).*

To further characterize the plasma cells for their capability to produce Ova-specific IgG subclass antibodies, flow cytometric analysis was performed early on day 8 post-immunization when plasma cell frequencies were the highest, as well as late on day 14 (Fig. 3.10 and Fig. 3.11). Additionally, the relative protein expression levels of alpha-2,6-sialyltransferase 1 (St6gal1) were measured intracellularly in Ova-specific IgG1 and IgG (but not IgG1) plasma cell subsets. St6gal1 catalyzes the addition of sialic acid onto galactosylated N-glycans, such as on IgG molecules (Moremen et al., 2012).

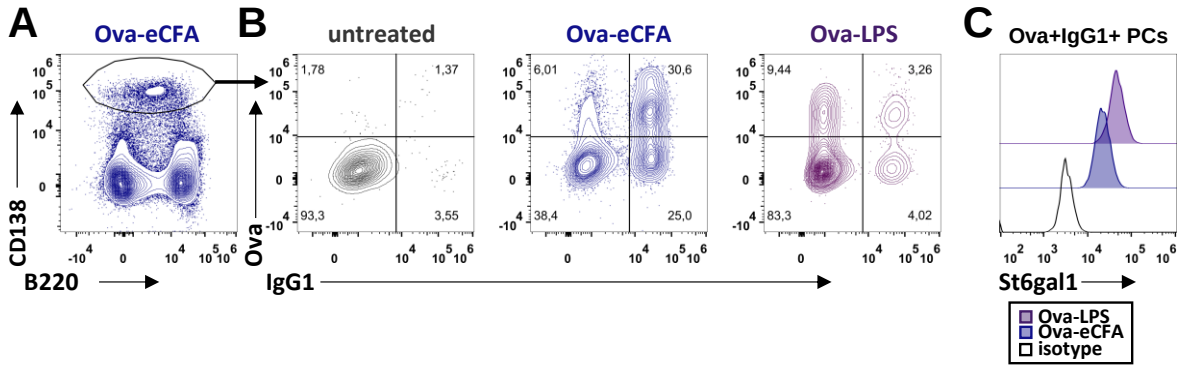

Fig. 3.11 ***Flow cytometry gating strategy for the identification of splenic Ova+ IgG1+ PCs and the subsequent intracellular measurement of St6gal1 protein expression in this population.*** *C57BL/6 WT mice were immunized i.p. with Ova-eCFA or Ova-LPS and were analyzed on day 8. Splenocytes were stained extra- and intracellularly, and flow cytometric analysis was performed. (A) PCs were identified by CD138 expression after pre-gating on single, viable lymphocytes. (B) Ova+ and IgG1+ gating in pre-gated PCs for untreated, Ova-eCFA or Ova-LPS immunized mice (day 8 upon immunization). The upper right square represents Ova+IgG1+ PCs. (C) St6gal1 fluorescent signal in pre-gated Ova+IgG1+ PCs after Ova-eCFA or Ova-LPS immunization or signal for isotype control antibody.*

On day 8, the plasma cell frequency was the highest for Ova-eCFA immunization (Fig. 3.12), with approximately 40% of all plasma cells recognizing Ova (Ova+) after immunization with eCFA, while only approx. 20% did so upon Ova-LPS immunization. Among the Ova+ plasma cells, more than 80% class-switched to IgG1 subclass after Ova-eCFA. Ova-LPS mainly induced other IgG subclasses (~60%), likely IgG2b or IgG2c but only 20% IgG1. However, independently of the IgG subclass, Ova-eCFA led to a lower expression of St6gal1 in Ova+ plasma cells compared to the Ova-LPS immunization (Fig. 3.12).

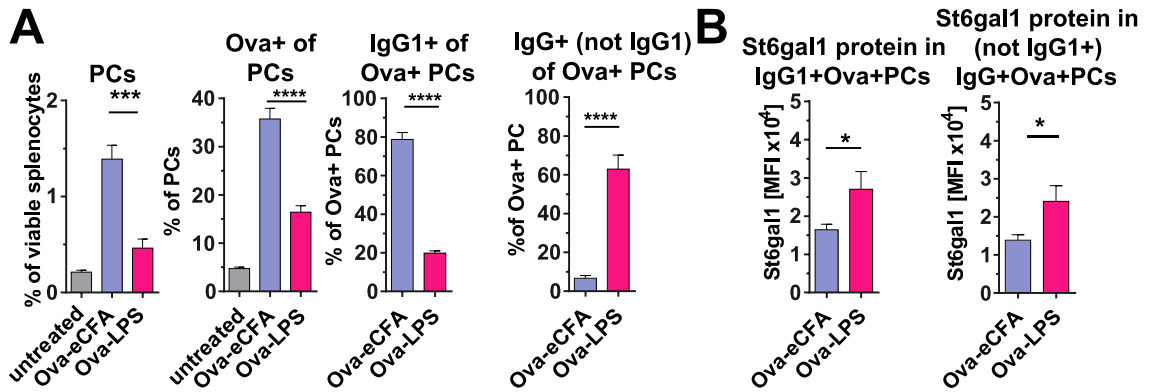

Fig. 3.12 ***Ova-eCFA but not Ova-LPS induces high frequencies of IgG1+Ova+ PCs with low expression of St6gal1 protein 8 days after vaccination.*** *C57BL/6 WT mice were immunized with either Ova-eCFA or Ova-LPS or left untreated. Spleens of the mice were harvested on day 8 post-immunization and flow cytometric analysis performed. (A) Frequencies of total PCs, Ova+ of PCs and IgG1+ or IgG+(not IgG1+) of Ova+PCs. (B) Median fluorescent intensities (MFI) of St6gal1 protein in IgG1+Ova+PCs or IgG+(notIgG1+)Ova+PCs. n = 6–8 mice per group pooled from two different experiments.*

On day 14, the frequency of plasma cells had already decreased; however, significant frequencies of Ova+ of plasma cells continued to be detected for both immunizations (Fig.

3.13). Likewise, the distinct IgG subclass distribution patterns between eCFA and LPS immunizations were conserved. Astonishingly, the overall frequency of all Ova-specific IgG (all subclasses) producing plasma cells was lower compared to day 8. However, also on day 14, Ova-specific IgG1-producing plasma cells expressed lower levels of St6gal1 in the eCFA group compared to the Ova-LPS group. The same tendency was observed for Ova+ plasma cells that produced one of the other IgG subclasses (IgG+notIgG1+) (Fig. 3.13).

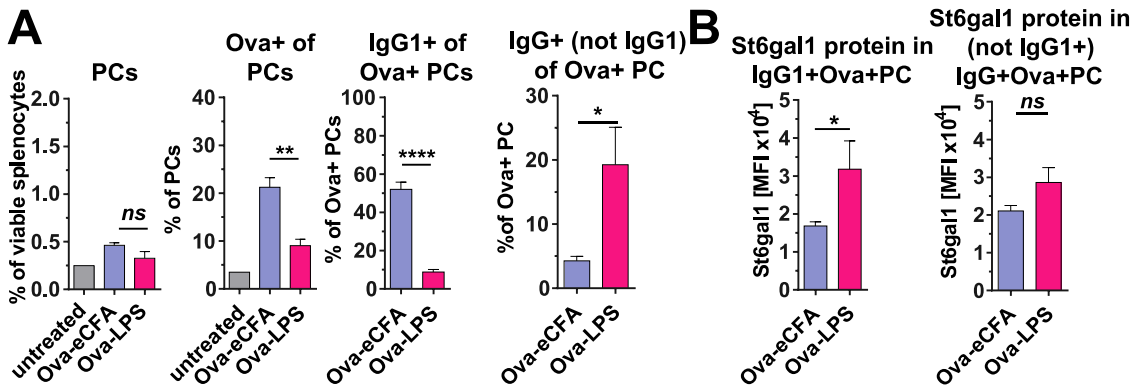

Fig. 3.13 ***Vaccination-induced differences in St6gal1 protein expression in Ova+IgG1+ plasma cells is maintained until 14 days after immunization.*** *C57BL/6 WT mice were immunized with either Ova-eCFA or Ova-LPS or left untreated. Spleens of the mice were harvested on day 14 post-immunization and flow cytometric analysis performed. (A) Frequencies of total PCs, Ova+ of PCs and IgG1+ or IgG+(not IgG1+) of Ova+PCs. (B) Median fluorescent intensities (MFI) of St6gal1 protein in IgG1+Ova+PCs or IgG+(notIgG1+)Ova+PCs. n = 6–7 mice per group pooled from two different experiments.*

In a second experiment, mice were vaccinated with Ova in eCFA, compared to Ova in Alum, which also resulted in a reduced inflammatory IgG Fc subclass glycosylation pattern, as shown in Fig. 3.6.

Immunization with Alum led to a comparable induction of plasma cells and even higher frequencies of Ova+ PCs on day 8 compared to the eCFA group (Fig. 3.14). Furthermore, Ova-Alum induced a stronger class-switch to IgG1 compared to Ova-eCFA, as already indicated by the data in Fig. 3.6 and Fig. 3.7. Comparable to Ova-LPS immunization, Ova-Alum showed higher St6gal1 expression levels in the Ova+IgG1+ and IgG+ (not IgG1+) plasma cells compared to Ova-eCFA immunization (Fig. 3.14).

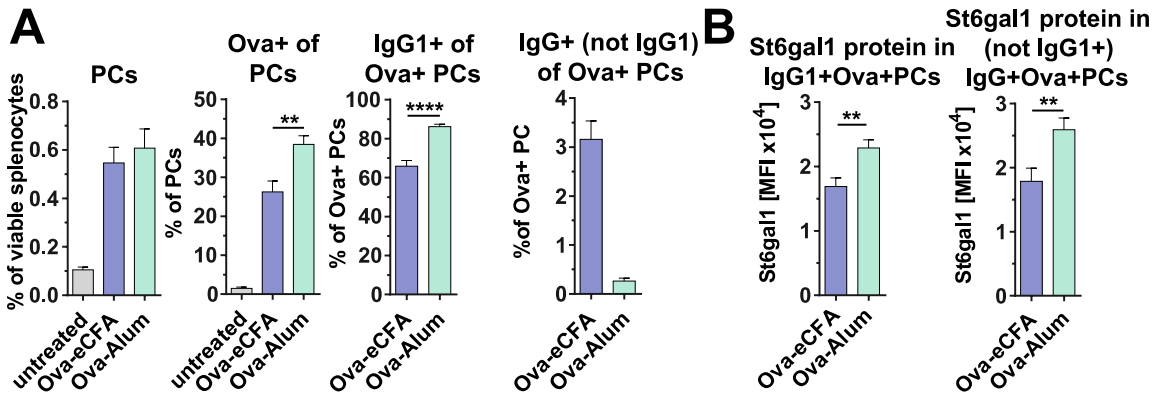

Fig. 3.14 ***Comparison of Ova+ PCs after vaccination with Ova-eCFA or Ova-Alum on day 8.*** *C57BL/6 WT mice were immunized with Ova in either eCFA or Alum or left untreated. Spleens of the mice were harvested on day 8 post-immunization and flow cytometric analysis performed. (A) Frequencies of total PCs, Ova+ of PCs and IgG1+ or IgG+(not IgG1+) of Ova+PCs. (B) Median fluorescent intensities (MFI) of St6gal1 protein in IgG1+Ova+PCs or IgG+(notIgG1+)Ova+PCs. n = 9 mice per group pooled from two different experiments.*

On day 14, the levels of plasma cells dropped tremendously for Ova-Alum immunizations (Fig. 3.15). However, the frequency of Ova+ of plasma cells was comparable to Ova-eCFA immunization, and the levels of IgG1 and IgG (not IgG1) class-switched Ova-specific plasma cells were comparable to the Ova-eCFA group. However, St6gal1 expression in IgG1+ and IgG+ (not IgG1+) Ova+ PCs was still higher in the Ova-Alum induced plasma cells (Fig. 3.15).

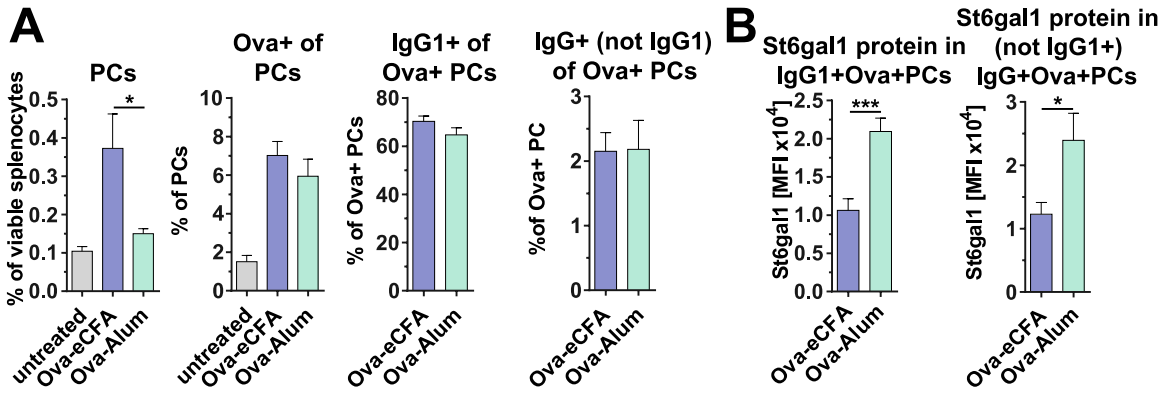

Fig. 3.15 ***Comparison of Ova+ PCs after vaccination with Ova-eCFA or Ova-Alum on day 14.*** *C57BL/6 WT mice were immunized with Ova in either eCFA or Alum or left untreated. Spleens of the mice were harvested on day 14 post-immunization and flow cytometric analysis performed. (A) Frequencies of total PCs, Ova+ of PCs and IgG1+ or IgG+(not IgG1+) of Ova+PCs. (B) Median fluorescent intensities (MFI) of St6gal1 protein in IgG1+Ova+PCs or IgG+(notIgG1+)Ova+PCs. n = 9–10 mice per group pooled from two different experiments.*

Together, the observed differences in the frequencies and St6gal1 expression levels of Ova-eCFA versus Ova-LPS or Ova-Alum immunizations were in line with the observed IgG subclass serum titers and glycosylation patterns (Fig. 3.6 - Fig. 3.8). In summary, Ova-eCFA induced a more pro-inflammatory IgG subclass Fc glycosylation pattern and Ova-specific IgG(1)+ PCs, which express lower levels of the St6gal1 protein compared to Ova-LPS or

Ova-Alum immunizations. Furthermore, the observed St6gal1 protein expression levels in Ova+IgG1+ PCs correlated with the observed Ova-specific IgG1 Fc subclass sialylation levels.

3.2 The role of IL-6 in IgG Fc glycosylation after Ova-eCFA immunization

Ova-specific IgG Fc glycosylation correlated with the expression level of St6gal1 protein in vaccination-induced Ova-specific IgG+ plasma cells, meaning that different adjuvants induced distinct St6gal1 expression levels. A mechanistic understanding how different adjuvants influence St6gal1 expression in plasma cells appears important for the development of new vaccination strategies. Cytokines like IL-17A, IFNγ and TNFα have already been noted as possible regulators of IgG glycosylation (Hess et al., 2013; Collins et al., 2013).

Hence, serum cytokine concentrations were measured via multiplex assay after immunization with Ova-eCFA or Ova-LPS. Interestingly, the inflammatory serum cytokines (IL-17A, IL-22, IL-6, IFNγ and TNFα) were clearly upregulated in the serum of Ova-eCFA immunized mice compared to Ova-LPS immunization (Fig. 3.16). Worthy of note is the fact that IL-10, IL-12p40, IL-17F and IL-21 were under the detection limit in all investigated serum samples. Recently, the involvement of Th17 cell derived IL-22 in downregulating of IgG sialylation has also been suggested (Pfeifle et al., 2017). Although IL-6 can induce Th17 cells (Bettelli et al., 2006), a role of IL-6 for IgG glycosylation has not been reported thus far.

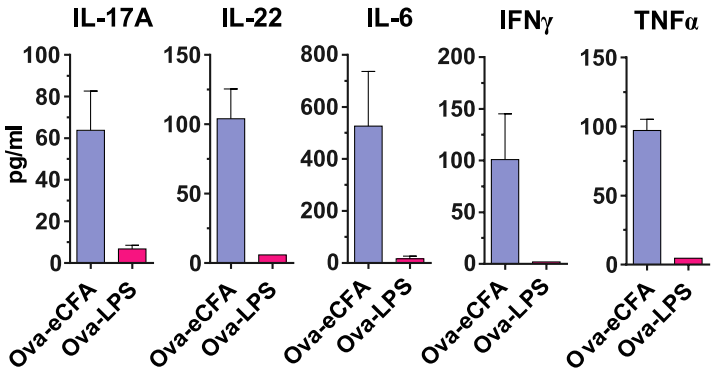

Fig. 3.16 ***Vaccination with Ova-eCFA but not with Ova-LPS induces pro-inflammatory cytokines.*** *C57BL/6 WT mice were immunized with either Ova-eCFA or Ova-LPS. Mice were bled eight days after immunization and serum cytokines subsequently analyzed via Legendplex™ mouse Th17+IL23p19 panel multiplex assay. Mean (+SEM) serum concentrations for IL-17A, IL-22, IL-6, IFNγ and TNFα are shown. IL-10, IL17F, IL-21 and IL-23p19 were under the detection limit (n = 5 per group).*

IL-6 was initially described as a stimulating factor for antibody production in B cell *in vitro* (Hirano et al., 1986; Muraguchi et al., 1988). Today, IL-6 is characterized as a pleiotropic

cytokine produced by immune cells such as antigen presenting cells (e.g., monocytes and dendritic cells) and B and T cells, as well as by non-immune cells including endothelial cells or fibroblasts (Ho et al., 2015b). Likewise, IL-6 has been shown to act on different immune and non-immune cells (Ho et al., 2015b). In addition, IL-6 is described as an important cytokine for T cell differentiation. IL-6 can skew the TGFβ mediated differentiation of regulatory T cells into the Th17 fate (Bettelli et al., 2006; Veldhoen et al., 2006). Misregulation of Treg/Th17 differentiation is associated with autoimmunity (Ho et al., 2015b). Moreover, IL-6 plays an important role in the initial differentiation of T_{FH} cells and subsequently the GC reaction (Choi et al., 2013; Riteau et al., 2016).

Consequently, to investigate the role of IL-6 on IgG Fc glycosylation, WT C57BL/6 mice and IL-6-deficient mice on the C57BL/6 background (IL-6 KO) were immunized with Ova-eCFA.

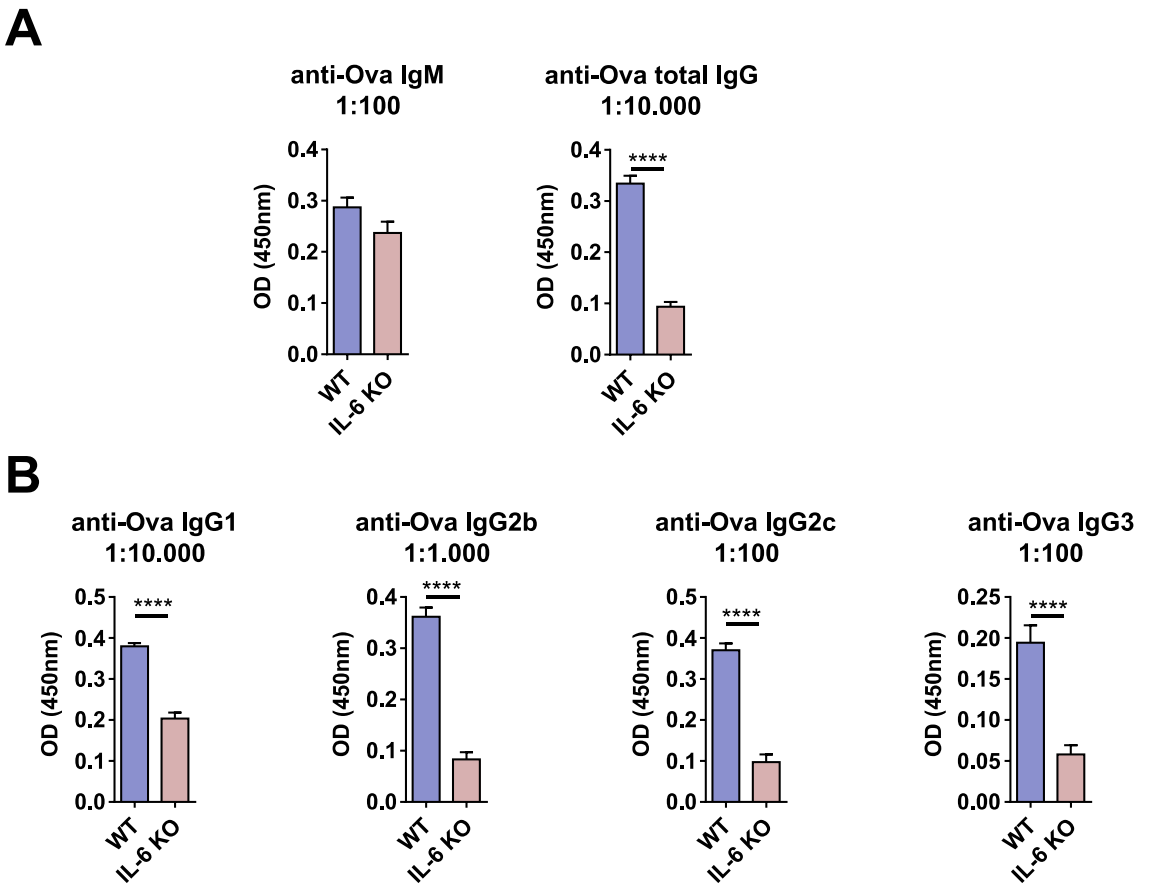

Fig. 3.17 ***IL-6 deficient mice show reduced Ova-specific IgG titers after immunization with Ova-eCFA on day 14.*** *C57BL/6 WT and IL-6 KO mice were immunized with Ova-eCFA. Mice were bled 14 days after vaccination and Ova-specific ELISA performed. (A) ELISAs for anti-Ova IgM and anti-Ova total IgG. (B) ELISAs for anti-Ova IgG1, IgG2b, IgG2c and IgG3. Serum dilutions are indicated in the graphs;* $n_{WT} = 7$, $n_{IL\text{-}6\ KO} = 20$.

At first, Ova-specific ELISA for IgM, IgG and IgG subclasses revealed a considerable downregulation of Ova-specific IgG, particular of IgG2 and 3 subclasses in the IL-6 KO

mice (Fig. 3.17) suggesting a reduced plasma cell response or IgG class switching, particularly for IgG2 and IgG3.

The resulting Fc glycosylation of Ova-specific IgG1 was analyzed by LC-MS 14 days after immunization (Fig. 3.18). The IL-6 KO mice clearly failed to induce the pro-inflammatory Ova-specific IgG1 glycosylation pattern that was observed in the WT controls. Instead, Ova-specific IgG1 Fc sialylation and galactosylation levels were comparable to Ova-Alum or Ova-LPS immunizations, as described above.

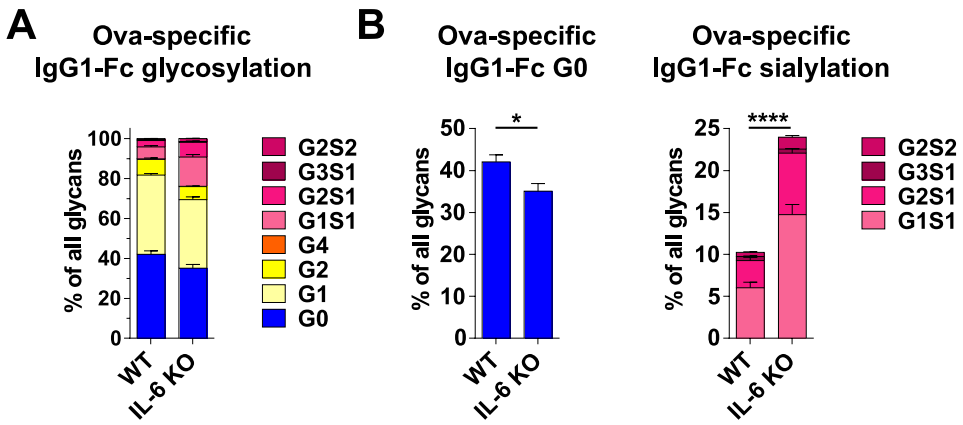

Fig. 3.18 ***Ova-eCFA vaccination in IL-6 KO mice fails to induce a pro-inflammatory IgG1 Fc glycosylation on day 14.*** *C57BL/6 WT and IL-6 KO mice were immunized with Ova-eCFA. Mice were bled 14 days after vaccination, and the Ova-specific IgG Fc glycosylation was investigated by LC-MS. (A) Fc glycosylation profile of Ova-specific IgG1. (B) Percentages of G0 and sialylated Ova-specific IgG1 Fc. Ova-specific IgG2b/c was not detectable in the IL-6 KO mice. n = 5 mice per group. The LC-MS analysis was performed by the PhD student in our laboratory, Alexander Wagt, at the Center for Proteomics and Metabolomics (in collaboration with Manfred Wuhrer), Leiden University Medical Center, Leiden, the Netherlands.*

To verify the importance of IL-6 on IgG Fc glycosylation, WT mice were treated with an IL-6 receptor- (IL-6R; CD126) blocking antibody (clone: MR16-1) (Tamura et al., 1993; Okazaki et al., 2002). Five hundred µg of the antibody were injected i.p. directly after immunization with Ova-eCFA, as well as three and six days thereafter. The Ova-specific serum IgG Fc subclass glycosylation was again analyzed 14 days after immunization (Fig. 3.19). IL-6R blocking led to increased levels of galactosylation and sialylation of Ova-specific IgG1 antibodies, which is comparable to the results obtained with the IL-6 KO mice (Fig. 3.18).

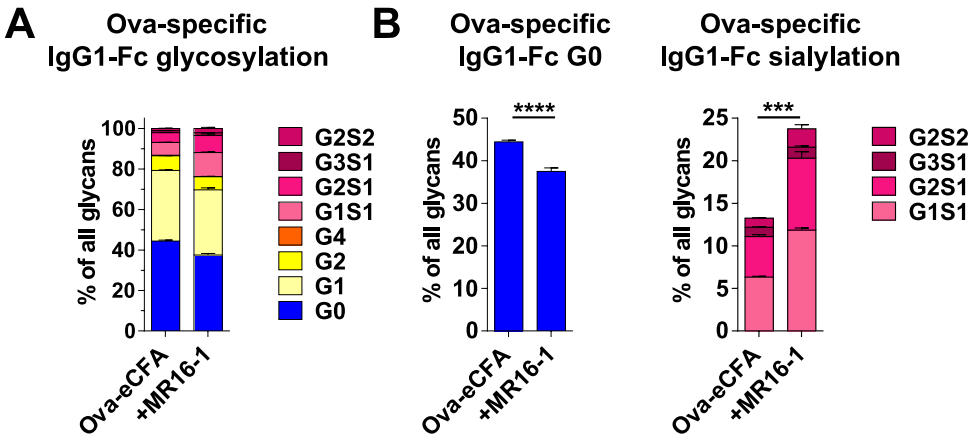

Fig. 3.19 ***Blocking of IL-6R after Ova-eCFA immunization led to comparable IgG1 Fc glycosylation pattern as observed in the IL-6 KO mice.*** *C57BL/6 WT mice were immunized with Ova-eCFA. One group was treated with 500 µg of the anti-IL-6R antibody (clone:MR16-1) on days 0, 3 and 5 ("+MR16-1"). Mice were bled 14 days after vaccination, and the Ova-specific IgG Fc glycosylation was investigated via LC-MS. (A) Glycosylation profile of Ova-specific IgG1 Fc. (B) Percentages of G0 and sialylated Ova-specific IgG1 Fc.* $n_{WT} = 5$, $n_{MR16\text{-}1} = 3$. *The experiments were conducted in collaboration with Chugai Pharmaceuticals Co., Ltd. (Japan). The LC-MS analysis was performed by the PhD student in our laboratory, Alexander Wagt, at the Center for Proteomics and Metabolomics (in collaboration with Manfred Wuhrer), Leiden University Medical Center, Leiden, the Netherlands.*

3.2.1 IL-6 is indispensable for the induction of plasma cells and their low expression of St6gal1 after Ova-eCFA immunization

As shown above, IL-6 signaling is important for high levels of Ova-specific IgG class-switched antibodies and the low level of IgG1 Fc sialylation upon Ova-eCFA vaccination.

To further analyze the cellular immune response, plasma cells were investigated in IL-6 KO mice early on day 8 and late on day 14 after immunization with Ova-eCFA. The general reduction in Ova-specific IgG antibodies was reflected in lower frequencies of splenic plasma cells in the IL-6KO (Fig. 3.20 and Fig. 3.21). However, similar proportions of plasma cells recognized Ova and among the Ova+ plasma cells are class-switched to IgG1 on day 8 (Fig. 3.20). This may indicate that the proliferation of plasmas cells might be dependent on IL-6 but general induction and activation upon antigen encounter was not. Intriguingly, the IgG1 sialylation correlated with the expression levels of St6gal1 in Ova+ IgG1 class-switched plasma cells. Compared to the IL-6 KO, the expression of St6gal1 was remarkably downregulated in WT mice (Fig. 3.20).

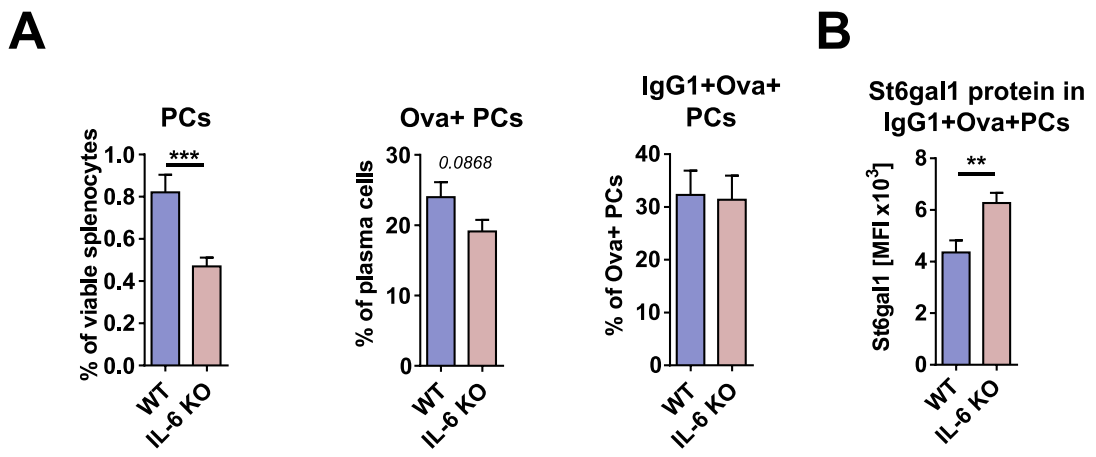

Fig. 3.20 ***IL-6 deficient mice have reduced splenic plasma cells and increased St6gal1 protein expression in Ova+IgG1+ plasma cells 8 days after immunization.*** *C57BL/6 WT and IL-6 KO mice were immunized with Ova-eCFA, and their spleens were harvested for flow cytometry analysis on day 8. (A) Frequencies of total PCs, Ova+ of PCs and IgG1+ of Ova+PCs. (B) Median fluorescent intensities (MFI) of St6gal1 protein in IgG1+Ova+PCs.* n_{WT} *= 9,* $n_{IL\text{-}6\ KO}$ *= 11 mice pooled from two independent experiments.*

Although the frequency of total plasma cells was not significantly different between WT and IL-6 KO mice on day 14 after immunization, WT mice had higher frequencies of Ova-recognizing and, among them, IgG1 class-switched plasma cells (Fig. 3.21). This may indicate that IL-6 KO mice fail to maintain an Ova-specific plasma cell response, which is in line with the reduction of Ova-specific IgG titers. Furthermore, Ova+IgG1+ plasma cells showed a higher expression of St6gal1 in the IL-6 KO mice compared to WT mice, which was reflected in the high degree of sialylated Ova-specific IgG1 (Fig. 3.18 and Fig. 3.21).

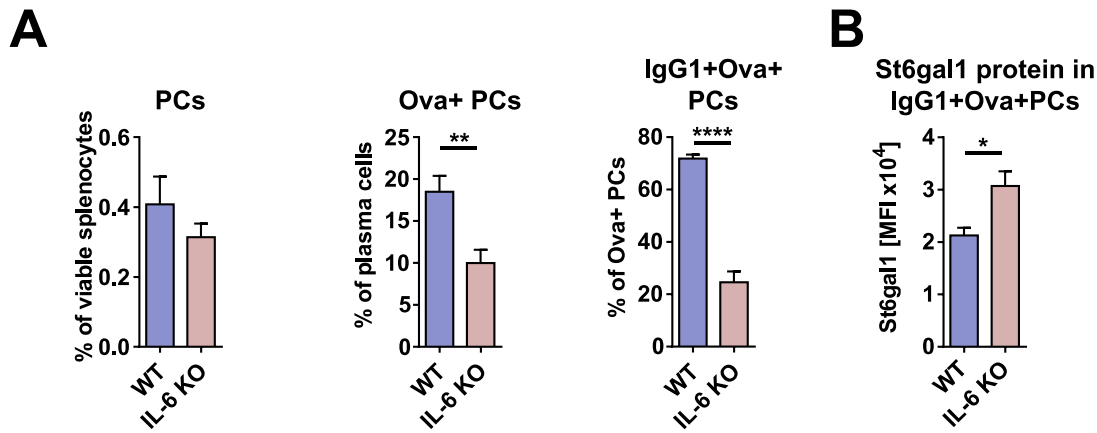

Fig. 3.21 ***IL-6 deficient mice have reduced Ova-specific IgG1 class-switched plasma cells and increased St6gal1 protein expression in IgG1+Ova+ plasma cells 14 days after immunization.*** *C57BL/6 WT and IL-6 KO mice were immunized with Ova-eCFA, and their spleens were harvested for flow cytometry analysis on day 14. (A) Frequencies of total PCs, Ova+ of PCs and IgG1+ of Ova+PCs. (B) Median fluorescent intensities (MFI) of St6gal1 protein in IgG1+Ova+PCs. n = 10 mice per group pooled from two independent experiments.*

Taken together, IL-6KO mice had an attenuated plasma cell response that led to decreased vaccine-induced IgG titers. Furthermore, IL-6 was important for the downregulation of

St6gal1 protein in plasma cells and subsequently the induction of low sialylated IgG antibodies after immunization with Ova-eCFA. The mechanism by which IL-6 may mediate these changes is further investigated in the following.

3.2.2 IL-6 dependent IL-17A signaling axis induces low St6gal1 expression upon vaccination with Ova-eCFA

IL-6 is involved in the induction of IL-17A producing CD4+ T helper cells (Th17). The IL-17A signaling axis has been reported to be involved in the regulation of pro-inflammatory IgG glycosylation (Hess et al., 2013; Pfeifle et al., 2017).

As expected, IL-6 KO mice induced less splenic Th17 cells and had reduced IL-17A serum concentrations on day 8 upon Ova-eCFA vaccination (Fig. 3.22).

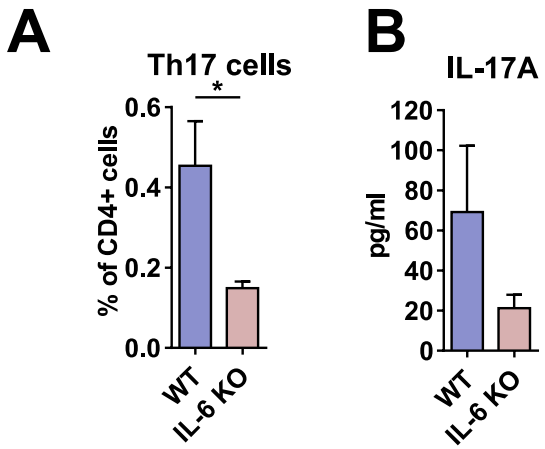

Fig. 3.22 ***Th17 cell differentiation and IL-17A levels are abrogated in IL-6 deficient mice after Ova-eCFA.*** *C57BL/6 WT and IL-6 KO mice were immunized with Ova-eCFA and spleens and serum were harvested on day 8. (A) Splenocytes were restimulated for intra-nuclear cytokine staining. Frequencies of IL-17A expressing CD4+ cells were analyzed. (B) Serum IL-17A cytokine was analyzed via multiplex assay. n = 5 mice per group.*

Accordingly, the Th17 pathway may also explain the effects on IgG glycosylation seen in the IL-6 KO mice. IL-17A signals then via a receptor heterodimer consisting of IL-17RA and IL-17RC (Gaffen, 2009). Thus, mice deficient in the IL-17RA (IL-17Ra KO) were immunized with Ova-eCFA, and the plasma cell response was investigated on days 8 and 14 after vaccination.

Interestingly, on day 8 after immunization, no difference between IL-17Ra KO and WT control mice was found in terms of the induction of total, Ova+ or Ova+IgG1+ plasma cells (Fig. 3.23). Additionally, the expression of St6gal1 appeared not to be influenced by the lack of IL-17RA signaling on that day.

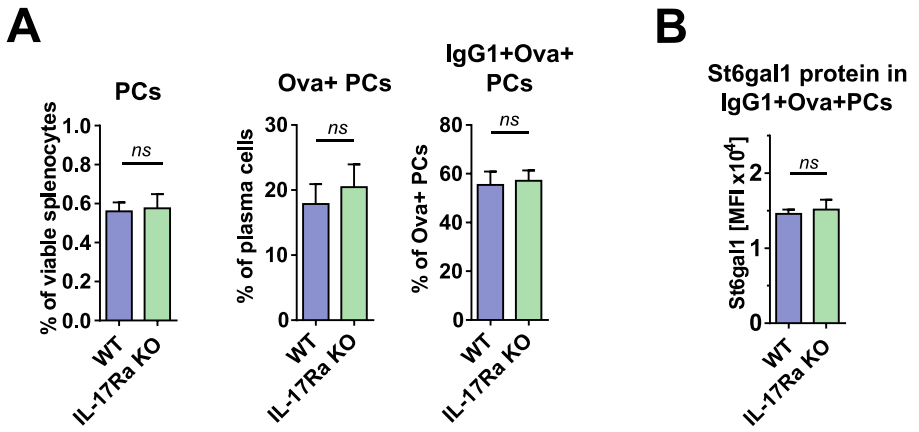

Fig. 3.23 ***IL-17RA signaling has no effect on the vaccination induced plasma cell response on day 8 after vaccination with Ova-eCFA.*** *C57BL/6 WT and IL-17Ra deficient mice were immunized with Ova-eCFA, and their spleens were harvested for flow cytometry analysis on day 8. (A) Frequencies of total PCs, Ova+ of PCs and IgG1+ of Ova+PCs. (B) Median fluorescent intensities (MFI) of St6gal1 protein in IgG1+Ova+PCs. n = 5 mice per group.*

On day 14, however, fewer IgG1 class switched plasma cells were observed among the Ova+ plasma cells. Moreover, St6gal1 expression in Ova+IgG1+ plasma cells was higher in the IL-17Ra deficient mice compared to WT mice (Fig. 3.24).

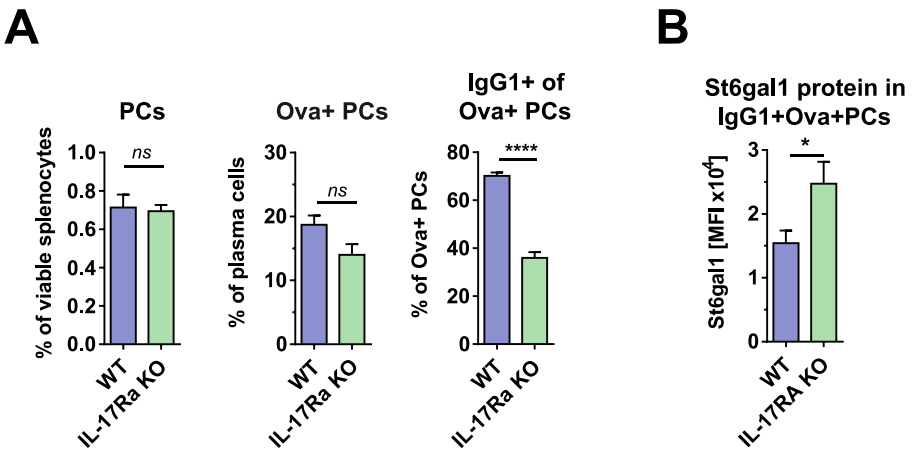

Fig. 3.24 ***Loss of IL-17RA signaling attenuates vaccination-induced IgG1 class-switch and St6gal1 expression in plasma cells 14 days after immunization with Ova-eCFA.*** *C57BL/6 WT and IL-17Ra deficient mice were immunized with Ova-eCFA, and their spleens were harvested for flow cytometry analysis on day 14. (A) Frequencies of total PCs, Ova+ of PCs and IgG1+ of Ova+PCs. (B) Median fluorescent intensities (MFI) of St6gal1 protein in IgG1+Ova+PCs. n_{WT} = 10, $n_{IL\text{-}17Ra}$ = 9 mice pooled from two independent experiments.*

To confirm these findings, mice deficient in IL-17A (IL-17A KO) were immunized with Ova-eCFA and analyzed on day 14. As in the IL-17Ra KO mice, IgG1+Ova+ plasma cells were less frequent but showed higher expression levels of St6gal1 on day 14 (Fig. 3.25). Consistently, IL-17A KO mice showed higher levels of sialylated Ova-specific IgG1 antibodies (Fig. 3.26).

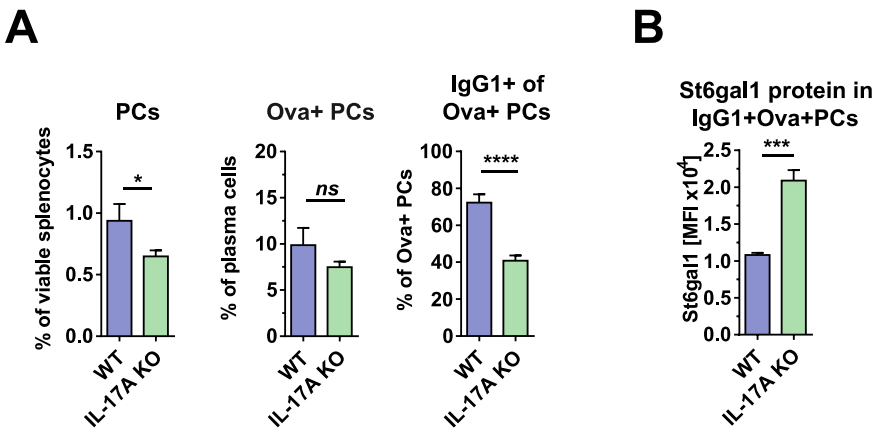

Fig. 3.25 ***Loss of IL-17A attenuates vaccination-induced IgG1 class-switch and St6gal1 expression in plasma cells 14 days after immunization.*** *C57BL/6 WT and IL-17A deficient mice were immunized with Ova-eCFA, and their spleens were harvested for flow cytometry analysis on day 14. (A) Frequencies of total PCs, Ova+ of PCs and IgG1+ of Ova+PCs. (B) Median fluorescent intensities (MFI) of St6gal1 protein in IgG1+Ova+PCs* $n_{WT} = 5$, $n_{IL\text{-}17AKO} = 7$. *The experiments were conducted in collaboration with Christoph Hölscher (Research Center Borstel, Borstel, Germany).*

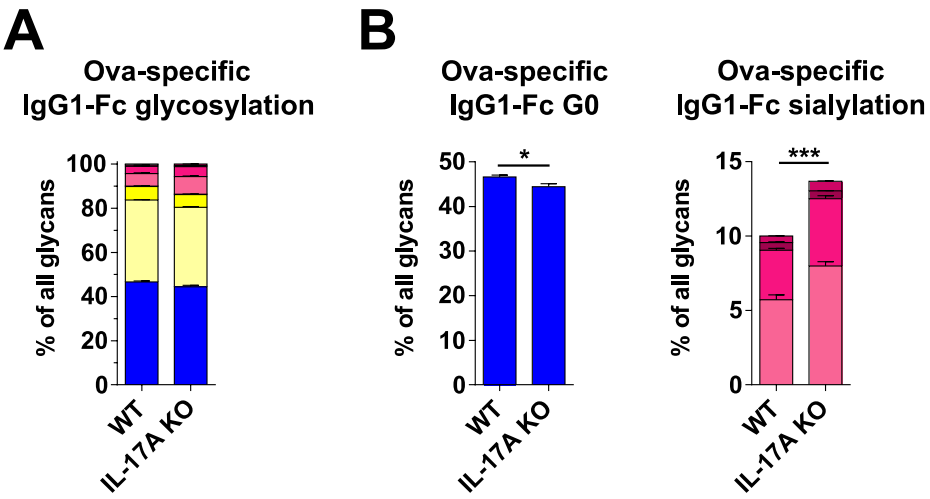

Fig. 3.26 ***IL-17A deficient mice have less pro-inflammatory Ova-specific IgG1 Fc glycosylation 14 days after vaccination with Ova-eCFA.*** *C57BL/6 WT or IL-17A KO mice were immunized with Ova-eCFA. Mice were bled 14 days after vaccination and the Ova-specific IgG Fc glycosylation investigated by LC-MS. (A) Glycosylation profile Ova-specific IgG1 Fc. (B) Percentages of G0 and sialylated Ova-specific IgG1 Fc.* $n_{WT} = 5$, $n_{IL\text{-}17A} = 7$. *The LC-MS analysis was performed by the PhD student in our laboratory, Alexander Wagt, at the Center for Proteomics and Metabolomics (in collaboration with Manfred Wuhrer), Leiden University Medical Center, Leiden, the Netherlands. The experiments were conducted in collaboration with Christoph Hölscher (Research Center Borstel, Borstel, Germany).*

Taken together, IL17A signaling appears dispensable for the induction of early plasma cells that were observed on day 8 after immunization with Ova-eCFA. Furthermore, no difference in the expression of St6gal1 was observed on day 8. However, on day 14, deficiency of either IL-17A or IL-17RA led to attenuated IgG1+ Ova-specific plasma cell development and failed to downregulate St6gal1 expression after immunization with Ova-eCFA. Furthermore, IL-17A-deficient mice induced higher sialylated Ova-specific IgG1 Abs as compared to WT mice, but they were not as high sialylated as in IL-6 KO mice (Fig. 3.18 and Fig. 3.26).

Recently, it has been reported that also IL-23 can induce pathogenic Th17 cells, which reduce St6gal1 expression in plasma cells and thus reduce the subsequent IgG sialylation in an induced autoimmune mouse model. These authors further suggested by *in vitro* experiments that IL-22 might be responsible for the observed downregulation (Pfeifle et al., 2017). IL-22 is often found co-expressed with IL-17A from Th17 cells (Liang et al., 2006). Here, IL-23p19 KO and IL-22 KO as compared to WT control mice were immunized with Ova-eCFA, and the specific IgG1 sialylation was analyzed 14 days after immunization (Fig. 3.27).

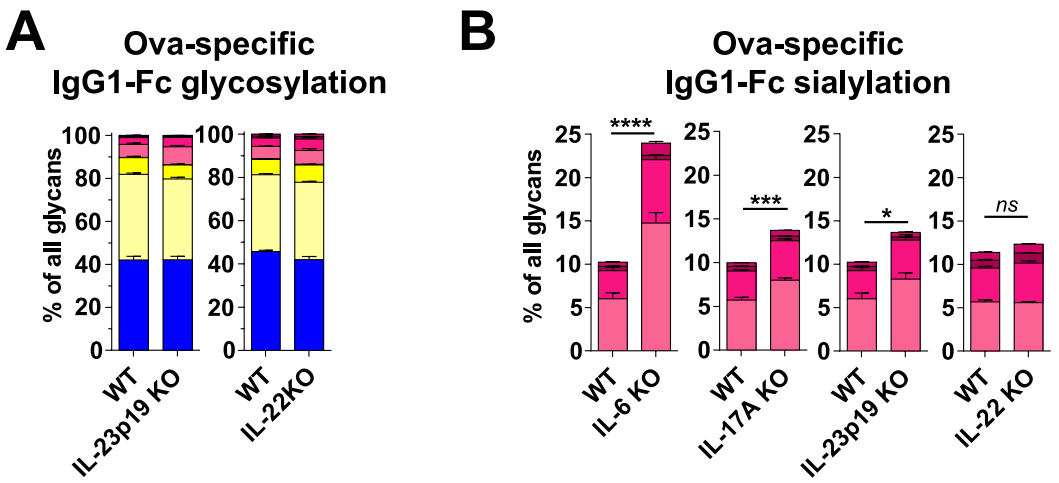

Fig. 3.27 ***Influence of the Th17-IL-23 axis on IgG1 glycosylation 14 days after immunization with Ova-eCFA.*** *C57BL/6 WT, IL-6, IL-17A, IL-23p19 and IL-22 deficient (KO) mice were immunized with Ova-eCFA in different experiments. Mice were bled 14 days after vaccination and the Ova-specific IgG1-Fc glycosylation investigated via LC-MS. (A) Fc Glycosylation profile of Ova-specific IgG1-antibodies of IL-23p19KO or IL-22KO or WT control mice. (B) Percent of sialylated anti-Ova IgG1-antibodies. IL-6 and IL-17A KO data were already shown in Fig. 3.18 and Fig. 3.26.* $n_{WT(each)} = 5$, $n_{IL\text{-}23p19} = 5$, $n_{IL\text{-}22} = 4$; $n_{IL\text{-}6} = 5$, $n_{IL\text{-}17A} = 7$. *The IL-17A KO experiments were conducted in collaboration with Christoph Hölscher (Research Center Borstel). The IL-22 KO experiments were conducted in collaboration with Anastasios Giannou (University Hospital Eppendorf, Hamburg, Germany). The LC-MS analysis was performed by the PhD student in our laboratory, Alexander Wagt, at the Center for Proteomics and Metabolomics (in collaboration with Manfred Wuhrer), Leiden University Medical Center, Leiden, the Netherlands.*

Interestingly, the suggested effects of IL-22 could not be reproduced in our *in vivo* model, and no difference between IL-22KO and WT control mice in terms of IgG1 Fc sialylation was observed. IL-23p19 deficient mice, however, showed increased portions of sialylated Ova-specific IgG1 Fc comparable to the changes observed in IL-17A KO mice (Fig. 3.27). However, the effects in IL-23p19 KO and IL-17A KO mice were not as strong as in IL-6 KO mice.

Additionally, on day 8, IL-22 and IL-17A serum concentrations were investigated in IL-23p19 KO and IL-6KO compared to WT control mice after immunization with Ova-eCFA (Fig. 3.28). While IL-17A expression was exclusively high in WT mice, which correlated with the observed low IgG1 sialylation level on day 14, IL-22 was only downregulated in IL-23p19 KO but not in IL-6 KO mice. This observation confirms an

IL-23p19 dependent secretion of IL-17A and IL-22 (Liang et al., 2006). However, IL-22 secretion was even upregulated in IL-6 KO. Together with the Ova-specific glycan analysis (Fig. 3.27), the cytokine levels indicate that IL-22 might not be involved in the downregulation of Ova-specific IgG1 sialylation in IL-6 KO mice.

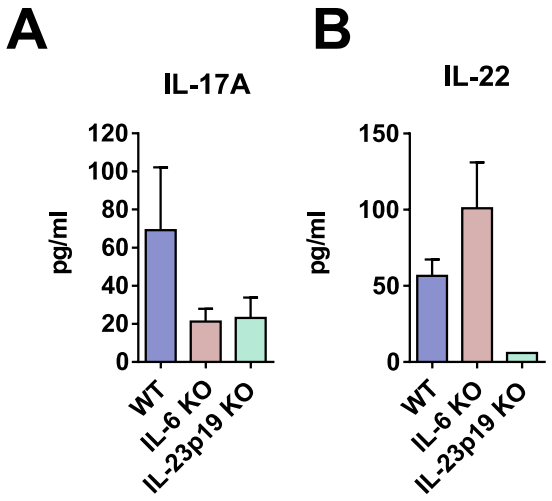

Fig. 3.28 ***Serum IL-17A and IL-22 are differently regulated in IL-6 KO, IL-23p19 KO and WT mice after Ova-eCFA immunization.*** *C57BL/6 WT, IL-6 KO or IL-23p19 KO mice were immunized with Ova-eCFA. Mice were bled eight days after immunization and serum (A) IL-17A and (B) IL-22 cytokines subsequently analyzed via Legendplex™ mouse Th17+ panel multiplex assay (n = 4–5 per group). IL-17A serum concentrations for IL-6 KO and WT mice are also shown in Fig. 3.22.*

Taken together, IL-6 and IL-23p19 are central cytokines for the induction of IL-17A producing CD4+ Th17 cells. IL-17A signaling is involved in the downregulation of St6gal1 protein in IgG1+Ova+ PCs after Ova-eCFA immunization and might explain, at least partially, the effects on St6gal1 expression and IgG1 sialylation observed in the IL-6 KO upon immunization with Ova-eCFA.

3.2.3 IL-6 receptor signaling on T cells reduces sialylation of vaccination induced IgG

The IL-23:IL-17A axis had significant impact on the induced Ova-specific IgG glycosylation pattern upon immunization with Ova-eCFA (see above). This result suggested the involvement of T cells, primarily Th17 cells, in the regulation of Ova-specific IgG Fc glycosylation.

Subsequently, to further investigate the role of IL-6 on T cells, mice that had a loxp site flanked IL-6 receptor gene (IL-6R; CD126) were crossed with mice that expressed a Cre recombinase under the control of the CD4 promotor. Hence, the generated mice were unable to produce the IL-6R in CD4 positive cells (or cells that were CD4+, e.g., during their development), that is, primarily T cells (Fig. A.5). As controls, littermates that had the IL-6R flox locus but did not express the Cre-recombinase were used.

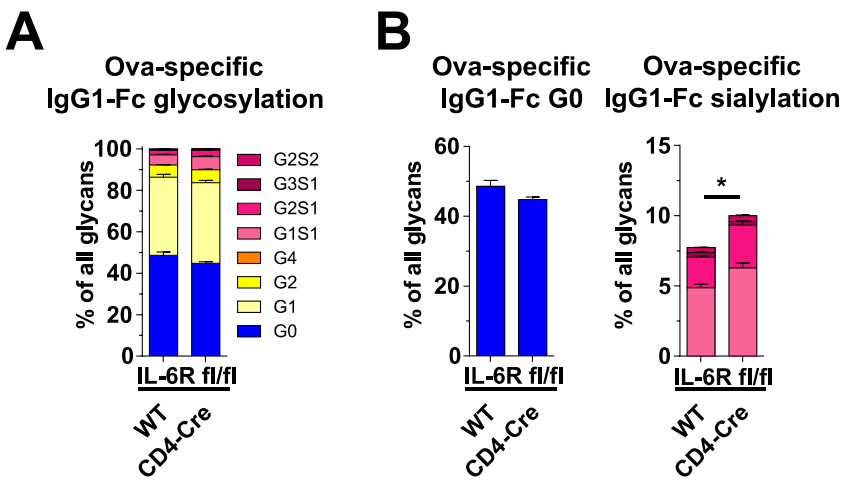

Fig. 3.29 ***IL-6 cis-signaling on T cells alters Ova-specific IgG1 Fc glycosylation after vaccination with Ova-eCFA on day 14.*** *CD4-specific IL-6R deficient (IL-6R fl/fl x CD4-Cre) or littermate control (IL-6R fl/fl; "WT") mice were immunized with Ova-eCFA. Mice were bled 14 days after vaccination and the Ova-specific IgG1 Fc glycosylation investigated by LC-MS. (A) Fc glycosylation profile of Ova-specific IgG1. (B) Percentages of G0 and sialylated Ova-specific IgG1. n = 4 mice per group. The LC-MS analysis was performed by the PhD student in our laboratory, Alexander Wagt, at the Center for Proteomics and Metabolomics (in collaboration with Manfred Wuhrer), Leiden University Medical Center, Leiden, the Netherlands. The experiments were conducted in collaboration with Nir Yogev and Ari Waisman (University of Mainz, Mainz, Germany).*

Interestingly, the analysis of Ova-specific IgG1 Fc glycosylation 14 days after Ova-eCFA immunization revealed a significant increase in sialylation between mice bearing IL-6R deficient T cells and respective controls (Fig. 3.29). Additionally, the total Ova-specific IgG and IgG2b titer was reduced in CD4+ T cell specific IL-6R KO mice (Fig. 3.30).

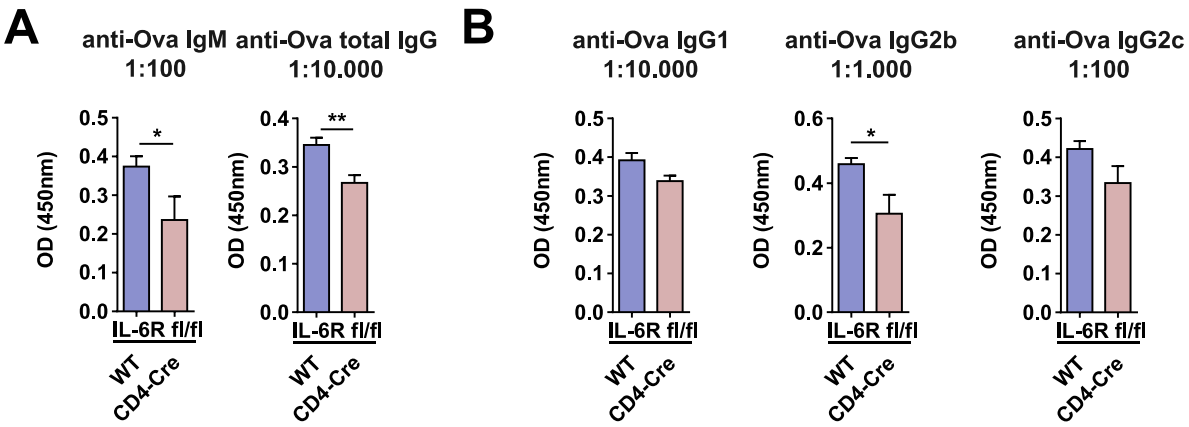

Fig. 3.30 ***IL-6 cis-signaling on T cells influences Ova-specific IgG titers after immunization with Ova-eCFA on day 14.*** *CD4-specific IL-6R deficient (IL-6Rfl/fl x CD4-Cre) or littermate control (IL-6Rfl/fl; "WT") mice were immunized with Ova-eCFA. Mice were bled 14 days after vaccination and Ova-specific ELISA performed. (A) ELISAs for anti-Ova IgM and anti-Ova total IgG. (B) ELISAs for anti-Ova IgG1, IgG2b and IgG2c. Serum dilutions are indicated in the graphs; n = 4 mice per group. The experiments were conducted in collaboration with Nir Yogev and Ari Waisman (University of Mainz, Mainz, Germany).*

In summary, the results obtained here indicate that the observed effects of IL-6 on St6gal1 expression and Ova-specific IgG1 Fc sialylation were (at least partly) mediated via direct signaling of IL-6 on T cells.

3.2.4 IL-6 trans-signaling, but not cis-signaling, drives Th17 differentiation

To confirm that the effects of IL-6 on IgG Fc glycosylation that were observed in the IL-6R flox x CD4-Cre model are mediated via the Th17 axis, T cell differentiation was investigated in this model on day 8 after Ova-eCFA immunization.

Surprisingly, IL-6 signaling on CD4+ T cells showed no influence on the establishment of Th17 cells as well as Foxp3+ CD4+ T cells (Fig. 3.31). Accordingly, comparable IL-17A serum concentrations were observed in these mice compared to the control mice (Fig. 3.31).

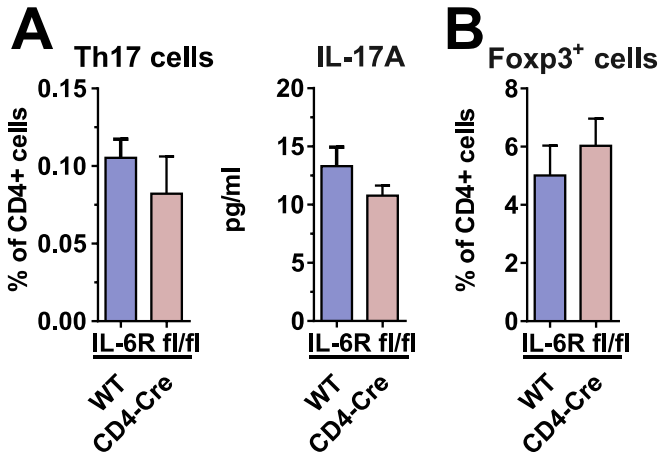

Fig. 3.31 ***IL-6 cis-signaling on T cells does not influence Th17 differentiation.*** *CD4-specific IL-6R deficient (IL-6Rfl/fl x CD4-Cre) or littermate control (IL-6Rfl/fl; "WT") mice were immunized with Ova-eCFA, and their spleens were harvested for flow cytometry analysis on day 8. (A) Splenocytes were re-stimulated and frequency of IL-17A producing CD4+ (Th17) cells determined by flow cytometry. IL-17A serum concertation was determined by Legendplex assay. (B) Splenocytes were also stained intranuclear for the expression of Foxp3. Frequency of Foxp3+ CD4 T cells. n = 5 mice per group. The experiments were conducted in collaboration with Nir Yogev and Ari Waisman (University of Mainz, Mainz, Germany).*

IL-6 has been shown to act on different cells, both immune and non-immune (Ho et al., 2015b), which became even more evident when the three modes of IL-6 signaling were elucidated, as summarized in Fig. 3.32. In the IL-6 cis signaling, IL-6 is recognized by the membrane-bound IL-6 receptor, and intracellular signaling is mediated after engagement and by the ubiquitously expressed co-receptor gp130 (CD130) (Garbers et al., 2015). The IL-6R has no intracellular signaling domain. In the IL-6 trans-signaling, soluble IL-6R (sIL-6R) binds to IL-6 and facilitates signaling via gp130. Thus, IL-6 trans-signaling can act on nearly all cells of the body (Garbers et al., 2015). By contrast, the classical or cis-signaling

involves the membrane bound IL-6R and is restricted to cells that express IL-6R on their surfaces.

Recently, a third mode of signaling has been suggested (Heink et al., 2017). During trans-presentation IL-6:IL-6R binding takes place inside the cell (e.g., in dendritic cells), and this complex is then processed to the cell surface, where it can activate gp130 on neighboring cells (Heink et al., 2017).

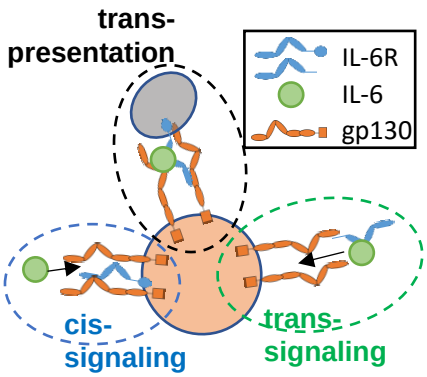

Fig. 3.32 Schematic overview of the three described IL-6 signaling pathways.

Downstream of gp130, Janus kinase (Jak) dependent phosphorylation activates the signal transducer and activator of transcription (STAT3) (Garbers et al., 2015). Since the requirement for gp130 is independent of the mode of signaling, the intracellular signal transduction of gp130 is believed to be identical for the three signaling modes (Garbers et al., 2018). However, the tropism of IL-6 is clearly different between the three signaling modes.

Under physiological conditions, a soluble form of gp130 (sgp130) exists (Narazaki et al., 1993). It has been shown that sgp130 can interact with the IL-6:sIL-6R complex and thereby inhibit trans-signaling, but neither cis-signaling nor trans-presentation (Jostock et al., 2001; Heink et al., 2017).

In the IL-6R flox x CD4-Cre model, only the cis-signaling pathway is compromised. Hence, to elucidate the role of IL-6 trans-signaling on Th17 differentiation, a transgenic mouse that overexpresses sgp130 (fused to a murine IgG1 Fc part; sgp130Fc tg; Rabe et al., 2008) was immunized with Ova-eCFA. Intriguingly, Th17 differentiation was completely inhibited in the sgp130Fc tg mice on day 8 after immunization, as observed for the complete IL-6 KO (Fig. 3.33). Likewise, serum IL-17A concentrations were reduced in the sgp130Fc tg mice compared to controls.

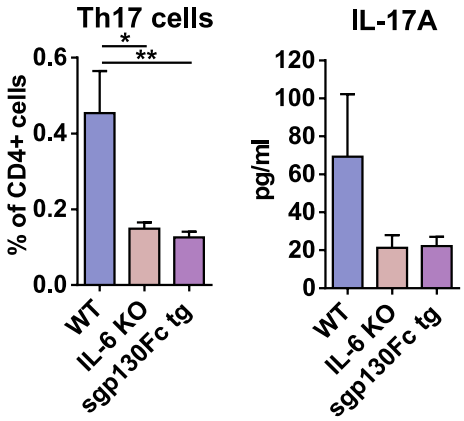

Fig. 3.33 ***Th17 cell differentiation and IL-17 secretion requires IL-6 trans-signaling****. C57BL/6 WT, IL-6 KO and sgp130Fc tg mice were immunized with Ova-eCFA, and their spleens and serum were harvested on day 8. (A) Splenocytes were restimulated for intracellular cytokine staining. Frequencies IL-17A expressing CD4+ cells were analyzed. (B) Serum IL-17A cytokine was analyzed via multiplex assay. Compare also Fig. 3.22.*

These data clearly indicated that IL-6 trans-signaling is important for Th17 cell induction upon Ova-eCFA immunization. Targeted inhibition of IL-6 trans-signaling (e.g., with sgp130Fc) can abrogate Th17 differentiation and may resolve the Th17 mediated effects on St6gal1 expression levels in PCs and IgG Fc sialylation. However, this must be confirmed in future experiments, for example, after immunization of sgp130Fc tg mice and subsequent analysis of Ova-specific IgG Fc glycosylation.

Notably, IL-6 trans-presentation via IL-6:IL-6R complexes on CD11c+ DCs and gp130 on CD4+ T cells, as described recently, did not play here a role in determining the IgG Fc glycosylation, as IL-6R flox x CD11c-Cre mice showed no IgG Fc glycosylation changes compared to their controls upon Ova-eCFA immunization (Fig. 3.34). Furthermore, the result showed that IL-6 cis-signaling on CD11c+ cells was not required for the effects as well.

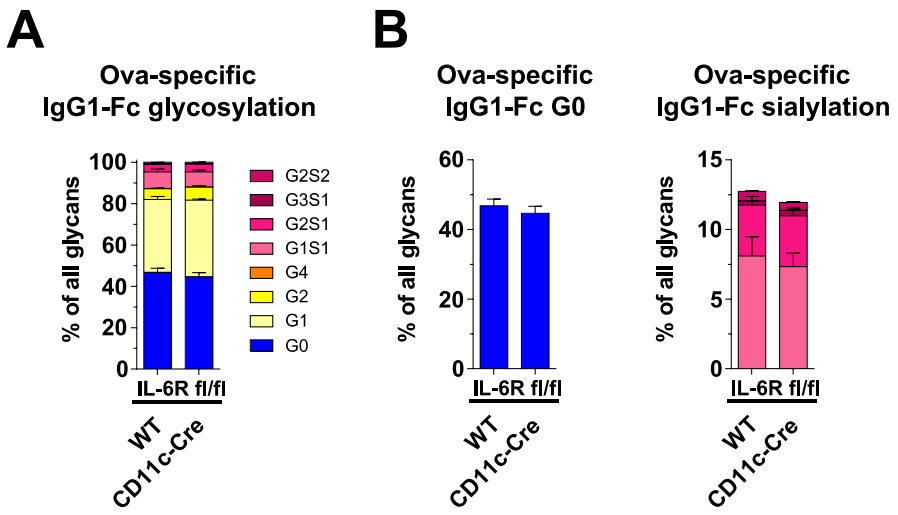

Fig. 3.34 ***IL-6 trans-presentation by CD11c+ cells has no effects on Ova-specific IgG1 Fc glycosylation after vaccination with Ova-eCFA.*** *CD11c-specific IL-6R deficient (IL-6R fl/fl x CD11c-Cre) or littermate control (IL-6R fl/f; "WT"l) mice were immunized with Ova-eCFA. Mice were bled 14 days after vaccination and the Ova-specific IgG-Fc glycosylation investigated by LC-MS. (A) Glycosylation profile Ova-specific IgG1. (B) Percentages of G0 and sialylated Ova-specific IgG1.* $n_{WT} = 3$, $n_{CD11c} = 5$. *The LC-MS analysis was performed by the PhD student in our laboratory, Alexander Wagt, at the Center for Proteomics and Metabolomics (in collaboration with Manfred Wuhrer), Leiden University Medical Center, Leiden, the Netherlands. The experiments were conducted in collaboration with Nir Yogev and Ari Waisman (University of Mainz, Mainz, Germany).*

3.2.5 IL-6 cis-signaling induces T follicular helper cell differentiation and promotes germinal centers

Th17 cells were not affected by the IL-6R deficiency in T cells and, hence, could not explain the IgG glycosylation difference seen in this model. Therefore, T cell differentiation was further analyzed in this mice. Aside from Th17 differentiation, IL-6 has additionally been described as important for the induction of T follicular helper cells after vaccination (Riteau et al., 2016). These cells are characterized by the expression of ICOS and CXCR5 (Fig. 3.35) and support B cell maturation in the GC reaction (Crotty, 2011). T follicular helper cells can be further discriminated by the expression of Foxp3. Foxp3-non-expressing CD4+ T follicular helper cells have been termed T_{FH} cells, and Foxp3-expressing cells have been termed regulatory T follicular helper cells (T_{FR}). T_{FR} cells are involved in suppressing and resolving the GC reaction. The ratio of the frequencies of activating T_{FH} and suppressing T_{FR} cells was used here to assess the strength of the GC reaction. A ratio towards T_{FH} cells (T_{FH} >> T_{FR}) accounts for an ongoing pro-inflammatory GC reaction (Vaeth et al., 2014).

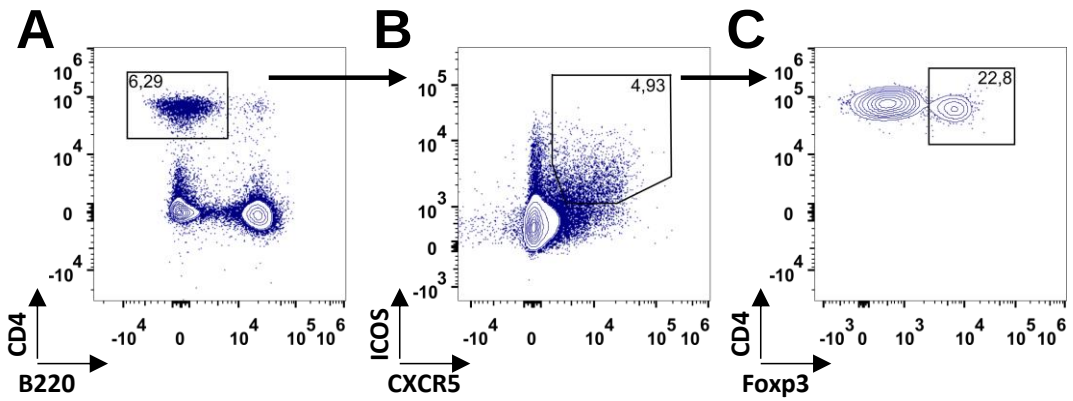

Fig. 3.35 ***Representative flow cytometric gating strategy for identifying effector and regulatory T follicular helper cells.*** *Splenocytes were stained extra- and intracellularly, as described, and flow cytometric analysis was performed on the Attune Nxt flow cytometer. Cells were pre-gated on single, viable lymphocytes. (A) Gating for CD4+ T cells. (B) T follicular helper cells were identified by the expression of CXCR5 and ICOS among the CD4+ population. (C) CXCR5+ICOS+CD4+ cells were further characterized by the nuclear expression of Foxp3. Cells that fall into the Foxp3+ gate are designated T_{FR}, while Foxp3- cells are designated T_{FH}.*

Indeed, T follicular helper cells were considerably reduced in IL-6R flox x CD4-Cre mice eight days after Ova-eCFA vaccination compared to respective controls (Fig. 3.36). In particular, the frequency with which T_{FH} cells were activated was affected, while the frequency of regulatory T_{FR} cells remained indistinguishable between the genotypes. Likewise, the ratio of T_{FH}:T_{FR} cells indicated a stronger GC reaction in the control group.

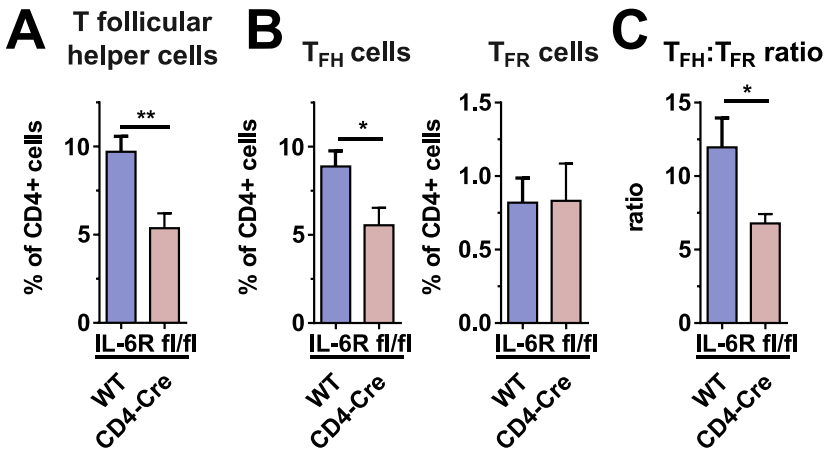

Fig. 3.36 ***IL-6 cis-signaling in T cells skew T cell differentiation towards T follicular helper cells phenotype.*** *CD4-specific IL-6R deficient (IL-6Rfl/fl x CD4-Cre) or littermate control (IL-6Rfl/fl; "WT") mice were immunized with Ova-eCFA, and their spleens were harvested for flow cytometry analysis on day 8. (A) Frequencies of all CXCR5+ICOS+ T follicular helper cells (B) T follicular helper cells were further discriminated by the expression of Foxp3 into T_{FH} (Foxp3-) and T_{FR} (Foxp3+) cells (C) Ratio of T_{FH} to T_{FR} cells. n = 4–5 mice per group. The experiments were conducted in collaboration with Nir Yogev and Ari Waisman (University of Mainz, Mainz, Germany).*

T_{FH} cells are critical for the induction and progress of the GC reaction, whereas T_{FR} cells are responsible for resolving a GC reaction. During the GC reaction, T_{FH} cells provide T cell

help to GC B cells and drive their affinity maturation, class switch and differentiation into memory or plasma cells. GC B cells, by contrast, can also provide stimulatory signals to T_{FH} cells, which subsequently further provokes the GC reaction. IL-6 cis-signaling had an important effect on the differentiation of T follicular helper cells, and hence, the question of whether germinal center B cells were compromised upon the loss of IL-6R on T cells is analyzed. Aside from the pan-B cell marker B220 (CD45R), GC B cells were identified by the co-expression of the activation marker GL7 and CD95 (Fas) (Victora & Nussenzweig, 2012) (Fig. 3.37).

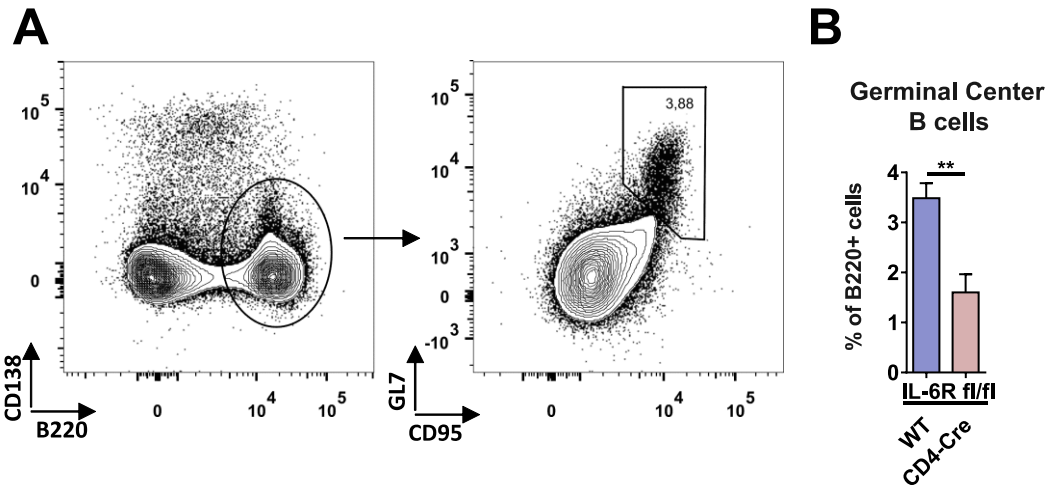

Fig. 3.37 ***Representative flow cytometric gating strategy for identifying germinal center B cells****. Splenocytes were stained extra- and intracellularly as described, and flow cytometric analysis was performed on the Attune Nxt flow cytometer. Cells were pre-gated on single, viable lymphocytes. (A) Germinal center cells were gated as CD138-,B220+ and GL7+CD95(Fas)+. (B) Frequency of germinal center B cells on day 8 after Ova-eCFA in CD4-specific IL-6R deficient (IL-6Rfl/fl x CD4-Cre) or littermate control (IL-6Rfl/fl; "WT") mice. n = 4–5 mice per group. The CD4-Cre experiment was conducted in collaboration with Nir Yogev and Ari Waisman (University of Mainz, Mainz, Germany).*

As expected, the reduced differentiation of T_{FH} in the IL-6R flox x CD4-Cre mice was accompanied by reduced frequencies of GC B cells (Fig. 3.37). Likewise, a reduction of T_{FH} and GC B cells was observed in mice that were completely deficient in IL-6 (IL-6 KO) (Fig. 3.38). Interestingly, IL-6 KO mice did not completely fail to induce GC B cells on day 8 following Ova-eCFA immunization (Fig. 3.38). However, in contrast to the WT controls, GC B cells were not maintained until day 14 post-immunization (Fig. 3.39). Moreover, T follicular helper cell induction was comparably low between days 8 and 14 in the IL-6KO mice. Worthy of note is that IL-6 trans-signaling had no effect on the induction of GC B cells or T follicular helper cells on day 8 since no difference was observed in sgp130Fc tg mice (Fig. 3.38).

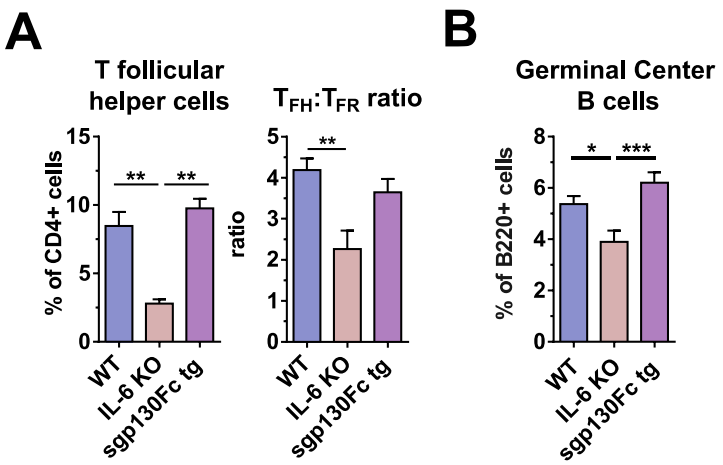

Fig. 3.38 ***IL-6 cis but not trans-signaling is indispensable for the induction of germinal center B and T cells on day 8 after Ova-eCFA immunization.*** *C57BL/6 WT, IL-6 KO or sgp130FC tg mice were immunized with Ova-eCFA and their spleens were harvested for flow cytometry analysis on day 8. (A) Frequencies of all T follicular helper cells and the ratio of T_{FH}:T_{FR} cells. (B) Frequency of germinal center B cells. n_{WT} = 9, $n_{IL\text{-}6}$ = 10, n_{sgp130} = 9 pooled from two different experiments.*

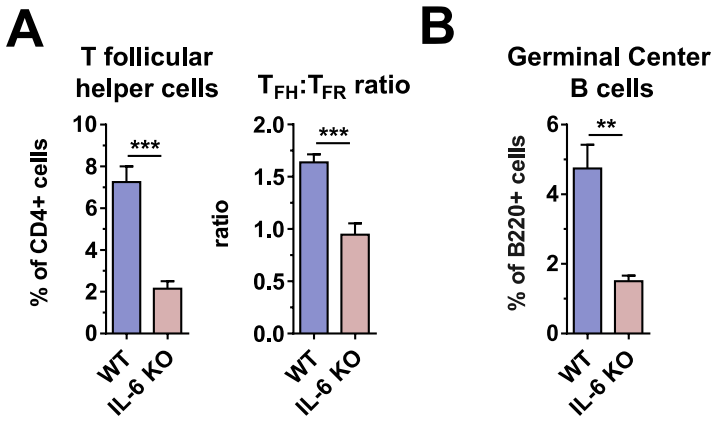

Fig. 3.39 ***IL-6 is indispensable for the induction of germinal center B and T cells on day 14 after Ova-eCFA immunization.*** *C57BL/6 WT and IL-6 KO mice were immunized with Ova-eCFA, and their spleens were harvested for flow cytometry analysis on day 14. (A) Frequencies of all T follicular helper cells and the ratio of T_{FH}:T_{FR} cells. (B) Frequency of germinal center B cells. n = 5 mice per group.*

Taken together, a clear influence of IL-6 on the induction of germinal center cells after Ova-eCFA immunization was observed. Interestingly, the data indicate that IL-6 cis-signaling preferentially induces germinal centers (most likely via the induction of T_{FH} cells), while IL-6 trans-signaling skewed T cell differentiation towards a Th17 phenotype.

Whether these IL-6 mediated effects also play a role in the adjuvant-induced immune responses of mice is investigated for germinal center and Th17 differentiation after immunization with Ova-eCFA and Ova-Alum in the following.

3.2.6 Ova-eCFA but not Ova-Alum leads to a more durable germinal center and Th17 differentiation

Germinal centers are source of class-switched and affinity maturated plasma and memory B cells. Hence, GCs play a critical role in vaccine-induced protection. Remarkably, vaccination with Ova-eCFA and Ova-Alum induced comparable levels of GC B cells on day 8 after immunization (Fig. 3.40). However, T follicular helper cells and the ratio of T_{FH} to T_{FR} cells were upregulated upon Ova-eCFA vaccination. Appropriately, GC B cells disappeared until day 14 after Ova-Alum vaccination, while in the case of Ova-eCFA, GC B cells and T follicular helper cells continued to be present even up to day 14 (Fig. 3.41).

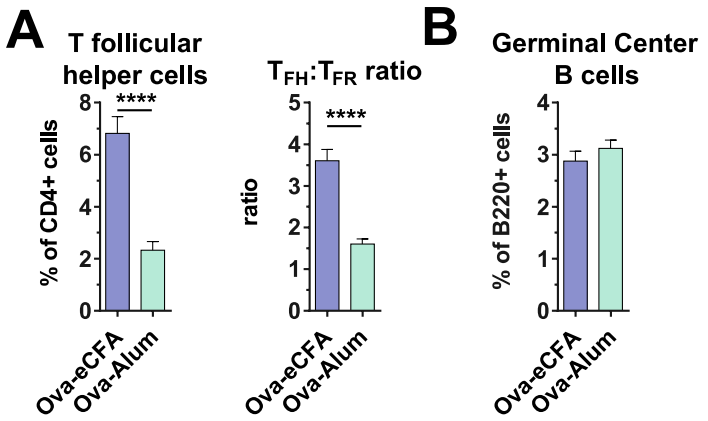

Fig. 3.40 ***Vaccination with Ova-Alum induces lower T follicular helper cells than Ova-eCFA on day 8 after immunization.*** *C57BL/6 WT mice were immunized with Ova-eCFA or Ova-Alum and spleens for flow cytometry analysis harvested on day 8. (A) Frequencies of all T follicular helper cells and the ratio of T_{FH}:T_{FR} cells. (B) Frequency of germinal center B cells. n = 9 mice per group pooled from two independent experiments.*

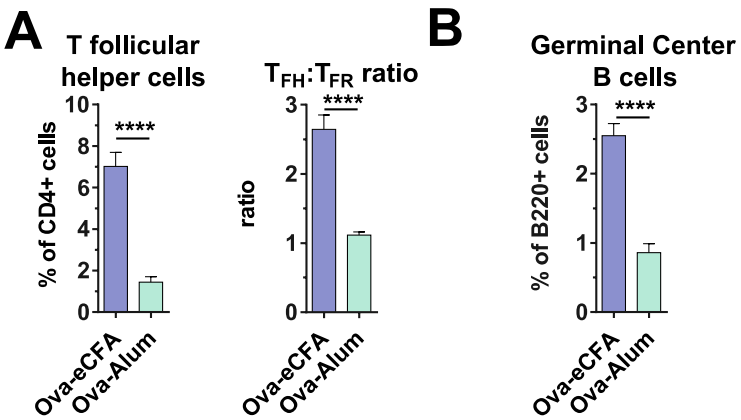

Fig. 3.41 ***Ova-eCFA but not Ova-Alum vaccination induces long-lasting germinal centers until day 14 after immunization****. C57BL/6 WT mice were immunized with Ova-eCFA or Ova-Alum, and their spleens were harvested for flow cytometry analysis on day 14. (A) Frequencies of all T follicular helper cells and the ratio of T_{FH}:T_{FR} cells. (B) Frequency of germinal center B cells. n = 9 mice per group pooled from two independent experiments.*

IL-6 trans-signaling was responsible for the induction of Th17 cells after Ova-eCFA immunization. Consequently, Th17 responses after immunizations with different adjuvants are compared.

First, immunization of IL-17A reporter (IL-17A-eGFP) mice with different adjuvants revealed an adjuvant-dependent induction of Th17 cells (Fig. 3.42). The amount of Mycobacteria tuberculosis (Mtb.) that was used to complete Freund's Adjuvant correlated with the induction of Th17 cells, with 5 mg/ml Mtb. in eCFA inducing the most Th17 cells. While 1 mg/ml (CFA) or no Mtb. (IFA) induced comparable intermediate Th17 cells, Alum immunizations induced the least Th17 cells.

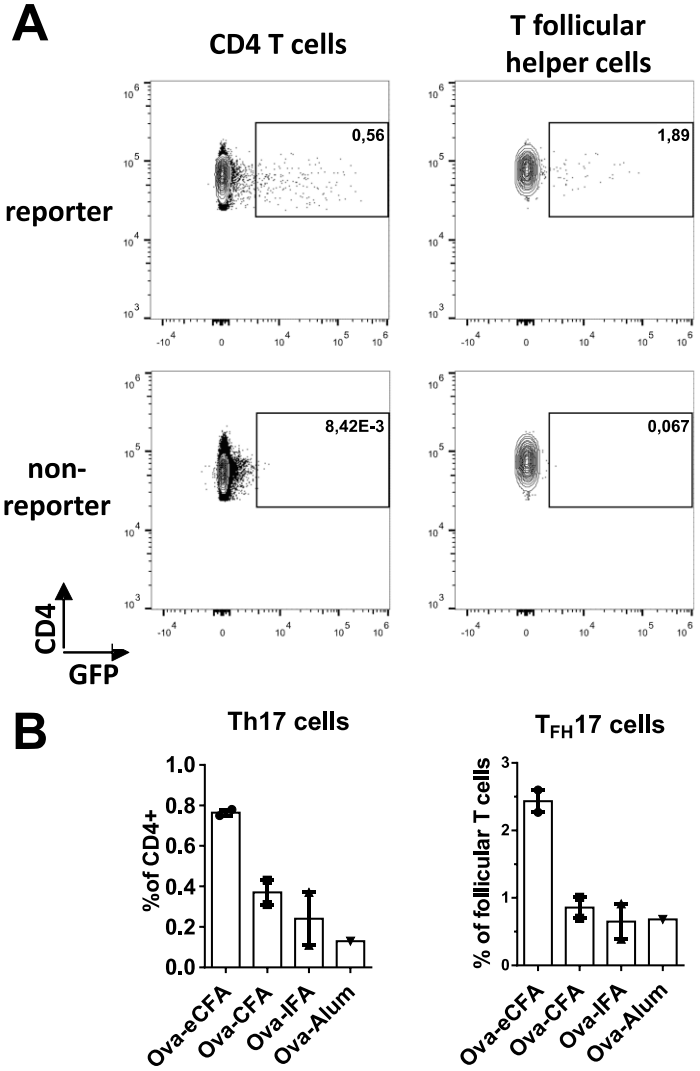

Fig. 3.42 ***IL-17A reporter mice identify IL-17A producing CXCR5+ICOS+ T follicular helper cells.*** *IL-17A-eGFP reporter mice were immunized with Ova and different adjuvants. Spleens were harvested for flow cytometric analysis on day 14 after immunization. Splenocytes were stained for extracellular markers (A) Representative flow cytometric gating strategy for IL-17A expressing CD4+ T cells and T follicular helper cells upon Ova-eCFA immunization in reporter (upper panel) or naive non-reporter (lower panel) mice. Cells were pre-gated on single, viable lymphocytes. T follicular helper cells were identified by the expression of CD4, ICOS and CXCR5. (B) Frequency of IL-17A expressing CD4+ T cells (Th17 cells) and IL-17A expressing T follicular helper cells ($T_{FH}17$ cells) upon the different immunizations ($n_{eCFA} = 2$, $n_{CFA} = 2$, $n_{IFA} = 2$, $n_{Alum} = 1$). The experiments were conducted in collaboration with Christoph Hölscher (Research Center Borstel).*

Moreover, the analysis of CXCR5+ICOS+ T follicular helper cells identified an IL-17A producing subset that is referred to as $T_{FH}17$ cells in the following. $T_{FH}17$ cells were only upregulated when high amounts of Mtb. in eCFA were used as an adjuvant (Fig. 3.42).

Next, the IL-17A expression findings were confirmed by intracellular IL-17A staining after *ex vivo* re-stimulation of CD4+ T cells from WT animals after eCFA and Alum immunizations (Fig. 3.43). Interestingly, on day 8 after immunization, there was no induction of Th17 cells compared to untreated controls detectable for Ova-eCFA and Ova-Alum immunizations. On day 14, however, only eCFA immunizations led to increased differentiation of Th17 cells. In contrast, induction of $T_{FH}17$ cells were already observed early on day 8 upon Ova-eCFA. The induction of $T_{FH}17$ differentiation was not detectable in Ova-Alum immunizations (Fig. 3.43).

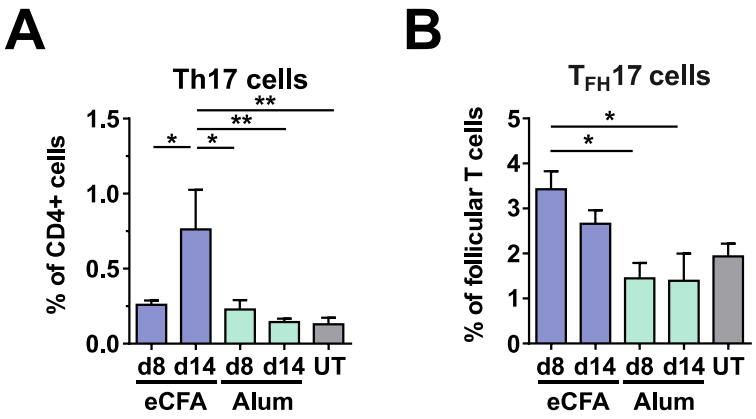

Fig. 3.43 ***Th17 and T_{FH}17cell differentiation upon vaccination.*** *C57BL/6 WT mice were immunized with Ova-eCFA or Ova-Alum or left untreated. Spleens were harvested on days 8 or 14 after immunization. Splenocytes were restimulated for intracellular cytokine staining. (A) Frequencies IL-17A expressing cells of CD4+ T cells and (B) Frequencies of IL-17A expressing cells of CXCR5+ICOS+CD4+ T follicular helper cells on the indicated day. UT = untreated, n = 5 mice per group and day.*

In summary, Ova-Alum immunization led to reduced induction of T follicular helper cells compared to Ova-eCFA. Likewise, only Ova-eCFA immunization led to an increased induction of Th17 cells. Interestingly, $T_{FH}17$ cells were also induced upon Ova-eCFA but not upon Ova-Alum immunization. It might be possible that $T_{FH}17$ cells play a particular role in regulating IgG Fc glycosylation and are required, for example, to maintain the GC reaction up to day 14 after Ova-eCFA immunization. Accordingly, the effect of IL-17A on the durability of GC cells is subsequently investigated.

3.2.7 IL-17A signaling does not influence germinal center cell frequencies

To investigate whether IL-17A derived from Th17 or, in particular, from $T_{FH}17$ cells influences the GC reaction and whether this may explain the changes in the IgG Fc

glycosylation between IL-17A KO and WT mice, the GC was analyzed in these two strains after immunization with Ova-eCFA. Because the differences in Th17 cells were more pronounced on day 14 in the aforementioned models, this day was selected for analysis (Fig. 3.44). Remarkably, no differences in the frequencies of GC B cells and T follicular helper cells, or on the ratio of T_{FH}:T_{FR} cells, was observed.

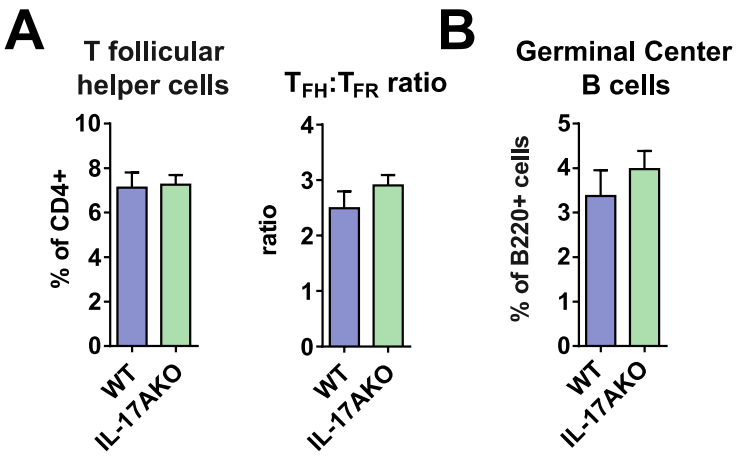

Fig. 3.44 ***IL-17A has no influence on the germinal center reaction.*** *C57BL/6 WT or IL-17A KO mice were immunized with Ova-eCFA, and their spleens were harvested for flow cytometry analysis on day 14. (A) Frequencies of all T follicular helper cells and the ratio of T_{FH}:T_{FR} cells. (B) Frequency of germinal center B cells. n_{WT} = 5, $n_{IL\text{-}17A}$ = 7. The experiments were conducted in collaboration with Christoph Hölscher (Research Center Borstel).*

These data suggested that the quantity of GC cells was not influenced by IL-17A. However, the data did not completely rule out an involvement of IL-17A on the quality of the GC reaction (differentiation, class-switching or regulation of St6gal1 expression of plasma cells during the GC reaction).

Overall, the quantity of T follicular helper cells and the ratio of T_{FH}:T_{FR}, but also qualitative differences of the T follicular helper cell response (e.g., cytokine, such as IL-17A, expression) might influence the GC response and therefore the St6gal1 expression level in the PCs.

3.2.8 Enhanced T_{FH}:T_{FR} ratios led to more pro-inflammatory IgG Fc glycosylation pattern upon vaccination

The vaccination-induced IgG Fc glycosylation pattern seemed to correlate with the strength of the induced GC reaction (frequency of GC B cells, ratio T_{FH}:T_{FR} and perhaps the induced cytokine profile). To functionally test whether alteration in the GC could indeed influence the IgG glycosylation, mice with Foxp3-specific deficiency in the Nuclear factor of activated

T cells 2 transcription factor (Nfat2/Nfat-c1; Nfat-c1 flox x Foxp3+-Cre mice) were investigated upon Ova-LPS immunization. It has been shown that the specific depletion of Nfat-c1 alters the homing behavior of TFR cells, and these mice subsequently showed reduced frequencies of TFR cells and an elevated GC reaction (Vaeth et al., 2014).

Vaccination with Ova-eCFA induced strong GC responses, and the ratio of follicular T cells is clearly on the side of promoting T_{FH} cells. Immunization with Ova-LPS, by contrast, showed a lower induction of GCs and equalized ratios of T_{FH} and T_{FR} cells. Hence, Ova-LPS was chosen for the vaccination of the T_{FR} deficient Nfat-c1 fl x Foxp3-Cre ("Nfat") mice. As controls, mice that had the Nfat-c1 flox locus but no locus for the Cre-recombinase were used as controls ("WT").

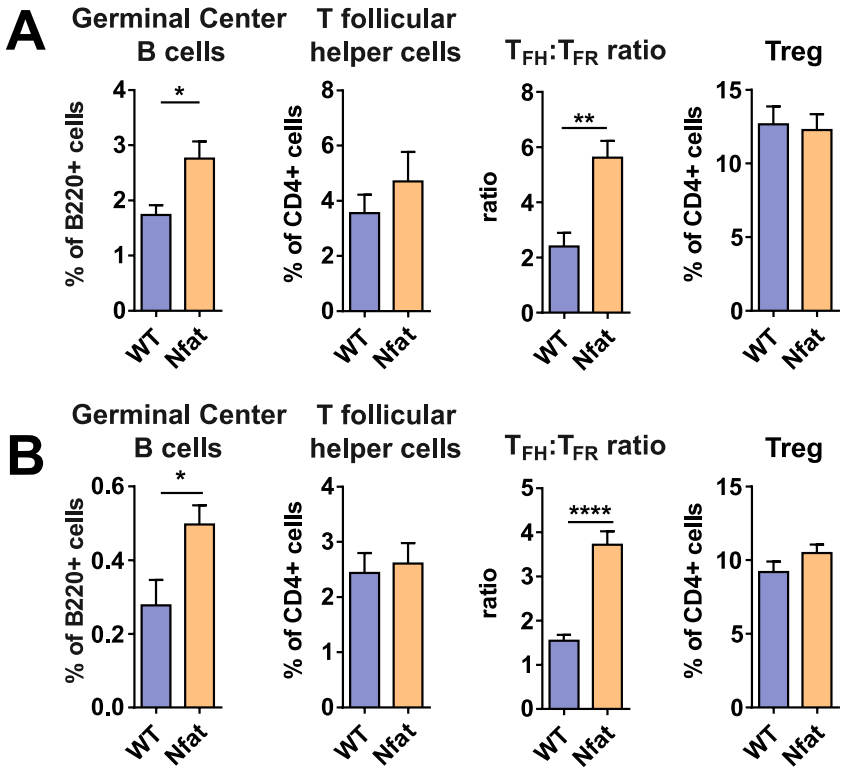

Fig. 3.45 ***Loss of "Nuclear-factor of activated T cells 2" (NFAT-c1) in Foxp3+ cells alters Germinal centers.*** *Foxp3-specific Nfat-c1 deficient (Nfat) or littermate control (WT) mice were immunized with Ova-LPS, and their spleens were harvested for flow cytometry analysis on days 8 (A) and 14 (B). Shown is the frequency of Foxp3+ CD4 T cells and of all T follicular helper cells and the ratio of T_{FH}:T_{FR} cells for both days. (A) n_{WT} = 5, n_{Nfat} = 6; (B) n_{WT} = 8, n_{Nfat} = 6. The experiments were conducted in collaboration with Raghu Erapaneedi and Friederike Berberich-Siebelt (University of Würzburg, Würzburg, Germany).*

Indeed, 8 and 14 days after immunization with Ova-LPS, the loss of T_{FR} cells in the Nfat mice led to an augmented the GC reaction, which was indicated by increased frequencies of GC B cells, T follicular helper cells and an increased T_{FH}:T_{FR} ratio (Fig. 3.45). Foxp3 specific deletion of Nfat-c1 had no effect on the overall Treg population (Fig. 3.45).

Furthermore, Nfat-c1 deficiency in Foxp3+ cells led to an overall upregulation of plasma cells on days 8 and 14 after vaccination (Fig. 3.46). Intriguingly, St6gal1 expression of IgG1 producing Ova-recognizing plasma cells was not altered on day 8, the point at which GCs are just established. However, 14 days after the immunization St6gal1 expression was significantly decreased in the T_{FR} deficient mice (Fig. 3.46).

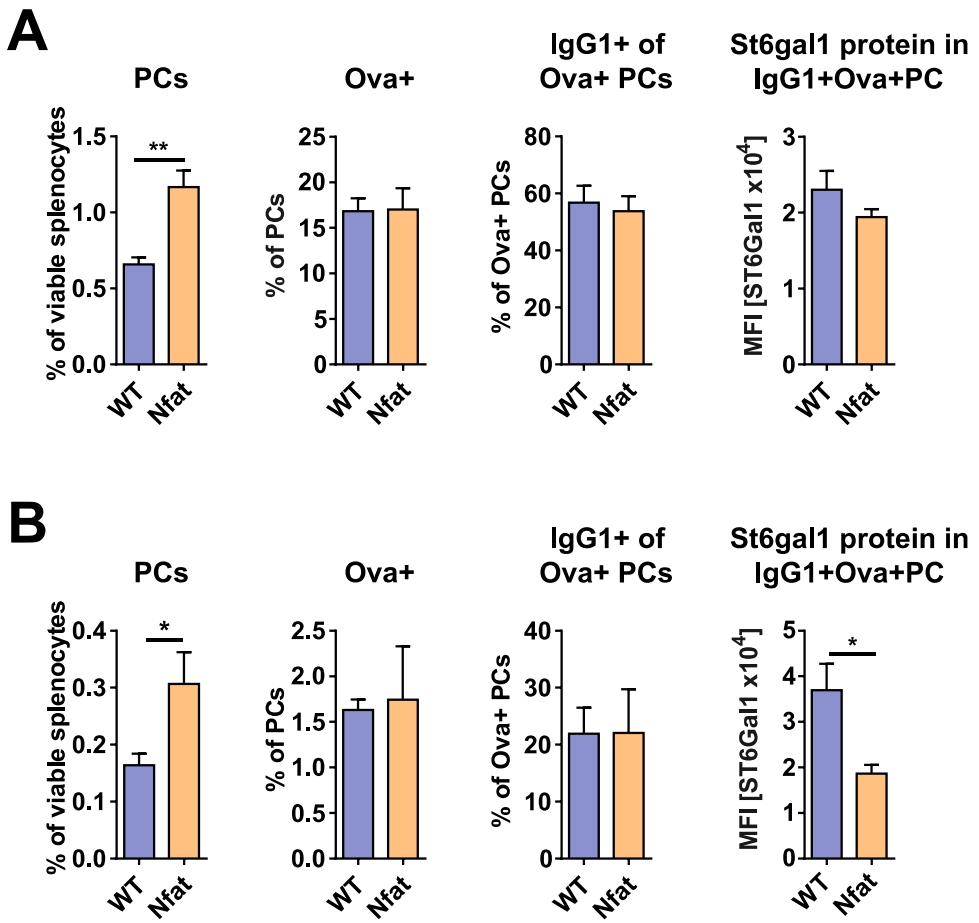

Fig. 3.46 ***Loss of "Nuclear-factor of activated T cells 2" (NFAT-c1) in Foxp3+ cells alters vaccination induced plasma cell responses.*** *Foxp3-specific Nfat-c1 deficient (Nfat) or littermate control (WT) mice were immunized with Ova-LPS, and their spleens were harvested for flow cytometry analysis on days 8 (A) and 14 (B). Shown is the frequency of plasma cells, Ova+ plasma cells and IgG1+ of Ova+ PCs, as well as St6gal1 expression in IgG1+Ova+ plasma cells on days 8 (A) and 14 (B), respectively. (A) n_{WT} = 5, n_{Nfat} = 6; (B) n_{WT} = 8, n_{Nfat} = 6. The experiments were conducted in collaboration with Raghu Erapaneedi and Friederike Berberich-Siebelt (University of Würzburg, Würzburg, Germany).*

Unfortunately, Ova-specific IgG1 glycosylation could not be determined by LC-MS. Nevertheless, IgG2 Fc sialylation of Ova-specific antibodies was reduced in Nfat-c1 fl x Foxp3-Cre mice (Fig. 3.47).

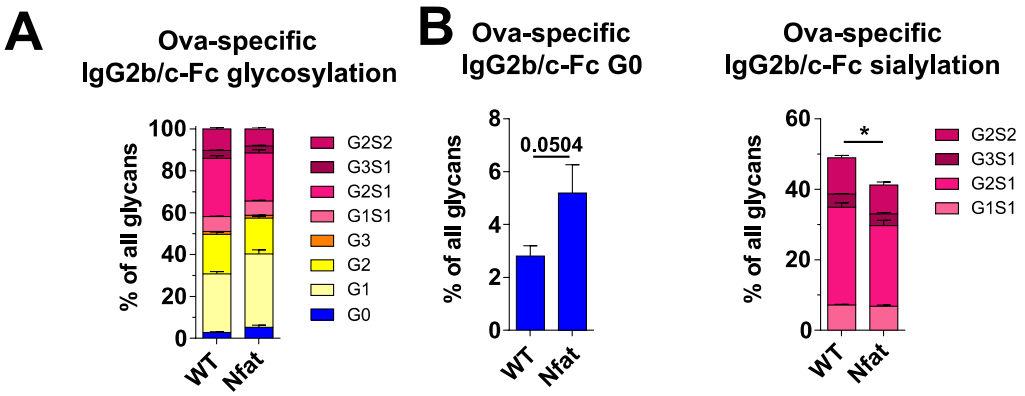

Fig. 3.47 ***Loss of "Nuclear-factor of activated T cells 2" (NFAT-c1) in Foxp3+ cells leads to attenuation of IgG2b/c Fc sialylation 14 days after vaccination.*** *Foxp3-specific Nfat-c1 deficient (Nfat) or littermate control (WT) mice were immunized with Ova-LPS. Mice were bled 14 days after vaccination, and the Ova-specific IgG2b/c Fc glycosylation was investigated by LC-MS. (A) Glycosylation profile Ova-specific IgG2b/c. (B) Percentages of G0 and sialylated Ova-specific IgG2b/c. n = 6 mice per group. The LC-MS analysis was performed by the PhD student in our laboratory, Alexander Wagt, at the Center for Proteomics and Metabolomics (in collaboration with Manfred Wuhrer), Leiden University Medical Center, Leiden, the Netherlands. The experiments were conducted in collaboration with Raghu Erapaneedi and Friederike Berberich-Siebelt (University of Würzburg, Würzburg, Germany).*

Together, these data demonstrate that augmented GC reactions upon the loss of T_{FR} cells had a significant influence on the St6gal1 expression in Ova+IgG1+ PCs and Ova-specific IgG sialylation.

4 Discussion

IgG Fc glycosylation is an important modulator of IgG-mediated effector functions, for example, in the context of autoimmune diseases or effective pathogen clearance (Collin & Ehlers, 2013; Alter et al., 2018). Agalactosylated IgG has been linked to pro-inflammatory effects (Ito et al., 2014; Parekh et al., 1985). By contrast, galactosylation and sialylation of IgG Fc molecules is linked to less-inflammatory or immunosuppressive functions (Kaneko et al., 2006; Karsten et al., 2012). Likewise, the sialylated portion of intravenous IgG (IVIG; pooled from healthy donors) has been shown to be beneficial as a treatment of autoimmune disorders (Schwab & Nimmerjahn, 2013). Moreover, the IgG glycosylation pattern appears to be more pro-inflammatory in patients with inflammatory diseases such as rheumatoid arthritis (RA), systemic lupus erythematosus (SLE), multiple sclerosis (MS) or inflammatory bowel diseases (IBD) (Parekh et al., 1985; Vučković et al., 2015; Wuhrer et al., 2015; Trbojević Akmačić et al., 2015).

Alterations in IgG glycosylation have also been found in other contexts such as cancer (Theodoratou et al., 2016) and chronic hepatitis infections (Ho et al., 2015a). In addition, as also shown here, vaccination can induce distinct antigen-specific glycosylation patterns (Selman et al., 2012a; Mahan et al., 2016; Kao et al., 2017). Genome-wide association studies suggested the involvement of inflammation-associated genes to IgG glycosylation (Lauc et al., 2013; Wahl et al., 2018).

These findings are, however, dependent on other factors. As such age, gender or smoking have been associated with differences in the IgG glycosylation patterns (Plomp et al., 2017). Likewise, the total IgG glycosylation of healthy human individuals investigated here was also dependent on age (Fig. 3.2 and Fig. 3.3). In the early years of the life (< 20 years), the IgG glycosylation pattern appears more pro-inflammatory (less galactosylated and sialylated), but levels of galactosylation and sialylation increase with age. From the mid of the twenties on, levels of galactosylation and sialylation begin once more to decrease, and the IgG glycosylation again becomes more pro-inflammatory with advancing age.

In this work, a high-throughput method for the analysis of IgG glycosylation was developed and used to analyze a cohort of people with a heterozygous mutation in their *CTLA4* allele compared to age and gender matched healthy controls. CTLA4 is an inhibitory T cell co-receptor that facilitates its function by competing with stimulatory co-receptors (e.g., CD28) for co-stimulatory molecules (e.g., CD80/86) on antigen-presenting cells (Wing et al., 2008; Sage et al., 2014). Likewise, CTLA4 deficiency can lead to a syndrome with diverse phenotypes that range from no symptoms over immune-deficiency syndromes (e.g., hypogammaglobulinemia) to increased (auto-) inflammatory diseases (Schwab et al., 2018).

Interestingly, compared to the healthy controls, people with a heterozygous mutation in their *CTLA4* allele demonstrated IgG glycosylation that was more pro-inflammatory with decreased levels of sialylation and galactosylation (Fig. 3.2 and Fig. 3.3).

Increased bisection was observed with the HPLC and LC-MS based methods. Although bisection is not directly linked to a pro- or anti-inflammatory phenotype, it has been described to counteract fucosylation (Ferrara et al., 2006; Vidarsson et al., 2014). Afucosylation is considered to be more pro-inflammatory. Afucosylated IgG has greater affinities to activating FcγR, and enhanced ADCC has been observed (Shields et al., 2002; Li et al., 2017). Fucosylation was only measured via the LC-MS approach, whereas in the HPLC analysis, IgG deglycosylation with EndoS hydrolyzed the glycan behind the fucosylated GlcNAc. Therefore, the fucosylated GlcNAc residue remains on the protein backbone and is not subject to the HPLC analysis. However, the degree of fucosylation measured by LC-MS was lower in *CTLA4* mutation carriers, which accords with observed differences in bisection between the two methods applied.

Interestingly, the shift in IgG glycosylation towards pro-inflammatory patterns (agalactosylated) was independent of the type of mutation or the developed phenotype (Tab. 3.1). Hence, the loss of CTLA4 led to a general reduction in IgG galactosylation and sialylation. In addition, CTLA4 has been described as an important co-receptor for T_{FR} cells and thus a regulator of GC reactions (Sage et al., 2014; Wing et al., 2014). Augmented GC reaction due to the loss of T_{FR} cells was shown here to lead to a more pro-inflammatory IgG glycosylation pattern in mice (Fig. 3.47). It is conceivable that CTLA4 from T_{FR} reduces the strength of the GC and thereby modulates the derived IgG glycosylation pattern. This might also explain the differences observed in the human CTLA4 cohort.

A comparable Fc glycosylation pattern within the individual samples was observed between human IgG subclasses (IgG1, IgG2, IgG3 and IgG4) (Fig. 3.3), the most prominent difference being the degree of fucosylation. For IgG4, no non-fucosylated glycopeptides were detected. However, this was not due to the absence of this glycans but rather due to the general low intensity of the IgG4 peaks (Selman et al., 2012b). All subclasses were detected within the same measurement, and the amount of sample had to be adjusted accordingly to avoid signals over the detection limit. Because IgG2/3 and IgG4 are usually less concentrated in human serum compared to human IgG1, the peaks of the spectra have lower intensities (Vidarsson et al., 2014). Peaks that were too low had to be excluded to avoid false positive values. For IgG1 17 different glycopeptides have been observed. For IgG2/3 and IgG4, only 14 and 9 glycopeptides have been measured, respectively (Tab. 3.2).

In contrast to human IgG subclasses, murine IgG subclasses showed huge differences in glycosylation pattern (Fig. 3.4). The levels of sialylation were found to be almost three times higher for IgG2b/c and two times higher for IgG3 subclasses compared to IgG1 in naïve

C57BL/6 serum. Interestingly, glycosylation differences within the same subclass but in different strains have also been found (Haan et al., 2017). In the study of Haan et al., IgG2b sialylation was higher in C57BL/6 compared to IgG2b from CD-1 or Swiss Webster mice. Nevertheless, no significant difference was found between IgG2b from C57BL/6 and Balb/c. Notably, Balb/c and C57BL/6 mice express different variants of the IgG1 heavy chain. Moreover, for the Balb/c heavy chain ($IgG1_{Balb}$), higher sialylation was observed. Because the two other strains investigated in their study expressed both IgG1 variants but maintained the glycosylation difference between IgG1 and $IgG1_{Balb}$, it is likely that the primary structure of the IgG subclasses influences the glycosylation itself, for example, due to different accessibility for glycosyltransferases (Haan et al., 2017). This structural influence might also explain the subclass-specific glycosylation differences observed here (Fig. 3.4).

Subclass-specific IgG Fc glycosylation was found in particular in mouse samples but was not as pronounced in human IgG samples. Likewise, HPLC analysis, which does not distinguish between the subclasses, was only comparable for human but not for mouse IgG analysis (Fig. 3.2, Fig. 3.3 and Fig. 3.4).

Interestingly, upon immunization in mice, the IgG glycosylation developed in a manner dependent on the adjuvant. The adjuvants MPLA and Alum maintained relatively high levels of galactosylation and sialylation, while eCFA led to reduced levels of galactosylation and sialylation (Fig. 3.5 and Fig. 3.6). Remarkably, this reduction was observed for both of the subclasses that were detected, namely, IgG1 and IgG2b/c. However, IgG2b/c maintained a higher sialylation compared to IgG1 for the three adjuvants that were tested (Fig. 3.6) (Epp et al., 2018). This trend was observed for all samples investigated by LC-MS in this research (Fig. A.7). In addition, an increase or decrease in IgG1-specific galactosylation, sialylation or both was always accompanied by the same trend in IgG2b/c glycosylation for all samples investigated here. This suggests that the adjuvant-dependent immune reactions do not alter IgG glycosylation in a subclass-specific manner. As mentioned, differences between the subclasses may be explained by differences in the primary structure and therewith the accessibility of the Fc glycosylation sides for the corresponding enzymes of the different IgG subclasses.

In the HPLC analysis, the glycans released from all IgG subclasses were analyzed. Hence, shifts in IgG subclasses can lead to differences in the observed total IgG glycosylation. For example, Alum induces an IgG1 dominated response, whereas IgG2b and IgG2c are higher upon MPLA vaccinations (Fig. 3.7). Total IgG glycosylation analyzed by HPLC showed a significant increased level of galactosylation and sialylation for the later adjuvant (Fig. 3.5). However, subclass-specific analysis revealed no differences in IgG1 and IgG2b/c for Alum and MPLA (Fig. 3.6) (Epp et al., 2018). Hence, the different expression of IgG subclasses upon Alum and MPLA immunization alone led to an apparent difference in the total IgG

glycosylation pattern. Thus, due to the intrinsic and significant difference in glycosylation between IgG subclasses, murine serum IgG samples should be analyzed according to subclass, for example, via LC-MS.

The majority of the immunization-induced IgG Abs is produced by plasma cells (Nutt et al., 2015). The IgG glycan is modified in the Golgi apparatus, wherein the St6gal1 enzyme catalyzes the transfer of sialic acid onto terminal galactose (Moremen et al., 2012). In line, plasma cell specific St6gal1 knockouts failed to produce sialylated IgG (Ohmi et al., 2016). Likewise, the expression of St6gal1 in Ova-specific IgG plasma cells correlated with the observed IgG glycosylation pattern (Fig. 3.12 - Fig. 3.15) (Hess et al., 2013; Bartsch et al., 2018; Pfeifle et al., 2017). However, on day 8, no differences in IgG sialylation were observed between Ova-eCFA and Ova-LPS immunization, but differences were apparent in the expression of St6gal1 in PCs for the two immunizations (Fig. 3.9 and Fig. 3.12). Intriguingly, sialylation for IgG1 was even elevated compared to the steady state IgG1 sialylation observed in naïve mice (Fig. 3.9). The exact source of the present antibodies on day 8, however, remains elusive, and it is likely that they were mainly not produced by the plasma cells that were observed on this day.

In contrast to the plasma cell response that peaked on day 8 (for Ova-eCFA; Fig. 3.10), Ova-specific IgG titers were low on that day (Fig. 3.8). Particularly in the case of Ova-eCFA, the titers raised from days 8 to 14 (Fig. 3.8), and similarly, the Fc sialylation level of these antibodies halved from days 8 to 14 (Fig. 3.9). Hence, IgG responses are behind the cellular plasma cell response, and IgG antibodies on day 8 were not from the observed plasma cells. These plasma cells, however, thenceforward began to secrete low sialylated IgG. Moreover, the half-life of IgG in circulation is between six and eight days (Vieira & Rajewsky, 1988). Likewise, serum titers accumulate until day 28, while splenic plasma cells are already almost at steady state levels on day 21 (Fig. 3.8 and Fig. 3.10 and data not shown).

Interestingly, the occurrence of sialylated early IgG Abs has been linked to early extrafollicular plasma cell responses and increased antigen-transport and vaccine efficacy (Wang et al., 2015). Like the findings enumerated above, an initial increase followed by a drop of sialylation levels of vaccine-induced IgG Abs was observed in this study. Furthermore, sialylated IgG has been linked to increased B cell activation and production of specific high-affinity IgG Abs (Wang et al., 2015). A possible source of these early IgG antibodies is plasmablasts differentiated, for example, from marginal zone B cells. These splenic cells can respond extremely quickly and do not require T cell help (Martin et al., 2001). Moreover, highly sialylated antibodies have been shown to be produced in response to T cell independent antigens (Hess et al., 2013). However, subsequent T cell-dependent extra-follicular plasma cell responses were very probably involved here before GC-derived PCs were also added to the antigen-specific PC pool.

Interestingly, St6gal1 can be produced in an extracellular form, mainly by hepatocytes (Kaplan et al., 1983). Recently, it has been suggested that this extracellular St6gal1 is solely responsible for IgG sialylation. In a mouse model wherein St6gal1 was specifically knocked out, levels of sialylated IgG similar to WT controls were observed upon immunization (Jones et al., 2016). However, the study has several limitations, particularly in terms of the quantification method employed for sialylated IgG. The authors used SNA (*Sambucus nigra agglutinin*) for the enrichment of sialylated IgG, which was then quantified. Nevertheless, SNA has been shown to easily bind to Fab sialylation but only to IgG Fc if two sialic acids are present in the Fc part (Stadlmann et al., 2010). Fab glycosylation sites are introduced by hypermutation and occur in about 15% of bulk IgG (Arnold et al., 2007). In addition, Fab glycosylation is often highly sialylated, probably, because it can be more easily accessed by St6gal1 (Arnold et al., 2007; Bondt et al., 2014). It is not clear whether the effects observed by Jones et.al. are Fc specific or whether Fab sialylation was responsible for the outcome.

Nevertheless, Fc sialylation has been shown to occur by exogenous St6gal1 in circulation (Pagan et al., 2018). Worthy of note is the fact that this exogenous sialylation, as well as the physiological production of hepatic St6gal1, requires a pro-inflammatory milieu, which is contradictory to the observed suppression of sialylation upon immunization (Kaplan et al., 1983; Pagan et al., 2018). Furthermore, other studies found a complete loss of Fc sialylation of antigen-specific immunization-induced IgG in mice with a plasma cell specific (AID-specific) deficiency in St6gal1 (Ohmi et al., 2016) and specific (monoclonal) IgG is often distinguishable from bulk IgG (Omtvedt et al., 2006). These findings suggest a specific control for IgG glycosylation, for example, by intracellular regulation of glycosyltransferases. Extracellular sialylation, however, would lack such regulation and sialylation would take place equally for all IgG abs. Taken together, although sialylation can take place in circulation, such is highly unlikely to occur under physiological conditions in mice and, hence, is not considered here.

The quality of a successful vaccination is often assessed by the induced antibody titers (Plotkin, 2010). Moreover, pro-inflammatory IgG glycosylation has been linked to increased effector function and, hence, amended vaccine-induced protection (Alter et al., 2018). Here, the vaccine-induced IgG glycosylation differed considerably depending on the adjuvant (Fig. 3.6). One aim of this thesis was to investigate the mechanisms that alter the immune response to a pro-inflammatory IgG glycosylation. Although adjuvants such as Alum have been used in numerous human vaccines for almost a century, the exact mode of action is not yet completely understood (Tab. 1.1) (Petrovsky & Aguilar, 2004; Marrack et al., 2009). Perhaps Alum leads to the activation of caspase 1 and, subsequently, to the release of pro-inflammatory cytokines, for example, IL-1ß, IL-4, IL-18 and IL-33 (Eisenbarth et al., 2008; Li et al., 2008; Marrack et al., 2009). These responses are linked to a Th2 type T cell response (Zhu et al., 2010; Coffman et al., 2010). CFA, by contrast, induces Th1- and Th17-like

cytokines such as IFNγ and IL-6 or IL-17, respectively (Fig. 3.16) (Shibaki & Katz, 2002; Coffman et al., 2010). Interestingly, incomplete Freund's adjuvant (IFA) that lacks Mycobacterial components favors a more Th2-like response (Billiau & Matthys, 2001; Shibaki & Katz, 2002). Moreover, mycobacterial components seem to be important for the induction of Th17 cells as they were absent upon IFA immunization (Fig. 3.42) (Coffman et al., 2010). MPLA is derived from LPS, and, likewise, MPLA mediates its effect via TLR4 and is described as a Th1-like adjuvant (Mata-Haro et al., 2007; Coffman et al., 2010). Strikingly, the different adjuvants induced distinct cytokine patterns, which shape the course of the immune reaction. Moreover, cytokines are critical for the type of IgG response, such as class-switch.

IL-6 is a pleiotropic cytokine and has a pivotal role in the innate and adaptive immune system. Likewise, it has a critical role in the pathology of autoimmune diseases as well as in protection against infections (Garbers et al., 2015). IL-6 seems to be particularly important in the defense and vaccine-induced protection against intracellular pathogens such as mycobacteria and viruses (Sodenkamp et al., 2012; Leal et al., 2001; Harker et al., 2011).

Interestingly, in gene association and protein association studies, IL-6 has also been suggested to correlate with pro-inflammatory IgG glycosylation patterns in humans (Lauc et al., 2013; Plomp et al., 2017). However, no functional evidence for the involvement of IL-6 on IgG glycosylation has thus far been published. In this study it was demonstrated that IL-6 deficient mice fail to induce pro-inflammatory IgG responses and do not downregulate the St6gal1 in PCs (Fig. 3.17, Fig. 3.20 and Fig. 3.21). Likewise, IgG Fc sialylation in IL-6 KO mice was comparable to immunizations with LPS in WT mice that did not induce IL-6 (Fig. 3.16 and Fig. 3.18). Treatment of WT mice with an IL-6R blocking antibody (clone: MR16-1) had similar effects on IgG glycosylation upon vaccination (Fig. 3.19). The MR16-1 antibody is a murine counterpart of human antibody Tocilizumab, which is used clinically, for example, for treatment of rheumatoid arthritis (Okazaki et al., 2002; Garbers et al., 2015). Remarkably, pro-inflammatory IgG glycosylation has been suggested as a patho-mechanism in RA (Ito et al., 2014; Pfeifle et al., 2017; Bartsch et al., 2018). Whether Tocilizumab treatment of such patients also effects IgG glycosylation and whether this contributes to the beneficial effect, must be determined in the future.

Previously, IL-6 has been described as a B cell stimulating factor (Hirano et al., 1986), as it consistently induces B cell differentiation and IgG secretion *in vitro* and *in vivo* ((Muraguchi et al., 1988; Kopf et al., 1998) (Fig. 3.17, Fig. 3.20, Fig. 3.21, Fig. 3.38 and Fig. 3.39). However, over recent decades, the involvement of IL-6 in T cell differentiation has been further investigated. For example, it plays a central role in skewing TGFβ dependent Treg differentiation towards Th17 differentiation (Bettelli et al., 2006). Strikingly, T cells, and particularly Th17, cells have been related to pro-inflammatory IgG glycosylation ((Hess et

al., 2013; Pfeifle et al., 2017), findings that were confirmed in this research. Mice deficient in IL-17A and IL-17RA failed to induce a low expression of St6gal1 in PCs and subsequently produced high sialylated IgG Abs upon vaccination with Ova-eCFA (Fig. 3.23-Fig. 3.26). Although the sources of IL-17A are not exclusively confined to Th17 cells (Korn et al., 2009), similar effects on IgG glycosylation were observed in IL-23p19 KO mice (Fig. 3.27). This cytokine is described as a Th17 maintaining and proliferating factor, which is reflected in the reduced levels of serum IL-17A and IL-22 upon IL-23p19 KO observed in this thesis (Fig. 3.28) (Floss et al., 2015).

IL-22 is a cytokine that is often co-expressed with IL-17A by Th17 cells. In contrast to the literature, an influence of IL-22 on IgG glycosylation could not be observed in this research upon Ova-eCFA immunization on the IgG Fc glycosylation pattern (Fig. 3.27) (Pfeifle et al., 2017). Interestingly, Th17 differentiation was inhibited in sgp130Fc tg mice and not affected in IL-6R flox x CD4-Cre mice (Fig. 3.31 and Fig. 3.33). These data indicate that IL-6 trans-signaling is responsible for the differentiation of Th17 cell, which has been suggested previously as well (Jones et al., 2010). In a recent study, the intracellular assembly of the IL-6:sIL-6R complex in CD11c+ cells and "trans-presentation" and activation of neighboring CD4+ T cells by gp130 was described to induce Th17 differentiation (Heink et al., 2017). Nevertheless, all varieties of IL-6 signaling are solely transmitted through gp130 and the subsequent Stat3 phosphorylation inside the cell (Garbers et al., 2018). However, trans-signaling may leads to augmented gp130 activation compared to classical signaling. Upon activation, CD4+ T cells downregulated the IL-6R by shedding into the soluble form (Briso et al., 2008; Jones et al., 2010). These cells do not respond to classical signaling, but the sIL-6R that is produced is eligible for ("autocrine") trans-signaling. Interestingly, sgp130Fc attenuated disease in the collagen induced arthritis (CIA) model (Nowell et al., 2009), which was induced by CFA adjuvanted collagen immunizations. Th17 cells have been shown to play a critical role in the CIA pathology (Nakae et al., 2003); however, a direct modulation of sgp130Fc on Th17 differentiation in the CIA has not been investigated, and the role of sgp130 and trans-signaling and Th17 cells must be further investigated after Ova-eCFA immunization (Nowell et al., 2009).

The unexpected observation that IL-6R flox x CD4-Cre mice had comparable levels of IL-17A producing Th17 cells (Fig. 3.31), while the IgG glycosylation pattern was clearly affected by the genotype (Fig. 3.29), suggested an additional role of IL-6 on the T cell mediated effect. Prominently, the frequency of CXCR5+ICOS+ follicular T cells was reduced upon the knockout (Fig. 3.36). In line, frequencies of GC B cells were compromised by IL-6 cis-signaling but not by IL-6 trans-signaling (Fig. 3.37, Fig. 3.38 and Fig. 3.39). Fittingly, IL-6 has been described as an inducer of T_{FH} cells and subsequent GC reactions (Eto et al., 2011; Riteau et al., 2016). The functional role of the GC reaction on IgG glycosylation was subsequently confirmed with the Nfat-c1 model (Fig. 3.45, Fig. 3.46 and

Fig. 3.47). In the "Nfat" mice, the transcription factor Nfat-c1 is flanked by loxp sites, and the Cre-recombinase is under the control of the Foxp3 promotor. Hence, Foxp3-expressing cells lose the Nfat-c1, which was shown to "exclusively" diminish the migration of T_{FR} cells into the GC, leading in turn to augmented GC reactions (Vaeth et al., 2014). The altered GC reaction observed in the Nfat mice translated into low St6gal1 expression in plasma cells and led to a reduced level of sialylation in the subsequent IgG Abs (Fig. 3.46 and Fig. 3.47). Likewise, the ratio of T_{FH}:T_{FR} cells shifted towards T_{FH} cells in these mice (Fig. 3.45) (Vaeth et al., 2014). These findings together indicate an ongoing or enhanced GC reaction.

T_{FR} cells keep the GC reaction in check and are critical in the GC resolution. Interestingly, the origin of T_{FH} and T_{FR} cells seem to be different. While T_{FH} cells are induced upon vaccination from the naïve T cell pool, T_{FR} cells dominantly develop from nTreg pool (Maceiras et al., 2017; Ritvo et al., 2018). nTregs are primed upon antigenic challenge in the thymus, whereas inducible Tregs (iTregs) differentiate upon antigen-recognition by the TCR in the periphery (Bilate & Lafaille, 2012). Hence, nTreg specificity is prone to auto-antigens and they play a critical role in maintaining central tolerance. Likewise, attenuated T_{FR} and the subsequently increased GC responses are linked to enhanced pro-inflammatory reactions and may lead to a loss of tolerance and the induction of auto-immunity (Vaeth et al., 2014; Wollenberg et al., 2011). Noteworthily, has been suggested that IL-6 skews only the differentiation of iTregs and, hence, plays minor roles in the induction of T_{FR} cells (Fujimoto et al., 2011). Likewise, in the IL-6 compromised models, T_{FH} cells were often elevated while T_{FR} remained unaffected (Fig. 3.36). In a spontaneous lupus mouse model, increased GC and PC frequencies and low expression of St6gal1 correlated with the occurrence of auto-antibodies (Fig. A.6) (Bartsch et al., 2018). Altered T_{FH}:T_{FR} ratios may induce the augmented GCs in this model and subsequently leads to loss of tolerance and pro-inflammatory IgG glycosylation. Although T_{FH} and T_{FR} were not investigated in this model, this may also be applicable to the human situation. For example, increased levels of blood T_{FH} cells have been observed to correlate with vaccine-induced protection (Locci et al., 2013). Moreover, they also appear elevated in autoimmune diseases, such as rheumatoid arthritis, which are linked to a pro-inflammatory IgG glycosylation pattern (Wang et al., 2013; Ueno, 2016). In addition, in humans, augmented GC reactions could explain how pro-inflammatory IgG glycosylation patterns develop. However, this is highly speculative, and more research must be conducted in this area. Moreover, in the aforementioned mouse and human scenario, not only Th17 but $T_{FH}17$ cells as well could be involved in the induction of pro-inflammatory IgG glycosylation.

Vaccination with a T cell dependent antigen led to distinct adjuvant-dependent IgG glycosylation patterns in this research. Reduced levels of IgG sialylation upon Ova-eCFA were shown to depend on IL-17A and, most likely, Th17 differentiation. Furthermore, GC reactions independently promote a pro-inflammatory glycosylation pattern, which highlights

the importance of T cell differentiation on the resulting cognate B and plasma cell response. The observed IgG glycosylation pattern was dynamic, with changes occurring over time. During the immune reaction, B and plasma cells may be influenced differently and accordingly produce differently glycosylated IgG antibodies. These antibodies are observable in circulation even after the corresponding plasma cells have disappeared. Hence, the observed IgG glycosylation is not only dependent on the type of current and past immune reactions but also on the titers that were produced by the different types of plasma cells (e.g., T cell-independent PCs or T cell-dependent extrafollicular PCs and GC-derived PCs). The mechanisms that may contribute, and how IL-6 may mediates its effects, resulting in the observed IgG glycosylation patterns are summarized in the model proposed below (Fig. 4.1).

The first IgG molecules on day 8 are highly sialylated independent of the adjuvant. Presumably, these antibodies are either derived from directly activated B cells (T cell independent) or may be influenced by first T cell help. Interestingly, IgG has already been suggested to be highly sialylated upon T cell independent reaction (Hess et al., 2013). Moreover, these antibodies may foster the adaptive immune response by transportation of immune complexes to APCs or GC structures in secondary lymphoid organs (Wang et al., 2015). T cell dependent immune responses usually require longer to develop. The differentiation of T helper cells is classified according to T cell derived cytokine patterns. Th1 and Th2 responses are well characterized and distinguished by the expression of, for example, IFNγ and IL-4, respectively (Zhu et al., 2010).

Interestingly, Alum is described as a Th2 inducing adjuvant, while LPS may favors a Th1 response (Coffman et al., 2010). These immunizations led to more sialylated IgG Fc glycosylation pattern which is may not distinguishable from T cell independent (or very early, or both) immune responses. However, the Th1 cytokine IFNγ has also been suggested to be involved in the induction of low-sialylated IgG after immunization (Hess et al., 2013).

IgG sialylation downregulation may be achieved upon Th17 cell induction by APC derived IL-6. Interestingly, Th17 cells were only upregulated upon Ova-eCFA immunization on day 14 (Fig. 3.43). Consistently, in the IL-17Ra KO mice, differences in plasma cell St6gal1 were only visible on day 14 but not on day 8 upon Ova-eCFA immunization (Fig. 3.23 and Fig. 3.24). This may indicate that Th17 responses require longer to develop and hence contribute only later to the antigen-specific IgG glycosylation pattern. In addition, GC derived plasma cells and corresponding IgG molecules were shown to have a more pro-inflammatory IgG glycosylation (Fig. 3.47).

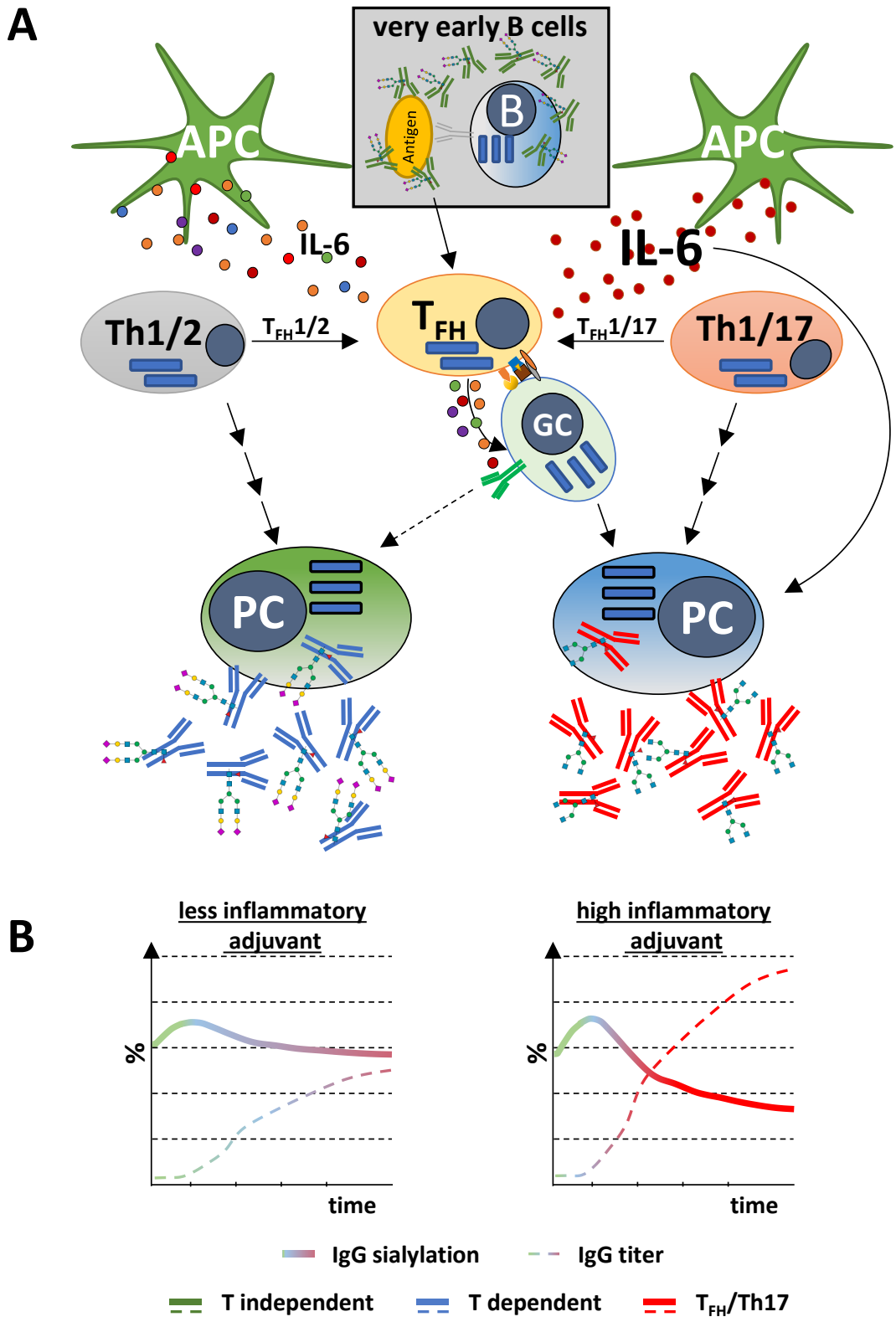

Fig. 4.1 ***Proposed model for the development of adjuvant-dependent IgG glycosylation pattern.*** *(A) Very early B cells (grey box) may produce early, highly sialylated IgG (green), which can promote GC reactions. Cytokines (e.g. IL-6) from antigen-presenting cells (APC) skew T cell differentiation, which, in turn, influences plasma cell differentiation and IgG glycosylation. Moreover, IL-6 may also influence B and plasma cells directly. Depending on the T cell subsets, plasma cells produce late, high (blue) or low (red) sialylated IgG. (B) Depending on the adjuvant, the relative amount (titer, dashed line) of early IgG (green), T cell dependent (blue) or T_{FH}/Th17 (red) dependent IgG antibodies varies. The composition of the induced IgG influences the observed IgG sialylation levels (solid line). The color of the line indicates the main source at a time.*

During the GC reaction, B cells are under the constant influence of T cell help, as a result of which they acquire somatic hypermutation and undergo class-switch. Furthermore, the GC reaction is crucial for the development of B cell memory (Victora & Nussenzweig, 2012).

Interestingly, both adjuvants, eCFA and Alum, induce strong GCs early on day 8 (Fig. 3.40); however, only in the case of eCFA is the GC perpetuated until day 14 (Fig. 3.41). The induction of T_{FH} cells and subsequently germinal center cells appeared highly dependent on IL-6 in this research (Fig. 3.36, Fig. 3.38 and Fig. 3.39). Several studies previously suggested that memory B cells occur early in the GC reaction while plasma cells often differentiate at later time points (Weisel et al., 2016; Shinnakasu et al., 2016; Kräutler et al., 2017). In a collaboration between our laboratory and Tomohiro Kurosaki and Hidehiro Fukuyama (RIKEN Center for Integrative Medical Sciences; Japan), the first experiments to investigate the source of plasma cells were conducted. In this model, GC derived B cells are marked irreversibly with a fluorescent dye, which makes them distinguishable from non-GC derived B cells (Shinnakasu et al., 2016). The first preliminary results suggested that on day 8, no plasma cells are derived from the GC (data not shown).

Neither IL-17Ra KO nor T_{FR}-compromised mice had different expressions of plasma cell St6gal1 on day 8, but they did on day 14, which indicates a delay in the development of pro-inflammatory IgG glycosylation (Fig. 3.23, Fig. 3.24 and Fig. 3.46). The frequency of plasma cells that arise from the GC reaction might differ considerably between the adjuvants. It could be possible that with Alum, fewer plasma cells are derived from the GC reaction. This might be reflected in the reduced frequency of plasma cells and the increased expression of St6gal1 compared to eCFA on day 14 observed in this study (Fig. 3.15). Moreover, IL-17A-producing T_{FH} cells ($T_{FH}17$) were identified here as upregulated upon eCFA but not upon Alum (Fig. 3.42 and Fig. 3.43). Although no influence of the IL-17A knockout was observed on the GC composition (Fig. 3.44), the possibility remains open of a qualitative difference, for example, in terms of cytokine production, between the GCs induced with eCFA or Alum.

The importance of the IgG glycosylation in antibody-mediated immune reactions against pathogens has been realized in recent years. Likewise, the glycosylation of vaccine-induced IgG influences the quality of vaccine-induced protection (Alter et al., 2018). However, little has been understood about the regulation of IgG glycosylation upon vaccination. The aim of this thesis was to investigate how different adjuvants can lead to differently glycosylated IgG upon vaccination with a T cell dependent antigen. Therefore, IgG glycosylation was investigated using LC-MS and HPLC based methods. Furthermore, in murine immunization models, T and B cell responses were investigated via flow cytometry, thereby identifying an IL-6-dependent downregulation of St6gal1 protein expression and subsequent suppression of IgG sialylation. It was further shown that the IL-6 effect was mediated by the

differentiation of Th17 cells and augmented GC reactions. Both Th17 cells and GC were functionally tested to be involved in the suppression of plasma cell St6gal1 and IgG sialylation. The results obtained here describe a new role of IL-6 in vaccine-induced IgG glycosylation. A sound understanding of the mechanisms that lead to distinct IgG glycosylation patterns may help develop future adjuvants that can induce the desired IgG Fc glycosylation patterns. Moreover, these mechanisms may also apply to the onset of pro-inflammatory IgG glycosylation that is observed in autoimmunity.

A References

Ackerman, ME, Crispin, M, Yu, X, Baruah, K, Boesch, AW, Harvey, DJ, Dugast, A-S, Heizen, EL, Ercan, A, Choi, I, Streeck, H, Nigrovic, PA, Bailey-Kellogg, C, Scanlan, C & Alter, G 2013, **'Natural variation in Fc glycosylation of HIV-specific antibodies impacts antiviral activity'** , *The Journal of clinical investigation*, 2013, pp. 2183–2192.

Ada, G 2005, **'Overview of Vaccines and Vaccination'** , *Molecular Biotechnology*, 2005, pp. 255–272.

Ahmed, R & Gray, D 1996, **'Immunological Memory and Protective Immunity: Understanding Their Relation'** , *Science (New York, N.Y.)*, 1996, pp. 54–60.

Allen, CDC & Cyster, JG 2008, **'Follicular dendritic cell networks of primary follicles and germinal centers: phenotype and function'** , *Seminars in immunology*, 2008, pp. 14–25.

Alter, G, Ottenhoff, THM & Joosten, SA 2018, **'Antibody glycosylation in inflammation, disease and vaccination'** , *Seminars in immunology*, 2018.

Anderson, RP & Jabri, B 2013, **'Vaccine against autoimmune disease: antigen-specific immunotherapy☆'** , *Current opinion in immunology*, 2013, pp. 410–417.

Anthony, RM, Kobayashi, T, Wermeling, F & Ravetch, JV 2011, **'Intravenous gammaglobulin suppresses inflammation through a novel T(H)2 pathway'** , *Nature*, 2011, pp. 110–113.

Anthony, RM, Wermeling, F & Ravetch, JV 2012, **'Novel roles for the IgG Fc glycan'** , *Annals of the New York Academy of Sciences*, 2012, pp. 170–180.

Arnold, JN, Wormald, MR, Sim, RB, Rudd, PM & Dwek, RA 2007, **'The impact of glycosylation on the biological function and structure of human immunoglobulins'** , *Annual review of immunology*, 2007, pp. 21–50.

Bartsch, YC, Rahmöller, J, Mertes, MMM, Eiglmeier, S, Lorenz, FKM, Stoehr, AD, Braumann, D, Lorenz, AK, Winkler, A, Lilienthal, G-M, Petry, J, Hobusch, J, Steinhaus, M, Hess, C, Holecska, V, Schoen, CT, Oefner, CM, Leliavski, A, Blanchard, V & Ehlers, M 2018, **'Sialylated Autoantigen-Reactive IgG Antibodies Attenuate Disease Development in Autoimmune Mouse Models of Lupus Nephritis and Rheumatoid Arthritis'** , *Frontiers in immunology*, 2018, p. 1183.

Behring, EV & Kitasato, S 1890, **'Ueber das Zustandekommen der Diphtherie-Immunität und der Tetanus-Immunität bei Thieren'** , *DMW - Deutsche Medizinische Wochenschrift*, 1890, pp. 1113–1114.

Bentebibel, S-E, Lopez, S, Obermoser, G, Schmitt, N, Mueller, C, Harrod, C, Flano, E, Mejias, A, Albrecht, RA, Blankenship, D, Xu, H, Pascual, V, Banchereau, J, Garcia-Sastre, A, Palucka, AK, Ramilo, O & Ueno, H 2013, **'Induction of ICOS+CXCR3+CXCR5+ TH cells correlates with antibody responses to influenza vaccination'** , *Science translational medicine*, 2013, p. 176ra32.

Bettelli, E, Carrier, Y, Gao, W, Korn, T, Strom, TB, Oukka, M, Weiner, HL & Kuchroo, VK 2006, **'Reciprocal developmental pathways for the generation of pathogenic effector TH17 and regulatory T cells'** , *Nature*, 2006, pp. 235–238.

Bigge, JC, Patel, TP, Bruce, JA, Goulding, PN, Charles, SM & Parekh, RB 1995, **'Nonselective and efficient fluorescent labeling of glycans using 2-amino benzamide and anthranilic acid'** , *Analytical biochemistry*, 1995, pp. 229–238.

Bilate, AM & Lafaille, JJ 2012, **'Induced CD4+Foxp3+ regulatory T cells in immune tolerance'** , *Annual review of immunology*, 2012, pp. 733–758.

Billiau, A & Matthys, P 2001, **'Modes of action of Freund's adjuvants in experimental models of autoimmune diseases'** , *Journal of leukocyte biology*, 2001, pp. 849–860.

Bondt, A, Rombouts, Y, Selman, MHJ, Hensbergen, PJ, Reiding, KR, Hazes, JMW, Dolhain, RJEM & Wuhrer, M 2014, **'Immunoglobulin G (IgG) Fab glycosylation analysis using a new mass spectrometric high-throughput profiling method reveals pregnancy-associated changes'** , *Molecular & cellular proteomics : MCP*, 2014, pp. 3029–3039.

Bonilla, FA 2018, **'Update: Vaccines in primary immunodeficiency'** , *The Journal of allergy and clinical immunology*, 2018, pp. 474–481.

Boursnell, ME, Rutherford, E, Hickling, JK, Rollinson, EA, Munro, AJ, Rolley, N, McLean, CS, Borysiewicz, LK, Vousden, K & Inglis, SC 1996, **'Construction and characterisation of a recombinant vaccinia virus expressing human papillomavirus proteins for immunotherapy of cervical cancer'** , *Vaccine*, 1996, pp. 1485–1494.

Brinkman-Van der Linden, ECM, Sjoberg, ER, Juneja, LR, Crocker, PR, Varki, N & Varki, A 2000, **'Loss of N -Glycolylneuraminic Acid in Human Evolution'** , *Journal of Biological Chemistry*, 2000, pp. 8633–8640.

Briso, EM, Dienz, O & Rincon, M 2008, **'Cutting edge: soluble IL-6R is produced by IL-6R ectodomain shedding in activated CD4 T cells'** , *Journal of immunology (Baltimore, Md. : 1950)*, 2008, pp. 7102–7106.

Browning, CH 1955, **'Emil Behring and Paul Ehrlich: Their Contributions to Science'** , *Nature*, 1955, pp. 570–575.

Bruhns, P & Jönsson, F 2015, **'Mouse and human FcR effector functions'** , *Immunological reviews*, 2015, pp. 25–51.

Cattoretti, G, Chang, CC, Cechova, K, Zhang, J, Ye, BH, Falini, B, Louie, DC, Offit, K, Chaganti, RS & Dalla-Favera, R 1995, **'BCL-6 protein is expressed in germinal-center B cells'** , *Blood*, 1995, pp. 45–53.

Caya, CA, Boikos, C, Desai, S & Quach, C 2015, **'Dosing regimen of the 23-valent pneumococcal vaccination: a systematic review'** , *Vaccine*, 2015, pp. 1302–1312.

Chiang, CL-L, Kandalaft, LE & Coukos, G 2011, **'Adjuvants for enhancing the immunogenicity of whole tumor cell vaccines'** , *International reviews of immunology*, 2011, pp. 150–182.

Choi, YS, Eto, D, Yang, JA, Lao, C & Crotty, S 2013, **'Cutting edge: STAT1 is required for IL-6-mediated Bcl6 induction for early follicular helper cell differentiation'** , *Journal of immunology (Baltimore, Md. : 1950)*, 2013, pp. 3049–3053.

Chung, Y, Tanaka, S, Chu, F, Nurieva, RI, Martinez, GJ, Rawal, S, Wang, Y-H, Lim, H, Reynolds, JM, Zhou, X-H, Fan, H-M, Liu, Z-M, Neelapu, SS & Dong, C 2011, **'Follicular regulatory T cells expressing Foxp3 and Bcl-6 suppress germinal center reactions'** , *Nature medicine*, 2011, pp. 983–988.

Coffman, RL, Sher, A & Seder, RA 2010, **'Vaccine adjuvants: putting innate immunity to work'** , *Immunity*, 2010, pp. 492–503.

Collin, M & Ehlers, M 2013, **'The carbohydrate switch between pathogenic and immunosuppressive antigen-specific antibodies'** , *Experimental dermatology*, 2013, pp. 511–514.

Collin, M & Olsén, A 2001, **'EndoS, a novel secreted protein from Streptococcus pyogenes with endoglycosidase activity on human IgG'** , *The EMBO journal*, 2001, pp. 3046–3055.

Collins, ES, Galligan, MC, Saldova, R, Adamczyk, B, Abrahams, JL, Campbell, MP, Ng, C-T, Veale, DJ, Murphy, TB, Rudd, PM & Fitzgerald, O 2013, **'Glycosylation status of serum in inflammatory arthritis in response to anti-TNF treatment'** , *Rheumatology (Oxford, England)*, 2013, pp. 1572–1582.

Coudeville, L, Bailleux, F, Riche, B, Megas, F, Andre, P & Ecochard, R 2010, **'Relationship between haemagglutination-inhibiting antibody titres and clinical protection against influenza: development and application of a bayesian random-effects model'** , *BMC medical research methodology*, 2010, p. 18.

Croce, A, Firuzi, O, Altieri, F, Eufemi, M, Agostino, R, Priori, R, Bombardieri, M, Alessandri, C, Valesini, G & Saso, L 2007, **'Effect of infliximab on the glycosylation of IgG of patients with rheumatoid arthritis'** , *Journal of clinical laboratory analysis*, 2007, pp. 303–314.

Crotty, S 2011, **'Follicular helper CD4 T cells (TFH)'** , *Annual review of immunology*, 2011, pp. 621–663.

Dekkers, G, Rispens, T & Vidarsson, G 2018, **'Novel Concepts of Altered Immunoglobulin G Galactosylation in Autoimmune Diseases'** , *Frontiers in immunology*, 2018, p. 553.

Di Noia, JM & Neuberger, MS 2007, **'Molecular mechanisms of antibody somatic hypermutation'** , *Annual review of biochemistry*, 2007, pp. 1–22.

Di Pasquale, A, Preiss, S, Tavares Da Silva, F & Garçon, N 2015, **'Vaccine Adjuvants: from 1920 to 2015 and Beyond'** , *Vaccines*, 2015, pp. 320–343.

Dvorak, AM & Dvorak, HF 1974, **'Structure of Freund's complete and incomplete adjuvants. Relation of adjuvanticity to structure'** , *Immunology*, 1974, pp. 99–114.

Edelman, GM, Cunningham, BA, Gall, WE, Gottlieb, PD, Rutishauser, U & Waxdal, MJ 1969, **'The covalent structure of an entire gammaG immunoglobulin molecule'** , *Proceedings of the National Academy of Sciences of the United States of America*, 1969, pp. 78–85.

Eibl, MM & Wolf, HM 2015, **'Vaccination in patients with primary immune deficiency, secondary immune deficiency and autoimmunity with immune regulatory abnormalities'** , *Immunotherapy*, 2015, pp. 1273–1292.

Eisen, HN 2014, '**Affinity enhancement of antibodies: how low-affinity antibodies produced early in immune responses are followed by high-affinity antibodies later and in memory B-cell responses**' , *Cancer immunology research*, 2014, pp. 381–392.

Eisenbarth, SC, Colegio, OR, O'Connor, W, Sutterwala, FS & Flavell, RA 2008, '**Crucial role for the Nalp3 inflammasome in the immunostimulatory properties of aluminium adjuvants**' , *Nature*, 2008, pp. 1122–1126.

Epp, A, Hobusch, J, Bartsch, YC, Petry, J, Lilienthal, G-M, Koeleman, CAM, Eschweiler, S, Möbs, C, Hall, A, Morris, SC, Braumann, D, Engellenner, C, Bitterling, J, Rahmöller, J, Leliavski, A, Thurmann, R, Collin, M, Moremen, KW, Strait, RT, Blanchard, V, et al. 2018, '**Sialylation of IgG antibodies inhibits IgG-mediated allergic reactions**' , *The Journal of allergy and clinical immunology*, 2018, pp. 399-402.e8.

Eto, D, Lao, C, DiToro, D, Barnett, B, Escobar, TC, Kageyama, R, Yusuf, I & Crotty, S 2011, '**IL-21 and IL-6 are critical for different aspects of B cell immunity and redundantly induce optimal follicular helper CD4 T cell (Tfh) differentiation**' , *PloS one*, 2011, p. e17739.

Ferrara, C, Brünker, P, Suter, T, Moser, S, Püntener, U & Umaña, P 2006, '**Modulation of therapeutic antibody effector functions by glycosylation engineering: influence of Golgi enzyme localization domain and co-expression of heterologous beta1, 4-N-acetylglucosaminyltransferase III and Golgi alpha-mannosidase II**' , *Biotechnology and bioengineering*, 2006, pp. 851–861.

Floss, DM, Schröder, J, Franke, M & Scheller, J 2015, '**Insights into IL-23 biology: From structure to function**' , *Cytokine & growth factor reviews*, 2015, pp. 569–578.

Freund, J, Casals, J & Hosmer, EP 1937, '**Sensitization and Antibody Formation after Injection of Tubercle Bacilli and Paraffin Oil**' , *Experimental Biology and Medicine*, 1937, pp. 509–513.

Fujimoto, M, Nakano, M, Terabe, F, Kawahata, H, Ohkawara, T, Han, Y, Ripley, B, Serada, S, Nishikawa, T, Kimura, A, Nomura, S, Kishimoto, T & Naka, T 2011, '**The influence of excessive IL-6 production in vivo on the development and function of Foxp3+ regulatory T cells**' , *Journal of immunology (Baltimore, Md. : 1950)*, 2011, pp. 32–40.

Gaffen, SL 2009, **'Structure and signalling in the IL-17 receptor family'** , *Nature reviews. Immunology*, 2009, pp. 556–567.

Garbers, C, Aparicio-Siegmund, S & Rose-John, S 2015, **'The IL-6/gp130/STAT3 signaling axis: recent advances towards specific inhibition'** , *Current opinion in immunology*, 2015, pp. 75–82.

Garbers, C, Heink, S, Korn, T & Rose-John, S 2018, **'Interleukin-6: designing specific therapeutics for a complex cytokine'** , *Nature reviews. Drug discovery*, 2018, pp. 395–412.

Ghilardi, N, Kljavin, N, Chen, Q, Lucas, S, Gurney, AL & Sauvage, FJ 2004, **'Compromised humoral and delayed-type hypersensitivity responses in IL-23-deficient mice'** , *Journal of immunology (Baltimore, Md. : 1950)*, 2004, pp. 2827–2833.

Glenny, AT, Pope, CG, Waddington, H & Wallace, U 1926, **'Immunological notes. XVII-XXIV'** , *The Journal of Pathology and Bacteriology*, 1926, pp. 31–40.

Haan, N, Reiding, KR, Krištić, J, Hipgrave Ederveen, AL, Lauc, G & Wuhrer, M 2017, **'The N-Glycosylation of Mouse Immunoglobulin G (IgG)-Fragment Crystallizable Differs Between IgG Subclasses and Strains'** , *Frontiers in immunology*, 2017, p. 608.

Harker, JA, Lewis, GM, Mack, L & Zuniga, EI 2011, **'Late interleukin-6 escalates T follicular helper cell responses and controls a chronic viral infection'** , *Science (New York, N.Y.)*, 2011, pp. 825–829.

Heink, S, Yogev, N, Garbers, C, Herwerth, M, Aly, L, Gasperi, C, Husterer, V, Croxford, AL, Möller-Hackbarth, K, Bartsch, HS, Sotlar, K, Krebs, S, Regen, T, Blum, H, Hemmer, B, Misgeld, T, Wunderlich, TF, Hidalgo, J, Oukka, M, Rose-John, S, et al. 2017, **'Trans-presentation of IL-6 by dendritic cells is required for the priming of pathogenic TH17 cells'** , *Nature immunology*, 2017, pp. 74–85.

Hess, C, Winkler, A, Lorenz, AK, Holecska, V, Blanchard, V, Eiglmeier, S, Schoen, A-L, Bitterling, J, Stoehr, AD, Petzold, D, Schommartz, T, Mertes, MMM, Schoen, CT, Tiburzy, B, Herrmann, A, Köhl, J, Manz, RA, Madaio, MP, Berger, M, Wardemann, H, et al. 2013, **'T cell-independent B cell activation induces immunosuppressive sialylated IgG antibodies'** , *The Journal of clinical investigation*, 2013, pp. 3788–3796.

Hinman, A 1999, **'Eradication of vaccine-preventable diseases'** , *Annual review of public health*, 1999, pp. 211–229.

Hirano, T, Yasukawa, K, Harada, H, Taga, T, Watanabe, Y, Matsuda, T, Kashiwamura, S, Nakajima, K, Koyama, K & Iwamatsu, A 1986, **'Complementary DNA for a novel human interleukin (BSF-2) that induces B lymphocytes to produce immunoglobulin'** , *Nature*, 1986, pp. 73–76.

Ho, C-H, Chien, R-N, Cheng, P-N, Liu, J-H, Liu, C-K, Su, C-S, Wu, I-C, Li, I-C, Tsai, H-W, Wu, S-L, Liu, W-C, Chen, S-H & Chang, T-T 2015a, **'Aberrant serum immunoglobulin G glycosylation in chronic hepatitis B is associated with histological liver damage and reversible by antiviral therapy'** , *The Journal of infectious diseases*, 2015a, pp. 115–124.

Hoff, J 2000, **'Methods of Blood Collection in the Mouse'** , *Lab Animal*, 2000, pp. 47-53.

Ho, L-J, Luo, S-F & Lai, J-H 2015b, **'Biological effects of interleukin-6: Clinical applications in autoimmune diseases and cancers'** , *Biochemical pharmacology*, 2015b, pp. 16–26.

Howell, JW, Hood, L & Sanders, BG 1967, **'Comparative analysis of the IgG heavy chain carbohydrate peptide'** , *Journal of molecular biology*, 1967, pp. 555–558.

Huffman, JE, Pučić-Baković, M, Klarić, L, Hennig, R, Selman, MHJ, Vučković, F, Novokmet, M, Krištić, J, Borowiak, M, Muth, T, Polašek, O, Razdorov, G, Gornik, O, Plomp, R, Theodoratou, E, Wright, AF, Rudan, I, Hayward, C, Campbell, H, Deelder, AM, et al. 2014, **'Comparative performance of four methods for high-throughput glycosylation analysis of immunoglobulin G in genetic and epidemiological research'** , *Molecular & cellular proteomics : MCP*, 2014, pp. 1598–1610.

Ishikawa, E, Ishikawa, T, Morita, YS, Toyonaga, K, Yamada, H, Takeuchi, O, Kinoshita, T, Akira, S, Yoshikai, Y & Yamasaki, S 2009, **'Direct recognition of the mycobacterial glycolipid, trehalose dimycolate, by C-type lectin Mincle'** , *The Journal of experimental medicine*, 2009, pp. 2879–2888.

Ito, K, Furukawa, J-I, Yamada, K, Tran, NL, Shinohara, Y & Izui, S 2014, **'Lack of galactosylation enhances the pathogenic activity of IgG1 but Not IgG2a anti-erythrocyte autoantibodies'** , *Journal of immunology (Baltimore, Md. : 1950)*, 2014, pp. 581–588.

Jackson, LA, Benson, P, Sneller, VP, Butler, JC, Thompson, RS, Chen, RT, Lewis, LS, Carlone, G, DeStefano, F, Holder, P, Lezhava, T & Williams, WW 1999, **'Safety of revaccination with pneumococcal polysaccharide vaccine'** , *JAMA*, 1999, pp. 243–248.

Jones, GW, McLoughlin, RM, Hammond, VJ, Parker, CR, Williams, JD, Malhotra, R, Scheller, J, Williams, AS, Rose-John, S, Topley, N & Jones, SA 2010, **'Loss of CD4+ T cell IL-6R expression during inflammation underlines a role for IL-6 trans signaling in the local maintenance of Th17 cells'** , *Journal of immunology (Baltimore, Md. : 1950)*, 2010, pp. 2130–2139.

Jones, MB, Oswald, DM, Joshi, S, Whiteheart, SW, Orlando, R & Cobb, BA 2016, **'B-cell-independent sialylation of IgG'** , *Proceedings of the National Academy of Sciences of the United States of America*, 2016, pp. 7207–7212.

Jostock, T, Müllberg, J, Ozbek, S, Atreya, R, Blinn, G, Voltz, N, Fischer, M, Neurath, MF & Rose-John, S 2001, **'Soluble gp130 is the natural inhibitor of soluble interleukin-6 receptor transsignaling responses'** , *European journal of biochemistry*, 2001, pp. 160–167.

Kaneko, Y, Nimmerjahn, F & Ravetch, JV 2006, **'Anti-inflammatory activity of immunoglobulin G resulting from Fc sialylation'** , *Science (New York, N.Y.)*, 2006, pp. 670–673.

Kao, D, Lux, A, Schaffert, A, Lang, R, Altmann, F & Nimmerjahn, F 2017, **'IgG subclass and vaccination stimulus determine changes in antigen specific antibody glycosylation in mice'** , *European journal of immunology*, 2017, pp. 2070–2079.

Kaplan, HA, Woloski, BM, Hellman, M & Jamieson, JC 1983, **'Studies on the effect of inflammation on rat liver and serum sialyltransferase. Evidence that inflammation causes release of Gal beta 1 leads to 4GlcNAc alpha 2 leads to 6 sialyltransferase from liver'** , *The Journal of biological chemistry*, 1983, pp. 11505–11509.

Karsten, CM, Pandey, MK, Figge, J, Kilchenstein, R, Taylor, PR, Rosas, M, McDonald, JU, Orr, SJ, Berger, M, Petzold, D, Blanchard, V, Winkler, A, Hess, C, Reid, DM, Majoul, IV, Strait, RT, Harris, NL, Köhl, G, Wex, E, Ludwig, R, et al. 2012, **'Anti-inflammatory activity of IgG1 mediated by Fc galactosylation and association of FcγRIIB and dectin-1'** , *Nature medicine*, 2012, pp. 1401–1406.

Kato, K, Lian, L-Y, Barsukov, IL, Derrick, JP, Kim, H, Tanaka, R, Yoshino, A, Shiraishi, M, Shimada, I, Arata, Y & Roberts, GCK 1995, **'Model for the complex between protein G and an antibody Fc fragment in solution'** , *Structure*, 1995, pp. 79–85.

Kawai, T & Akira, S 2010, **'The role of pattern-recognition receptors in innate immunity: update on Toll-like receptors'** , *Nature immunology*, 2010, pp. 373–384.

Kew, OM, Sutter, RW, Gourville, EM, Dowdle, WR & Pallansch, MA 2005, **'Vaccine-derived polioviruses and the endgame strategy for global polio eradication'** , *Annual review of microbiology*, 2005, pp. 587–635.

Khabbaz, RF, Moseley, RR, Steiner, RJ, Levitt, AM & Bell, BP 2014, **'Challenges of infectious diseases in the USA'** , *Lancet (London, England)*, 2014, pp. 53–63.

Kometani, K & Kurosaki, T 2015, **'Differentiation and maintenance of long-lived plasma cells'** , *Current opinion in immunology*, 2015, pp. 64–69.

Kopf, M, Baumann, H, Freer, G, Freudenberg, M, Lamers, M, Kishimoto, T, Zinkernagel, R, Bluethmann, H & Köhler, G 1994, **'Impaired immune and acute-phase responses in interleukin-6-deficient mice'** , *Nature*, 1994, pp. 339–342.

Kopf, M, Herren, S, Wiles, MV, Pepys, MB & Kosco-Vilbois, MH 1998, **'Interleukin 6 influences germinal center development and antibody production via a contribution of C3 complement component'** , *The Journal of experimental medicine*, 1998, pp. 1895–1906.

Korn, T, Bettelli, E, Oukka, M & Kuchroo, VK 2009, **'IL-17 and Th17 Cells'** , *Annual review of immunology*, 2009, pp. 485–517.

Kräutler, NJ, Suan, D, Butt, D, Bourne, K, Hermes, JR, Chan, TD, Sundling, C, Kaplan, W, Schofield, P, Jackson, J, Basten, A, Christ, D & Brink, R 2017, **'Differentiation of germinal center B cells into plasma cells is initiated by high-affinity antigen and completed by Tfh cells'** , *The Journal of experimental medicine*, 2017, pp. 1259–1267.

Larché, M, Akdis, CA & Valenta, R 2006, **'Immunological mechanisms of allergen-specific immunotherapy'** , *Nature reviews. Immunology*, 2006, pp. 761–771.

Lauc, G, Huffman, JE, Pučić, M, Zgaga, L, Adamczyk, B, Mužinić, A, Novokmet, M, Polašek, O, Gornik, O, Krištić, J, Keser, T, Vitart, V, Scheijen, B, Uh, H-W, Molokhia, M, Patrick, AL, McKeigue, P, Kolčić, I, Lukić, IK, Swann, O, et al. 2013, **'Loci associated with N-glycosylation of human immunoglobulin G show pleiotropy with autoimmune diseases and haematological cancers'** , *PLoS genetics*, 2013, p. e1003225.

Leal, IS, Flórido, M, Andersen, P & Appelberg, R 2001, **'Interleukin-6 regulates the phenotype of the immune response to a tuberculosis subunit vaccine'** , *Immunology*, 2001, pp. 375–381.

Liang, SC, Tan, X-Y, Luxenberg, DP, Karim, R, Dunussi-Joannopoulos, K, Collins, M & Fouser, LA 2006, **'Interleukin (IL)-22 and IL-17 are coexpressed by Th17 cells and cooperatively enhance expression of antimicrobial peptides'** , *The Journal of experimental medicine*, 2006, pp. 2271–2279.

Li, T, DiLillo, DJ, Bournazos, S, Giddens, JP, Ravetch, JV & Wang, L-X 2017, **'Modulating IgG effector function by Fc glycan engineering'** , *Proceedings of the National Academy of Sciences of the United States of America*, 2017, pp. 3485–3490.

Lilienthal, G-M, Rahmöller, J, Petry, J, Bartsch, YC, Leliavski, A & Ehlers, M 2018, **'Potential of Murine IgG1 and Human IgG4 to Inhibit the Classical Complement and Fcγ Receptor Activation Pathways'** , *Frontiers in immunology*, 2018, p. 958.

Lindquist, L & Vapalahti, O 2008, **'Tick-borne encephalitis'** , *The Lancet*, 2008, pp. 1861–1871.

Litinskiy, MB, Nardelli, B, Hilbert, DM, He, B, Schaffer, A, Casali, P & Cerutti, A 2002, **'DCs induce CD40-independent immunoglobulin class switching through BLyS and APRIL'** , *Nature immunology*, 2002, pp. 822–829.

Li, H, Willingham, SB, Ting, JP-Y & Re, F 2008, **'Cutting Edge: Inflammasome Activation by Alum and Alum's Adjuvant Effect Are Mediated by NLRP3'** , *Journal of immunology (Baltimore, Md. : 1950)*, 2008, pp. 17–21.

Llewelyn, MB, Hawkins, RE & Russell, SJ 1992, **'Discovery of antibodies'** , *BMJ : British Medical Journal*, 1992, pp. 1269–1272.

Locci, M, Havenar-Daughton, C, Landais, E, Wu, J, Kroenke, MA, Arlehamn, CL, Su, LF, Cubas, R, Davis, MM, Sette, A, Haddad, EK, Poignard, P & Crotty, S 2013, **'Human circulating PD-1+CXCR3-CXCR5+ memory Tfh cells are highly functional and correlate with broadly neutralizing HIV antibody responses'** , *Immunity*, 2013, pp. 758–769.

Lu, LL, Chung, AW, Rosebrock, TR, Ghebremichael, M, Yu, WH, Grace, PS, Schoen, MK, Tafesse, F, Martin, C, Leung, V, Mahan, AE, Sips, M, Kumar, MP, Tedesco, J, Robinson, H, Tkachenko, E, Draghi, M, Freedberg, KJ, Streeck, H, Suscovich, TJ, et al. 2016, **'A Functional Role for Antibodies in Tuberculosis'** , *Cell*, 2016, pp. 433-443.e14.

Maceiras, AR, Almeida, SCP, Mariotti-Ferrandiz, E, Chaara, W, Jebbawi, F, Six, A, Hori, S, Klatzmann, D, Faro, J & Graca, L 2017, **'T follicular helper and T follicular regulatory cells have different TCR specificity'** , *Nature communications*, 2017, p. 15067.

Mahan, AE, Jennewein, MF, Suscovich, T, Dionne, K, Tedesco, J, Chung, AW, Streeck, H, Pau, M, Schuitemaker, H, Francis, D, Fast, P, Laufer, D, Walker, BD, Baden, L, Barouch, DH & Alter, G 2016, **'Antigen-Specific Antibody Glycosylation Is Regulated via Vaccination'** , *PLoS pathogens*, 2016, p. e1005456.

Malhotra, R, Wormald, MR, Rudd, PM, Fischer, PB, Dwek, RA & Sim, RB 1995, **'Glycosylation changes of IgG associated with rheumatoid arthritis can activate complement via the mannose-binding protein'** , *Nature medicine*, 1995, pp. 237–243.

Malkiel, S, Barlev, AN, Atisha-Fregoso, Y, Suurmond, J & Diamond, B 2018, **'Plasma Cell Differentiation Pathways in Systemic Lupus Erythematosus'** , *Frontiers in immunology*, 2018, p. 427.

Manz, RA, Thiel, A & Radbruch, A 1997, **'Lifetime of plasma cells in the bone marrow'** , *Nature*, 1997, pp. 133–134.

Marrack, P, McKee, AS & Munks, MW 2009, **'Towards an understanding of the adjuvant action of aluminium'** , *Nature reviews. Immunology*, 2009, pp. 287–293.

Martin, F, Oliver, AM & Kearney, JF 2001, **'Marginal Zone and B1 B Cells Unite in the Early Response against T-Independent Blood-Borne Particulate Antigens'** , *Immunity*, 2001, pp. 617–629.

Massoud, AH, Yona, M, Di Xue, Chouiali, F, Alturaihi, H, Ablona, A, Mourad, W, Piccirillo, CA & Mazer, BD 2014, **'Dendritic cell immunoreceptor: a novel receptor for intravenous immunoglobulin mediates induction of regulatory T cells'** , *The Journal of allergy and clinical immunology*, 2014, pp. 853-63.e5.

Mata-Haro, V, Cekic, C, Martin, M, Chilton, PM, Casella, CR & Mitchell, TC 2007, **'The vaccine adjuvant monophosphoryl lipid A as a TRIF-biased agonist of TLR4'** , *Science (New York, N.Y.)*, 2007, pp. 1628–1632.

Matthews, AJ, Zheng, S, DiMenna, LJ & Chaudhuri, J 2014, **'Regulation of immunoglobulin class-switch recombination: choreography of noncoding transcription, targeted DNA deamination, and long-range DNA repair'** , *Advances in immunology*, 2014, pp. 1–57.

Matzinger, P 2002, **'The danger model: a renewed sense of self'** , *Science (New York, N.Y.)*, 2002, pp. 301–305.

McNeil, MM & DeStefano, F 2018, **'Vaccine-associated hypersensitivity'** , *The Journal of allergy and clinical immunology*, 2018, pp. 463–472.

Miyauchi, K, Sugimoto-Ishige, A, Harada, Y, Adachi, Y, Usami, Y, Kaji, T, Inoue, K, Hasegawa, H, Watanabe, T, Hijikata, A, Fukuyama, S, Maemura, T, Okada-Hatakeyama, M, Ohara, O, Kawaoka, Y, Takahashi, Y, Takemori, T & Kubo, M 2016, **'Protective neutralizing influenza antibody response in the absence of T follicular helper cells'** , *Nature immunology*, 2016, pp. 1447–1458.

Mond, JJ, Vos, Q, Lees, A & Snapper, CM 1995, **'T cell independent antigens'** , *Current opinion in immunology*, 1995, pp. 349–354.

Moremen, KW, Tiemeyer, M & Nairn, AV 2012, **'Vertebrate protein glycosylation: diversity, synthesis and function'** , *Nature reviews. Molecular cell biology*, 2012, pp. 448–462.

Mufson, MA, Hughey, DF, Turner, CE & SCHIFFMAN, G 1991, **'Revaccination with pneumococcal vaccine of elderly persons 6 years after primary vaccination'** , *Vaccine*, 1991, pp. 403–407.

Muraguchi, A, Hirano, T, Tang, B, Matsuda, T, Horii, Y, Nakajima, K & Kishimoto, T 1988, **'The essential role of B cell stimulatory factor 2 (BSF-2/IL-6) for the terminal differentiation of B cells'** , *Journal of Experimental Medicine*, 1988, pp. 332–344.

Muramatsu, M, Kinoshita, K, Fagarasan, S, Yamada, S, Shinkai, Y & Honjo, T 2000, **'Class Switch Recombination and Hypermutation Require Activation-Induced Cytidine Deaminase (AID), a Potential RNA Editing Enzyme'** , *Cell*, 2000, pp. 553–563.

Murphy, KP, Janeway, C, Travers, P, Walport, M, Mowat, A & Weaver, CT 2012, *Janeway's immunobiology*, 8th edn, Garland Science, London.

Nakae, S, Komiyama, Y, Nambu, A, Sudo, K, Iwase, M, Homma, I, Sekikawa, K, Asano, M & Iwakura, Y 2002, **'Antigen-specific T cell sensitization is impaired in IL-17-deficient mice, causing suppression of allergic cellular and humoral responses'** , *Immunity*, 2002, pp. 375–387.

Nakae, S, Nambu, A, Sudo, K & Iwakura, Y 2003, **'Suppression of immune induction of collagen-induced arthritis in IL-17-deficient mice'** , *Journal of immunology (Baltimore, Md. : 1950)*, 2003, pp. 6173–6177.

Narazaki, M, Yasukawa, K, Saito, T, Ohsugi, Y, Fukui, H, Koishihara, Y, Yancopoulos, GD, Taga, T & Kishimoto, T 1993, **'Soluble forms of the interleukin-6 signal-transducing receptor component gp130 in human serum possessing a potential to inhibit signals through membrane-anchored gp130'** , *Blood*, 1993, pp. 1120–1126.

Nimmerjahn, F & Ravetch, JV 2008, **'Fcgamma receptors as regulators of immune responses'** , *Nature reviews. Immunology*, 2008, pp. 34–47.

Nowell, MA, Williams, AS, Carty, SA, Scheller, J, Hayes, AJ, Jones, GW, Richards, PJ, Slinn, S, Ernst, M, Jenkins, BJ, Topley, N, Rose-John, S & Jones, SA 2009, **'Therapeutic targeting of IL-6 trans signaling counteracts STAT3 control of experimental inflammatory arthritis'** , *Journal of immunology (Baltimore, Md. : 1950)*, 2009, pp. 613–622.

Nurieva, RI, Chung, Y, Martinez, GJ, Yang, XO, Tanaka, S, Matskevitch, TD, Wang, Y-H & Dong, C 2009, **'Bcl6 mediates the development of T follicular helper cells'** , *Science (New York, N.Y.)*, 2009, pp. 1001–1005.

Nutt, SL, Hodgkin, PD, Tarlinton, DM & Corcoran, LM 2015, **'The generation of antibody-secreting plasma cells'** , *Nature reviews. Immunology*, 2015, pp. 160–171.

Oefner, CM, Winkler, A, Hess, C, Lorenz, AK, Holecska, V, Huxdorf, M, Schommartz, T, Petzold, D, Bitterling, J, Schoen, A-L, Stoehr, AD, Vu Van, D, Darcan-Nikolaisen, Y, Blanchard, V, Schmudde, I, Laumonnier, Y, Ströver, HA, Hegazy, AN, Eiglmeier, S, Schoen, CT, et al. 2012, **'Tolerance induction with T cell-dependent protein antigens induces regulatory sialylated IgGs'** , *The Journal of allergy and clinical immunology*, 2012, pp. 1647-55.e13.

Ohmi, Y, Ise, W, Harazono, A, Takakura, D, Fukuyama, H, Baba, Y, Narazaki, M, Shoda, H, Takahashi, N, Ohkawa, Y, Ji, S, Sugiyama, F, Fujio, K, Kumanogoh, A, Yamamoto, K, Kawasaki, N, Kurosaki, T, Takahashi, Y & Furukawa, K 2016, **'Sialylation converts arthritogenic IgG into inhibitors of collagen-induced arthritis'** , *Nature communications*, 2016, p. 11205.

Okazaki, M, Yamada, Y, Nishimoto, N, Yoshizaki, K & Mihara, M 2002, **'Characterization of anti-mouse interleukin-6 receptor antibody'** , *Immunology letters*, 2002, pp. 231–240.

Omtvedt, LA, Royle, L, Husby, G, Sletten, K, Radcliffe, CM, Harvey, DJ, Dwek, RA & Rudd, PM 2006, **'Glycan analysis of monoclonal antibodies secreted in deposition disorders indicates that subsets of plasma cells differentially process IgG glycans'** , *Arthritis and rheumatism*, 2006, pp. 3433–3440.

Packer, NH, Lawson, MA, Jardine, DR & Redmond, JW 1998, **'A general approach to desalting oligosaccharides released from glycoproteins'** , *Glycoconjugate journal*, 1998, pp. 737–747.

Pagan, JD, Kitaoka, M & Anthony, RM 2018, **'Engineered Sialylation of Pathogenic Antibodies In Vivo Attenuates Autoimmune Disease'** , *Cell*, 2018, pp. 564-577.e13.

Pallikkuth, S, Parmigiani, A, Silva, SY, George, VK, Fischl, M, Pahwa, R & Pahwa, S 2012, **'Impaired peripheral blood T-follicular helper cell function in HIV-infected nonresponders to the 2009 H1N1/09 vaccine'** , *Blood*, 2012, pp. 985–993.

Parekh, RB, Dwek, RA, Sutton, BJ, Fernandes, DL, Leung, A, Stanworth, D, Rademacher, TW, Mizuochi, T, Taniguchi, T & Matsuta, K 1985, **'Association of rheumatoid arthritis and primary osteoarthritis with changes in the glycosylation pattern of total serum IgG'** , *Nature*, 1985, pp. 452–457.

Petrovsky, N & Aguilar, JC 2004, **'Vaccine adjuvants: current state and future trends'** , *Immunology and cell biology*, 2004, pp. 488–496.

Pfeifle, R, Rothe, T, Ipseiz, N, Scherer, HU, Culemann, S, Harre, U, Ackermann, JA, Seefried, M, Kleyer, A, Uderhardt, S, Haugg, B, Hueber, AJ, Daum, P, Heidkamp, GF, Ge, C, Böhm, S, Lux, A, Schuh, W, Magorivska, I, Nandakumar, KS, et al. 2017, **'Regulation of autoantibody activity by the IL-23-TH17 axis determines the onset of autoimmune disease'** , *Nature immunology*, 2017, pp. 104–113.

Pincetic, A, Bournazos, S, DiLillo, DJ, Maamary, J, Wang, TT, Dahan, R, Fiebiger, B-M & Ravetch, JV 2014, **'Type I and type II Fc receptors regulate innate and adaptive immunity'** , *Nature immunology*, 2014, pp. 707–716.

Plomp, R, Ruhaak, LR, Uh, H-W, Reiding, KR, Selman, M, Houwing-Duistermaat, JJ, Slagboom, PE, Beekman, M & Wuhrer, M 2017, **'Subclass-specific IgG glycosylation is associated with markers of inflammation and metabolic health'** , *Scientific reports*, 2017, p. 12325.

Plotkin, SA 2010, **'Correlates of Protection Induced by Vaccination ▿ '** , *Clinical and Vaccine Immunology : CVI*, 2010, pp. 1055–1065.

Pschyrembel, W, Witzel, S, Dornblüth, O (eds.) 2007, *Pschyrembel Klinisches Wörterbuch*, 261st edn, DE GRUYTER, Berlin.

Pucić, M, Knezević, A, Vidic, J, Adamczyk, B, Novokmet, M, Polasek, O, Gornik, O, Supraha-Goreta, S, Wormald, MR, Redzić, I, Campbell, H, Wright, A, Hastie, ND, Wilson, JF, Rudan, I, Wuhrer, M, Rudd, PM, Josić, D & Lauc, G 2011, **'High throughput isolation and glycosylation analysis of IgG-variability and heritability of the IgG glycome in three isolated human populations'** , *Molecular & cellular proteomics : MCP*, 2011, p. M111.010090.

Quast, I, Keller, CW, Maurer, MA, Giddens, JP, Tackenberg, B, Wang, L-X, Münz, C, Nimmerjahn, F, Dalakas, MC & Lünemann, JD 2015, **'Sialylation of IgG Fc domain impairs complement-dependent cytotoxicity'** , *The Journal of clinical investigation*, 2015, pp. 4160–4170.

Rabe, B, Chalaris, A, May, U, Waetzig, GH, Seegert, D, Williams, AS, Jones, SA, Rose-John, S & Scheller, J 2008, **'Transgenic blockade of interleukin 6 transsignaling abrogates inflammation'** , *Blood*, 2008, pp. 1021–1028.

Rashid, H, Khandaker, G & Booy, R 2012, **'Vaccination and herd immunity: what more do we know?'** , *Current opinion in infectious diseases*, 2012, pp. 243–249.

Reinhardt, RL, Liang, H-E & Locksley, RM 2009, **'Cytokine-secreting follicular T cells shape the antibody repertoire'** , *Nature immunology*, 2009, pp. 385–393.

Ricklin, D, Hajishengallis, G, Yang, K & Lambris, JD 2010, **'Complement: a key system for immune surveillance and homeostasis'** , *Nature immunology*, 2010, pp. 785–797.

Riedel, S 2005, **'Edward Jenner and the history of smallpox and vaccination'** , *Proceedings (Baylor University. Medical Center)*, 2005, pp. 21–25.

Riteau, N, Radtke, AJ, Shenderov, K, Mittereder, L, Oland, SD, Hieny, S, Jankovic, D & Sher, A 2016, **'Water-in-Oil-Only Adjuvants Selectively Promote T Follicular Helper Cell Polarization through a Type I IFN and IL-6-Dependent Pathway'** , *Journal of immunology (Baltimore, Md. : 1950)*, 2016, pp. 3884–3893.

Ritvo, P-G, Saadawi, A, Barennes, P, Quiniou, V, Chaara, W, El Soufi, K, Bonnet, B, Six, A, Shugay, M, Mariotti-Ferrandiz, E & Klatzmann, D 2018, **'High-resolution repertoire analysis reveals a major bystander activation of Tfh and Tfr cells'** , *Proceedings of the National Academy of Sciences of the United States of America*, 2018, pp. 9604–9609.

Rombouts, Y, Ewing, E, van de Stadt, LA, Selman, MHJ, Trouw, LA, Deelder, AM, Huizinga, TWJ, Wuhrer, M, van Schaardenburg, D, Toes, REM & Scherer, HU 2015, **'Anti-citrullinated protein antibodies acquire a pro-inflammatory Fc glycosylation phenotype prior to the onset of rheumatoid arthritis'** , *Annals of the rheumatic diseases*, 2015, pp. 234–241.

Rothstein, SS, Goldman, HS & Arcomano, A 1982, **'Passive immunization for hepatitis B'** , *Journal of Oral and Maxillofacial Surgery*, 1982, pp. 34–37.

Saade, F & Petrovsky, N 2012, **'Technologies for enhanced efficacy of DNA vaccines'** , *Expert Review of Vaccines*, 2012, pp. 189–209.

Sabin, AB & Boulger, LR 1973, **'History of Sabin attenuated poliovirus oral live vaccine strains'** , *Journal of Biological Standardization*, 1973, pp. 115–118.

Sage, PT, Paterson, AM, Lovitch, SB & Sharpe, AH 2014, **'The coinhibitory receptor CTLA-4 controls B cell responses by modulating T follicular helper, T follicular regulatory, and T regulatory cells'** , *Immunity*, 2014, pp. 1026–1039.

Sage, PT & Sharpe, AH 2015, **'T follicular regulatory cells in the regulation of B cell responses'** , *Trends in immunology*, 2015, pp. 410–418.

Salk, JE, Bazeley, PL, Bennett, BL, Krech, U, Lewis, LJ, Ward, EN & Youngner, JS 1954b, **'Studies in Human Subjects on Active Immunization Studies in Human Subjects on Active Immunization Against Poliomyelitis'** , *American Journal of Public Health and the Nations Health*, 1954b, pp. 994–1009.

Salk, JE, Krech, U, Youngner, JS, Bennett, BL, Lewis, LJ & Bazeley, PL 1954a, **'Formaldehyde treatment and safety testing of experimental poliomyelitis vaccines'** , *American Journal of Public Health and the Nations Health*, 1954a, pp. 563–570.

Sanderson, RD, Lalor, P & Bernfield, M 1989, **'B lymphocytes express and lose syndecan at specific stages of differentiation'** , *Cell regulation*, 1989, pp. 27–35.

Scallon, BJ, Tam, SH, McCarthy, SG, Cai, AN & Raju, TS 2007, **'Higher levels of sialylated Fc glycans in immunoglobulin G molecules can adversely impact functionality'** , *Molecular immunology*, 2007, pp. 1524–1534.

Schatz, DG & Ji, Y 2011, **'Recombination centres and the orchestration of V(D)J recombination'** , *Nature reviews. Immunology*, 2011, pp. 251–263.

Scherer, HU, Wang, J, Toes, REM, van der Woude, D, Koeleman, CAM, Boer, AR, Huizinga, TWJ, Deelder, AM & Wuhrer, M 2009, **'Immunoglobulin 1 (IgG1) Fc-glycosylation profiling of anti-citrullinated peptide antibodies from human serum'** , *Proteomics. Clinical applications*, 2009, pp. 106–115.

Schmitz, JE, Kuroda, MJ, Santra, S, Sasseville, VG, Simon, MA, Lifton, MA, Racz, P, Tenner-Racz, K, Dalesandro, M, Scallon, BJ, Ghrayeb, J, Forman, MA, Montefiori, DC, Rieber, EP, Letvin, NL & Reimann, KA 1999, **'Control of viremia in simian immunodeficiency virus infection by CD8+ lymphocytes'** , *Science (New York, N.Y.)*, 1999, pp. 857–860.

Schubert, D, Bode, C, Kenefeck, R, Hou, TZ, Wing, JB, Kennedy, A, Bulashevska, A, Petersen, B-S, Schäffer, AA, Grüning, BA, Unger, S, Frede, N, Baumann, U, Witte, T, Schmidt, RE, Dueckers, G, Niehues, T, Seneviratne, S, Kanariou, M, Speckmann, C, et al. 2014, **'Autosomal dominant immune dysregulation syndrome in humans with CTLA4 mutations'** , *Nature medicine*, 2014, pp. 1410–1416.

Schwab, C, Gabrysch, A, Olbrich, P, Patiño, V, Warnatz, K, Wolff, D, Hoshino, A, Kobayashi, M, Imai, K, Takagi, M, Dybedal, I, Haddock, JA, Sansom, DM, Lucena, JM, Seidl, M, Schmitt-Graeff, A, Reiser, V, Emmerich, F, Frede, N, Bulashevska, A, et al. 2018, **'Phenotype, penetrance, and treatment of 133 cytotoxic T-lymphocyte antigen 4-insufficient subjects'** , *The Journal of allergy and clinical immunology*, 2018.

Schwab, I & Nimmerjahn, F 2013, **'Intravenous immunoglobulin therapy: how does IgG modulate the immune system?'** , *Nature reviews. Immunology*, 2013, pp. 176–189.

Selman, MHJ, Derks, RJE, Bondt, A, Palmblad, M, Schoenmaker, B, Koeleman, CAM, van de Geijn, FE, Dolhain, RJEM, Deelder, AM & Wuhrer, M 2012b, **'Fc specific IgG glycosylation profiling by robust nano-reverse phase HPLC-MS using a sheath-flow ESI sprayer interface'** , *Journal of proteomics*, 2012b, pp. 1318–1329.

Selman, MHJ, Jong, SE, Soonawala, D, Kroon, FP, Adegnika, AA, Deelder, AM, Hokke, CH, Yazdanbakhsh, M & Wuhrer, M 2012a, **'Changes in antigen-specific IgG1 Fc N-glycosylation upon influenza and tetanus vaccination'** , *Molecular & cellular proteomics : MCP*, 2012a, p. M111.014563.

Sen, G, Khan, AQ, Chen, Q & Snapper, CM 2005, **'In vivo humoral immune responses to isolated pneumococcal polysaccharides are dependent on the presence of associated TLR ligands'** , *Journal of immunology (Baltimore, Md. : 1950)*, 2005, pp. 3084–3091.

Shade, K-T & Anthony, R 2013, **'Antibody Glycosylation and Inflammation'** , *Antibodies*, 2013, pp. 392–414.

Shade, K-TC, Platzer, B, Washburn, N, Mani, V, Bartsch, YC, Conroy, M, Pagan, JD, Bosques, C, Mempel, TR, Fiebiger, E & Anthony, RM 2015, **'A single glycan on IgE is indispensable for initiation of anaphylaxis'** , *The Journal of experimental medicine*, 2015, pp. 457–467.

Shibaki, A & Katz, SI 2002, **'Induction of skewed Th1/Th2 T-cell differentiation via subcutaneous immunization with Freund's adjuvant'** , *Experimental dermatology*, 2002, pp. 126–134.

Shields, RL, Lai, J, Keck, R, O'Connell, LY, Hong, K, Meng, YG, Weikert, SHA & Presta, LG 2002, **'Lack of fucose on human IgG1 N-linked oligosaccharide improves binding to human Fcgamma RIII and antibody-dependent cellular toxicity'** , *The Journal of biological chemistry*, 2002, pp. 26733–26740.

Shinnakasu, R, Inoue, T, Kometani, K, Moriyama, S, Adachi, Y, Nakayama, M, Takahashi, Y, Fukuyama, H, Okada, T & Kurosaki, T 2016, **'Regulated selection of germinal-center cells into the memory B cell compartment'** , *Nature immunology*, 2016, pp. 861–869.

Sodenkamp, J, Waetzig, GH, Scheller, J, Seegert, D, Grötzinger, J, Rose-John, S, Ehlers, S & Hölscher, C 2012, **'Therapeutic targeting of interleukin-6 trans-signaling does not affect the outcome of experimental tuberculosis'** , *Immunobiology*, 2012, pp. 996–1004.

Stadlmann, J, Pabst, M & Altmann, F 2010, **'Analytical and Functional Aspects of Antibody Sialylation'** , *Journal of clinical immunology*, 2010, pp. S15-9.

Tamura, T, Udagawa, N, Takahashi, N, Miyaura, C, Tanaka, S, Yamada, Y, Koishihara, Y, Ohsugi, Y, Kumaki, K & Taga, T 1993, **'Soluble interleukin-6 receptor triggers osteoclast formation by interleukin 6'** , *Proceedings of the National Academy of Sciences of the United States of America*, 1993, pp. 11924–11928.

Tao, MH & Morrison, SL 1989, **'Studies of aglycosylated chimeric mouse-human IgG. Role of carbohydrate in the structure and effector functions mediated by the human IgG constant region'** , *Journal of immunology (Baltimore, Md. : 1950)*, 1989, pp. 2595–2601.

Taranger, J, Trollfors, B, Lagergård, T, Sundh, V, Bryla, DA, Schneerson, R & Robbins, JB 2000, **'Correlation between pertussis toxin IgG antibodies in postvaccination sera and subsequent protection against pertussis'** , *The Journal of infectious diseases*, 2000, pp. 1010–1013.

Theodoratou, E, Thaçi, K, Agakov, F, Timofeeva, MN, Štambuk, J, Pučić-Baković, M, Vučković, F, Orchard, P, Agakova, A, Din, FVN, Brown, E, Rudd, PM, Farrington, SM, Dunlop, MG, Campbell, H & Lauc, G 2016, **'Glycosylation of plasma IgG in colorectal cancer prognosis'** , *Scientific reports*, 2016, p. 28098.

Trbojević Akmačić, I, Ventham, NT, Theodoratou, E, Vučković, F, Kennedy, NA, Krištić, J, Nimmo, ER, Kalla, R, Drummond, H, Štambuk, J, Dunlop, MG, Novokmet, M, Aulchenko, Y, Gornik, O, Campbell, H, Pučić Baković, M, Satsangi, J & Lauc, G 2015, **'Inflammatory bowel disease associates with proinflammatory potential of the immunoglobulin G glycome'** , *Inflammatory bowel diseases*, 2015, pp. 1237–1247.

Twisselmann, N, Bartsch, YC, Pagel, J, Wieg, C, Hartz, A, Ehlers, M & Härtel, C 2019, **'IgG Fc Glycosylation Patterns of Preterm Infants Differ With Gestational Age'** , *Frontiers in Immunology*, 2019, p. 548.

Ueno, H 2016, **'T follicular helper cells in human autoimmunity'** , *Current opinion in immunology*, 2016, pp. 24–31.

Vaccari, M, Gordon, SN, Fourati, S, Schifanella, L, Liyanage, NPM, Cameron, M, Keele, BF, Shen, X, Tomaras, GD, Billings, E, Rao, M, Chung, AW, Dowell, KG, Bailey-Kellogg, C, Brown, EP, Ackerman, ME, Vargas-Inchaustegui, DA, Whitney, S, Doster, MN, Binello, N, et al. 2016, **'Adjuvant-dependent innate and adaptive immune signatures of risk of SIVmac251 acquisition'** , *Nature medicine*, 2016, pp. 762–770.

Vaeth, M, Müller, G, Stauss, D, Dietz, L, Klein-Hessling, S, Serfling, E, Lipp, M, Berberich, I & Berberich-Siebelt, F 2014, **'Follicular regulatory T cells control humoral autoimmunity via NFAT2-regulated CXCR5 expression'** , *The Journal of experimental medicine*, 2014, pp. 545–561.

Vaeth, M, Schliesser, U, Müller, G, Reissig, S, Satoh, K, Tuettenberg, A, Jonuleit, H, Waisman, A, Müller, MR, Serfling, E, Sawitzki, BS & Berberich-Siebelt, F 2012, **'Dependence on nuclear factor of activated T-cells (NFAT) levels discriminates conventional T cells from Foxp3+ regulatory T cells'** , *Proceedings of the National Academy of Sciences of the United States of America*, 2012, pp. 16258–16263.

van de Geijn, FE, Wuhrer, M, Selman, MH, Willemsen, SP, Man, YA, Deelder, AM, Hazes, JM & Dolhain, RJ 2009, **'Immunoglobulin G galactosylation and sialylation are associated with pregnancy-induced improvement of rheumatoid arthritis and the postpartum flare: results from a large prospective cohort study'** , *Arthritis research & therapy*, 2009, p. R193.

Vanderschaeghe, D, Meuris, L, Raes, T, Grootaert, H, van Hecke, A, Verhelst, X, van de Velde, F, Lapauw, B, van Vlierberghe, H & Callewaert, N 2018, **'Endoglycosidase S enables a highly simplified clinical chemistry assay procedure for direct assessment of serum IgG undergalactosylation in chronic inflammatory disease'** , *Molecular & cellular proteomics : MCP*, 2018.

Veldhoen, M, Hocking, RJ, Atkins, CJ, Locksley, RM & Stockinger, B 2006, **'TGFbeta in the context of an inflammatory cytokine milieu supports de novo differentiation of IL-17-producing T cells'** , *Immunity*, 2006, pp. 179–189.

Victora, GD & Nussenzweig, MC 2012, **'Germinal centers'** , *Annual review of immunology*, 2012, pp. 429–457.

Vidarsson, G, Dekkers, G & Rispens, T 2014, **'IgG subclasses and allotypes: from structure to effector functions'** , *Frontiers in immunology*, 2014, p. 520.

Vieira, P & Rajewsky, K 1988, **'The half-lives of serum immunoglobulins in adult mice'** , *European journal of immunology*, 1988, pp. 313–316.

Vučković, F, Krištić, J, Gudelj, I, Teruel, M, Keser, T, Pezer, M, Pučić-Baković, M, Štambuk, J, Trbojević-Akmačić, I, Barrios, C, Pavić, T, Menni, C, Wang, Y, Zhou, Y, Cui, L, Song, H, Zeng, Q, Guo, X, Pons-Estel, BA, McKeigue, P, et al. 2015, **'Association of systemic lupus erythematosus with decreased immunosuppressive potential of the IgG glycome'** , *Arthritis & rheumatology (Hoboken, N.J.)*, 2015, pp. 2978–2989.

Wahl, A, van den Akker, E, Klaric, L, Štambuk, J, Benedetti, E, Plomp, R, Razdorov, G, Trbojević-Akmačić, I, Deelen, J, van Heemst, D, Slagboom, PE, Vučković, F, Grallert, H, Krumsiek, J, Strauch, K, Peters, A, Meitinger, T, Hayward, C, Wuhrer, M, Beekman, M, et al. 2018, **'Genome-Wide Association Study on Immunoglobulin G Glycosylation Patterns'** , *Frontiers in immunology*, 2018, p. 277.

Wang, TT, Maamary, J, Tan, GS, Bournazos, S, Davis, CW, Krammer, F, Schlesinger, SJ, Palese, P, Ahmed, R & Ravetch, JV 2015, **'Anti-HA Glycoforms Drive B Cell Affinity Selection and Determine Influenza Vaccine Efficacy'** , *Cell*, 2015, pp. 160–169.

Wang, J, Shan, Y, Jiang, Z, Feng, J, Li, C, Ma, L & Jiang, Y 2013, **'High frequencies of activated B cells and T follicular helper cells are correlated with disease activity in patients with new-onset rheumatoid arthritis'** , *Clinical and experimental immunology*, 2013, pp. 212–220.

Weisel, F & Shlomchik, M 2017, **'Memory B Cells of Mice and Humans'** , *Annual review of immunology*, 2017, pp. 255–284.

Weisel, FJ, Zuccarino-Catania, GV, Chikina, M & Shlomchik, MJ 2016, **'A Temporal Switch in the Germinal Center Determines Differential Output of Memory B and Plasma Cells'** , *Immunity*, 2016, pp. 116–130.

Wieland, A, Kamphorst, AO, Valanparambil, RM, Han, J-H, Xu, X, Choudhury, BP & Ahmed, R 2018, **'Enhancing FcγR-mediated antibody effector function during persistent viral infection'** , *Science immunology*, 2018.

Wing, JB, Ise, W, Kurosaki, T & Sakaguchi, S 2014, **'Regulatory T cells control antigen-specific expansion of Tfh cell number and humoral immune responses via the coreceptor CTLA-4'** , *Immunity*, 2014, pp. 1013–1025.

Wing, K, Onishi, Y, Prieto-Martin, P, Yamaguchi, T, Miyara, M, Fehervari, Z, Nomura, T & Sakaguchi, S 2008, **'CTLA-4 control over Foxp3+ regulatory T cell function'** , *Science (New York, N.Y.)*, 2008, pp. 271–275.

Wollenberg, I, Agua-Doce, A, Hernández, A, Almeida, C, Oliveira, VG, Faro, J & Graca, L 2011, **'Regulation of the germinal center reaction by Foxp3+ follicular regulatory T cells'** , *Journal of immunology (Baltimore, Md. : 1950)*, 2011, pp. 4553–4560.

World Health Assembly 1980, **'Declaration of global eradication of smallpox. World Health Organization'**, 33, <http://www.who.int/iris/handle/10665/155528>.

Wuhrer, M, Selman, MHJ, McDonnell, LA, Kümpfel, T, Derfuss, T, Khademi, M, Olsson, T, Hohlfeld, R, Meinl, E & Krumbholz, M 2015, **'Pro-inflammatory pattern of IgG1 Fc glycosylation in multiple sclerosis cerebrospinal fluid'** , *Journal of neuroinflammation*, 2015, p. 235.

Wuhrer, M, Stam, JC, van de Geijn, FE, Koeleman, CAM, Verrips, CT, Dolhain, RJEM, Hokke, CH & Deelder, AM 2007, **'Glycosylation profiling of immunoglobulin G (IgG) subclasses from human serum'** , *Proteomics*, 2007, pp. 4070–4081.

Ye, P, Rodriguez, FH, Kanaly, S, Stocking, KL, Schurr, J, Schwarzenberger, P, Oliver, P, Huang, W, Zhang, P, Zhang, J, Shellito, JE, Bagby, GJ, Nelson, S, Charrier, K, Peschon, JJ & Kolls, JK 2001, **'Requirement of interleukin 17 receptor signaling for lung CXC chemokine and granulocyte colony-stimulating factor expression, neutrophil recruitment, and host defense'** , *The Journal of experimental medicine*, 2001, pp. 519–527.

Zhang, Y, Tech, L, George, LA, Acs, A, Durrett, RE, Hess, H, Walker, LSK, Tarlinton, DM, Fletcher, AL, Hauser, AE & Toellner, K-M 2018, **'Plasma cell output from germinal centers is regulated by signals from Tfh and stromal cells'** , *The Journal of experimental medicine*, 2018, pp. 1227–1243.

Zheng, Y, Danilenko, DM, Valdez, P, Kasman, I, Eastham-Anderson, J, Wu, J & Ouyang, W 2007, '**Interleukin-22, a T(H)17 cytokine, mediates IL-23-induced dermal inflammation and acanthosis**' , *Nature*, 2007, pp. 648–651.

Zhu, J, Yamane, H & Paul, WE 2010, '**Differentiation of effector CD4 T cell populations**' , *Annual review of immunology*, 2010, pp. 445–489.

B Supplement

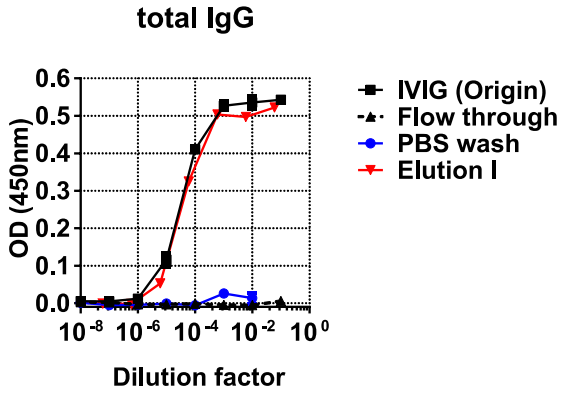

Fig. A.1 ***Total IgG purification for glyco-analysis.*** *Protein G purification of human pooled IgG (IVIG) was performed as described (see 2.2.1.1). Human IgG was completely retained by Protein G because the flow through and wash fractions contained no IgG, as determined by ELISA. IgG was completely recovered in the elution fraction.*

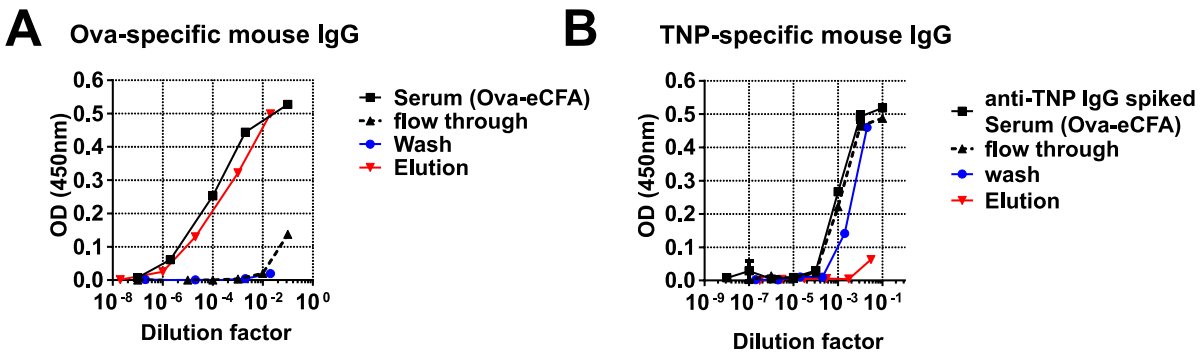

Fig. A.2 ***Ova-specific IgG purification for glyco-analysis retains the majority of specific IgG but not of other specificities.*** *(A) Serum from Ova-eCFA immunized mice (d14) was purified by Ova-sepharose as described (see 2.2.1.3). Different dilutions of serum, flow through after the Ova-sepharose, as well as PBS wash fraction and the elution, were tested by ELISA for Ova-specific IgG. Flow through and wash do not show remarkable amounts of Ova-specific IgG, which indicates that all Ova-IgG was retained by the column. After elution, almost all Ova-specific IgG was recovered. (B) Serum was spiked with monoclonat anti-TNP IgG1 (clone: H5), and Ova-specific purification was performed. The different fractions were then subject to TNP-specific IgG. Almost all TNP-specific IgG was found in the flow through and wash fractions, indicating no retention by the Ova-sepharose. TNP-specific IgG was almost absent in the elution.*

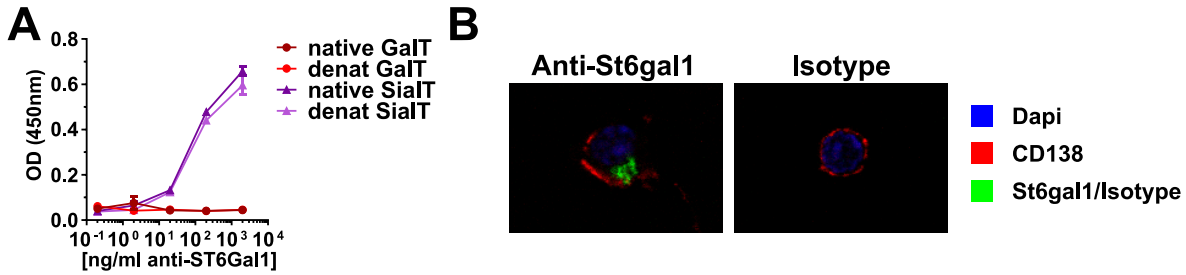

Fig. A.3 ***Binding behavior of anti-St6gal1 antibody used for flow cytometric measurement of mouse St6gal1.*** *(A) Native or heat denaturated St6gal1(SialT) or B4galT1 (GalT) was coupled to microtiter plate, and different dilutions of anti-St6gal1 antibody were detected with HRP-coupled anti-goat-IgG. The St6gal1 antibody binds only to native and denaturated St6gal1 but not to B4galT1. Splenocytes from naïve mice were stained with anti-CD138-PE and anti-St6gal1-AF488 or normal goat IgG-AF488 (isotype). CD138+ lymphocytes were sorted by FACS directly on a microscopic slide and counterstained with Dapi. Sorted cells were analyzed with a Confocal Laser Scanning Biological Microscope FV1000 (Olympus). Shown below are representative pictures of CD138+ cells that were stained with anti-St6gal1 (left) or isotype control (right). Only the anti-St6gal1 shows intracellular staining.*

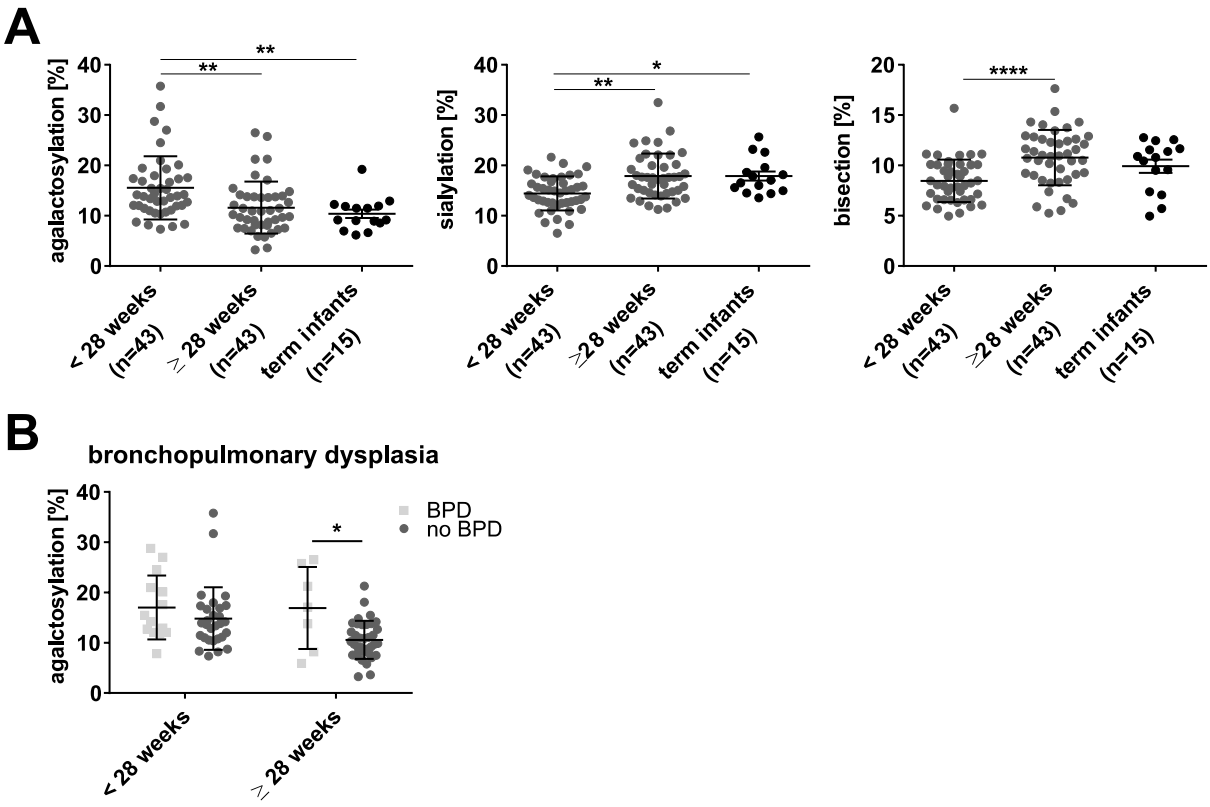

Fig. A. 4 ***IgG Fc glycosylation in preterm infants is dependent on gestational age and inflammatory status****. The IgG Fc glycosylation patterns in plasma sqmples of preterm infants (n = 86, 23–34 weeks of gestation) and term infants (n = 15) was analyzed by HPLC. (A) The IgG Fc glycosylation pattern of early preterm infants (< 28 weeks of gestation) is significantly less galactosylated (more aglactosylated) and sialylated compared to late born preterm infants (> 28 weeks of gestation) and normal (term) infants. Bisecting Fc glycans were only significantly decreased in preterm infants born after < 28 weeks of gestational age (mean ± SD, Kruskal-Wallis test). (B) Correlation of agalactosylated IgG Fc glycan with the occurrence of bronchopulmonary dysplasis (BPD) reveled significant increased agalactosylated IgG glycans in late born preterm (> 28 weeks) infants with BPD (mean ± SD, two-way ANOVA, multiple comparison within groups to adjust for gestational age). The data shown here was published in Twisselmann, et al., 2018.*

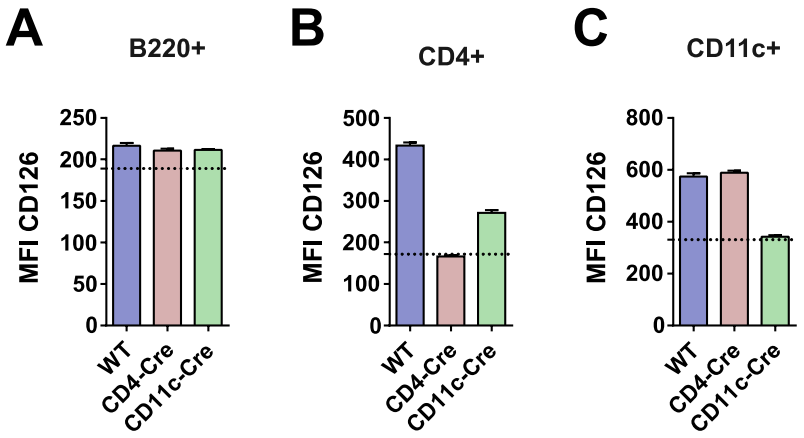

Fig. A.5 ***Flow cytometric control of IL-6R surface expression upon different genotypes****. IL-6R flox mice crossed to either CD4-Cre, CD11c-Cre or Cre negative littermates (WT) were analyzed for IL-6R expression by flow cytometry on day 8 after Ova-eCFA. IL6R MFI was analyzed in B220+ B cells (A), CD4+ (B) and CD11c+ (C) cells.*

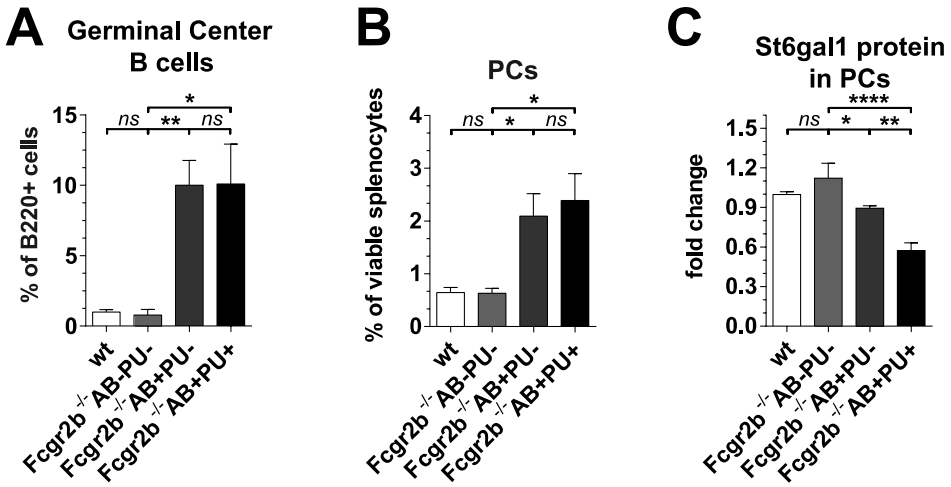

Fig. A.6 ***Augmented GC and PC frequencies in autoimmune prone FcγRiiB KO mice correlates with disease progression****. Eight- to 20-week-old FcγRiiB KO mice were tested and grouped for the presence of anti-dsDNA binding autoantibodies (AB- or AB+) and proteinuria (PU- or PU+). Proteinuria was only observed in auto-antibody positive animals. WT controls were negative for autoantibodies and showed no proteinuria. Mice were analyzed by flow cytometry in different ages and grouped according to the presence of auto-antibodies and proteinuria. Frequencies of (A) GC B cells and (B) plasma cells is augmented upon occurrence of auto-antibodies. (C) St6gal1 expression in PCs gradually decreases with the presence of autoantibodies and development of proteinuria. Some data shown here was published in Bartsch et al., 2018.*

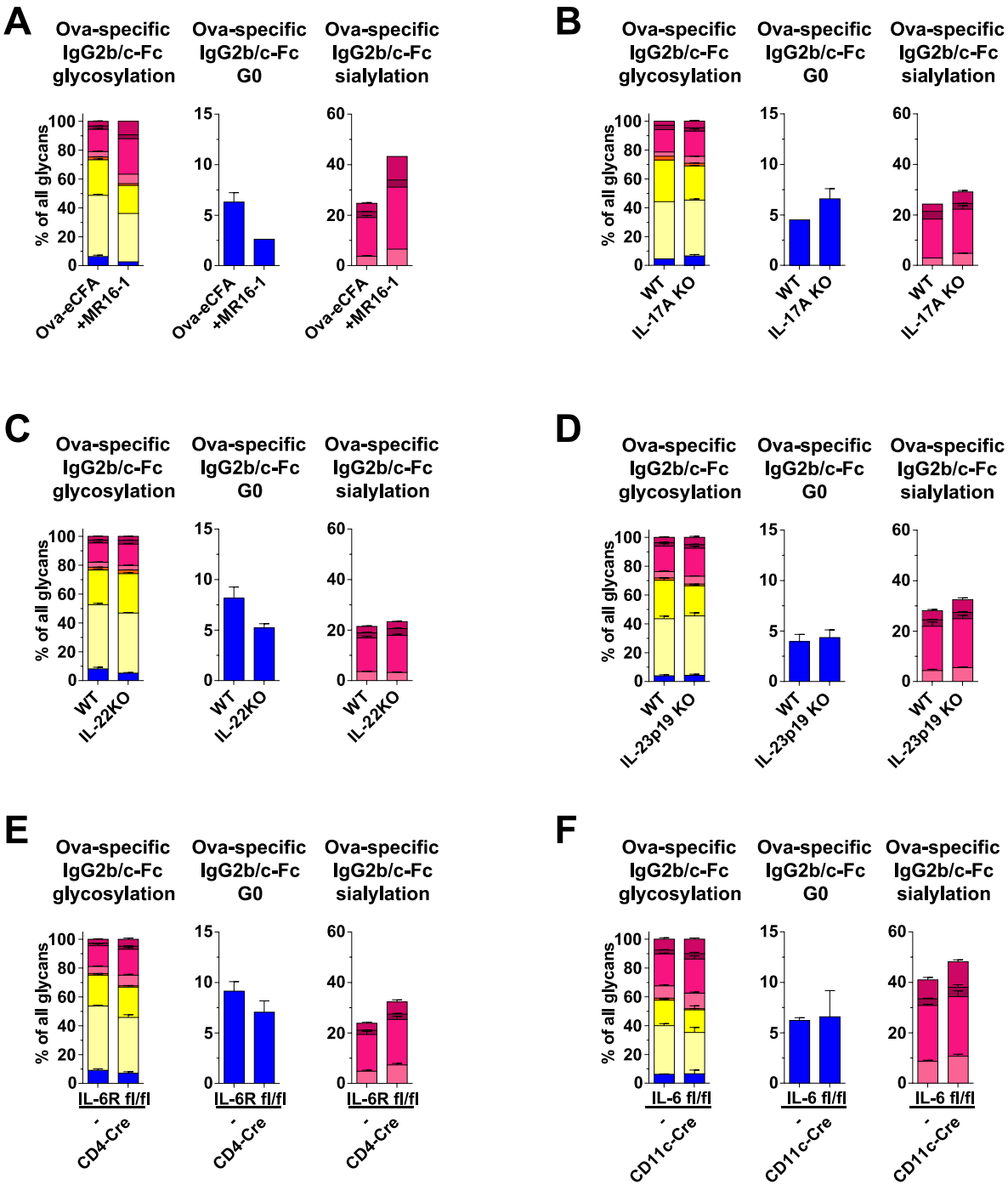

Fig. A.7 ***Ova-specific IgG2b/c Fc glycosylation upon Ova-eCFA immunization under different conditions on day 14****. Ova-specific IgG2b/c glycosylation pattern, G0 and sialylation of the experiments for which IgG1 Fc data is shown in the main figures. (A) MR16-1 treatment shown in Fig. 3.19, (B) IL-17A KO shown in Fig. 3.26, (C, D) IL-22KO and IL-23p19 KO shown in Fig. 3.27, (E) CD4-Cre shown in Fig. 3.29 and (F) CD11c-Cre shown in Fig. 3.34.*

C Abbreviations

Abs	antibodies
ACN	acetonitrile
ADCC	antibody-dependent cytotoxicity
ADCVI	antibody-dependent cell-mediated virus-inhibition
AF	Alexa Fluor®
AID	activation-induced cytidine deaminase
AIT	antigen-specific immune therapy
Alum	Aluminum hydroxide
ANOVA	analysis of variance
APC	antigen-presenting cell
Asn	asparagine
B4galt1	β-1,4-galactosyltransferase 1
Bcl-6	B-cell lymphoma 6 protein
BCR	B cell receptor
BV	Brilliant Violet™
C1q	complement component 1q
CD	cluster of differentiation
CFA	Complete Freund's Adjuvant
CMP	Cytidine monophosphate
CTL	cytotoxic T lymphocyte
CTLA4	cytotoxic T-lymphocyte-associated protein 4
CXCR5	C-X-C chemokine receptor type 5
d	day
DAMP	danger associated molecular pattern
DC	dendritic cell
DCIR	Dendritic cell immunoreceptor
DNA	Deoxyribonucleic acid
DZ	dark zone
eCFA	enriched Complete Freund's Adjuvant
ELISA	enzyme-linked immunosorbent assay
EndoS	Endoglycosidase S
ER	endoplasmic reticulum
Fab	fragment antigen-binding
FACS	fluorescence-activated cell sorting
Fc	fragment crystallizable
FDC	follicular dendritic cell

fl	flox
FLD	fluorescence detector
Foxp3	forkhead box P3
G0	agalactosylated
GC	germinal center
GlcNAc	N-Acetylglucosamine
GPI	glycophosphatidylinositol
HILIC	hydrophilic interaction liquid chromatography
HPLC	High Performance Liquid Chromatography
HRP	horseradish peroxidase
i.p.	intraperitoneal
IBD	Inflammatory bowel disease
IC	immune complex
ICOS	inducible T-cell costimulator
IFA	Incomplete Freund’s Adjuvant
Ig	immunoglobulin
IL	interleukin
ITAM	immunoreceptor tyrosine-based activation motif
ITIM	immunoreceptor tyrosine-based inhibitory motif
iTreg	inducible regulatory T cells
IVIG	intravenous IgG (pooled from healthy donor)
Jak	Janus kinase
KO	knockout
LC-MS	Liquid Chromatography Mass Spectrometry
LPS	Lipopolysaccharide
LZ	light zone
MAC	membrane attack complex
MBP	Mannose binding protein
MHC	major histocompatibility complex
MPLA	Monophosphoryl Lipid A
MS	Multiple Sclerosis
Mtb	Mycobacterium tuberculosis
MZ	marginal zone
Neu5Ac	N-acetylneuraminic acid
Neu5Gc	N-glycolylneuraminic acid
Nfat	nuclear factor of activated T-cells
nTreg	natural regulatory T cells
Ova	Ovalbumin
PAMP	pathogen associated molecular pattern
PBS	Phosphate-buffered saline

PC	plasma cell
PE	Phycoerythrin
PMA	phorbol 12-myristate 13-acetate
PRR	pattern recognition receptor
RA	rheumatoid arthritis
rpm	rounds per minute
RT	room temperature
SEM	standard error of the mean
SHIP	SH2 domain containing inositol phosphatase
SIGN-R1	specific ICAM-3 grabbing nonintegrin-related 1
SLE	systemic lupus erythematosus
SNA	Sambucus nigra agglutinin
St6gal1	α-2,6-sialyltransferase
STAT	signal transducer and activator of transcription 3
SYK	spleen tyrosine kinase
TCR	T cell receptor
TD	T cell (thymus) dependent
TFA	Trifluoroacetic acid
tg	transgene
TGFβ	transforming growth factor β
Th	T helper cell
TI	T cell (thymus) independent
TLR	Toll-like receptor
TNFα	tumor necrosis factor α
WHO	World Health Organization
WT	wildtype
y	Year

D Acknowledgements

I would like to thank all those who accompanied me on the path to completing my dissertation, especially those who provided all the reagents and mice and the experimental, scientific and social input. Without this support, it would have been a rocky road.

Special thanks to my supervisor, Marc Ehlers, who provided me with the opportunity to conduct this work in his laboratory. The many hours we discussed the experiments and results were extremely helpful. Equally helpful was the structure of the RTG1727 and the mentoring provided by Katja Bieber and Ralf Ludwig. I was never without contact persons and scientific support.

I would like to thank all members of AG Ehlers: Johann Rahmöller, Alexei Leliavski, Simon Eschweiler, Moritz Steinhaus, Alexander Epp, Julian Hobusch and in particular Gina Lilienthal and Janina Petry for the extent of their support in the many experiments and beyond. I would also like to thank Sander Wagt and Manfred Wuhrer from LUMC who agreed to analyze the many Glyco samples using LC-MS and thus made an important contribution to this project.

Special thanks, of course, also go to Lea, who always supported and motivated me and, above all, had understanding for my many hours in the lab.

Lastly, of course, I would like to thank my family and friends, who always supported me and provided a necessary balance.